

REPORT DOCUMENTATION PAGE

**Form Approved
OMB No. 0704-0188**

Public reporting burden for this collection of information is estimated to average 1 hour per response, including the time for reviewing instructions, searching existing data sources, gathering and maintaining the data needed, and completing and reviewing this collection of information. Send comments regarding this burden estimate or any other aspect of this collection of information, including suggestions for reducing burden, to Department of Defense, Washington Headquarters Services, Directorate for Information Operations and Reports (0704-0188), 1215 Jefferson Davis Highway, Suite 1204, Arlington, VA 22202. Respondents should be aware that notwithstanding any other provision of law, no person shall be subject to any penalty for failing to comply with a collection of information if it does not display a currently valid OMB control number. PLEASE DO NOT RETURN YOUR FORM TO THE ABOVE ADDRESS.

1. REPORT DATE (DD-MM-YYYY) 31/05/2002		2. REPORT TYPE Final Technical		3. DATES COVERED (From - To) 15/06/1992 - 14/07/1995	
4. TITLE AND SUBTITLE Optoelectronic Integrated Circuits Fabricated Using Atomic Layer Epitaxy				5a. CONTRACT NUMBER	
				5b. GRANT NUMBER DAAL03-92-G-0234	
				5c. PROGRAM ELEMENT NUMBER	
6. AUTHOR(S) P. Daniel Dapkus				5d. PROJECT NUMBER	
				5e. TASK NUMBER	
				5f. WORK UNIT NUMBER	
7. PERFORMING ORGANIZATION NAME(S) AND ADDRESS(ES)				8. PERFORMING ORGANIZATION REPORT NUMBER	
Univ. of Southern California Dept. of Contracts & Grants 837 West 36th Place, STO-330 University Park Los Angeles, CA 90089-1147					
9. SPONSORING / MONITORING AGENCY NAME(S) AND ADDRESS(ES) Closeout Unit Office of Naval Research, San Diego Region 4520 Executive Dr., Suite 300 San Diego, CA 92121-3019				10. SPONSOR/MONITOR'S ACRONYM(S) 30500.1-EL-SDI	
				11. SPONSOR/MONITOR'S REPORT NUMBER(S)	
12. DISTRIBUTION / AVAILABILITY STATEMENT APPROVED FOR PUBLIC RELEASE, DISTRIBUTION UNLIMITED					
13. SUPPLEMENTARY NOTES 20030310 027					
14. ABSTRACT Atomic Layer Epitaxy (ALE) is studied for use in the fabrication of optoelectronics integrated circuits. A new approach to ALE is investigated in which the process is performed under UHV conditions using organometallic compounds as sources for the reactive species. A vacuum ALE system was constructed and the mechanisms for growth of GaAs using trimethylgallium (TMGa) and tertiarybutylarsine (TBAs) were investigated using a set of insitu tools - reflection difference spectroscopy, mass spectroscopy, and reflection high energy electron diffraction. Studies of the interplay of total growth rate and background impurity (Carbon) incorporation were investigated. The growth rate was found to be limited by the exposure time required to insure complete removal of the CH₃ species from the surface to reduce C incorporation. Selective area growth of GaAs on patterned substrates was undertaken to investigate the orientation dependences of the growth morphology on pattern direction.					
15. SUBJECT TERMS Laser assisted growth, atomic layer epitaxy, optoelectronics integration, organometallics					
16. SECURITY CLASSIFICATION OF:			17. LIMITATION OF ABSTRACT	18. NUMBER OF PAGES	19a. NAME OF RESPONSIBLE PERSON P. Daniel Dapkus
a. REPORT UNCLASSIFIED	b. ABSTRACT UNCLASSIFIED	c. THIS PAGE UNCLASSIFIED	UL	134	19b. TELEPHONE NUMBER (include area code) (213) 740-4414

1.0 Introduction

This report describes the research carried out under ARO grant # DAAL03-92-G-0234 titled "Optoelectronic Integrated Circuits Fabricated Using Atomic Layer Epitaxy." This grant was a three-year program proposed to explore the possibility of using atomic layer epitaxy (ALE) and laser assisted ALE (LALE) as technologies to fabricate optoelectronic integrate circuits. ALE is the epitaxial growth technique that is characterized by sequentially exposing the wafer surface with III and V reactants under conditions in which a single atomic layer is formed during each exposure cycle. ALE was chosen as an approach to investigate because it is possible to control the layer thickness and uniformity of materials over large areas by the inherent saturated layer-by-layer growth¹⁻³. Furthermore, we had shown in a series of papers that selective area growth using localized laser assistance was possible in this growth regime as well⁴⁻¹⁰. This opened up the possibility that different devices structures could be grown on different parts of the wafer by changing the laser excitation pattern during growth. The early work on ALE and LALE was performed in small atmospheric pressure reactor vessels that were not amenable to the fabrication of large devices or integrated circuits. Furthermore, the use of atmospheric pressure made it impossible to devise a reactor in which light access was possible in a practical way. As a result, we planned to investigate the use of a UHV reactor chamber on which high quality quartz windows could be placed to allow high-resolution optical access to the wafer surface. It also made it possible to access the surface with other beams such as electron beams and ion beams. E-beams were viewed as a means to achieve high resolution localized growth and ion beams were viewed as a possible means to investigate growth with other sources and to alter the surface reaction kinetics.

The research was divided into three distinct areas of work: fundamental studies of the ALE process, studies of the growth of GaAs by ultrahigh vacuum ALE (VALE) and selected area growth of GaAs by laser assisted ALE. The fundamental studies were part of a more general program to investigate surface reactions in ALE and were jointly supported by ONR and the National Renewable Energy Laboratory. The VALE studies and the selected area growth studies were also jointly supported by NREL.

Section 1.0 References

1. S. P. Denbaars, P. D. Dapkus, J. S. Osinski, M. Zandian, C. A. Beyler, and K. M. Dzurko, "Thermal and laser assisted atomic layer epitaxy of compound semiconductors", Proc. of Int. Symp. GaAs and Related Compounds; Inst. Phys. Conf. Ser. No. 96, 89 (1989).
2. Q. Chen, J. A. Osinski, C. A. Beyler, and P. D. Dapkus, "Quantum well lasers with active regions grown by laser assisted atomic layer epitaxy", Appl. Phys. Letters 57, 1437 (1990)
3. Q. Chen, J. S. Osinski, C. A. Beyler, and P. D. Dapkus, "Laser assisted atomic layer epitaxy - a vehicle to optoelectronic integration," Proc. Mat. Res. Soc. Symp., Atomic Layer Growth and Processing, 222, 109 (1991)
4. Q. Chen, C. A. Beyler, P. D. Dapkus, J. J. Alwan, and J. J. Coleman, "The use of tertiarybutylarsine in atomic layer epitaxy and laser assisted epitaxy of device quality GaAs," Appl. Phys Lett. 60, 2418 (1992)
5. Q. Chen and P. D. Dapkus, "Growth and Characterization of device quality GaAs produced by laser assisted atomic layer epitaxy using triethylgallium," Thin Solid Films 225, 115 (1993).

DISTRIBUTION STATEMENT A
Approved for Public Release
Distribution Unlimited

2.0 Fundamental Studies

In order to be able to scale up the VALE process and to control the residual doping in the material, a system for the investigation of surface reaction mechanisms was established in previous programs and expanded in this program to include new techniques for understanding the surface reactions. A reaction chamber was added to a commercial ESCA system to allow rapid transfer of samples between the reaction chamber and the analysis chamber. This system was further modified to include the following analysis tools on the reaction chamber: RHEED, mass spectroscopy (MS), and reflection difference spectroscopy (RDS). Earlier studies of our group had used the RDS¹⁻⁷ and MS⁸ tools to correlate the changes in surface structure with evolution of gaseous species from the surface after exposure with ALE reactants. During this program these studies were expanded to focus on the correlation between the RDS transients and the RHEED transients after exposure. These studies are described in Appendix 1 attached to this document:

Appendix 1

B. Y. Maa, P. D. Dapkus, P. Chen, and A. Madhukar, "A Real-Time Study of the Reflection High Energy Electron Diffraction Specular Beam Intensity During Atomic Layer Epitaxy of GaAs" Appl. Phys. Lett. 62, 2551 (1993)

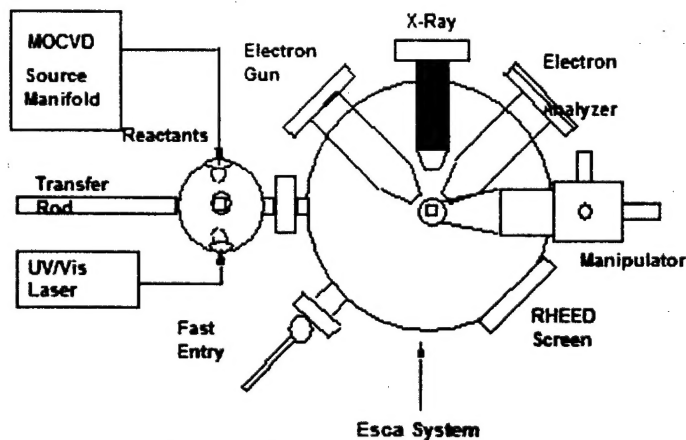


Figure 1 Schematic diagram of reaction system for studies of surface reactions in ALE.

Section 2 References

1. B. Y. Maa and P. D. Dapkus, "RHEED and XPS observations of trimethylgallium adsorption on (001) GaAs surfaces - relevance to atomic layer epitaxy", J. Electronic Materials 19, 289 (1990)
2. B. Y. Maa and P. D. Dapkus, "Studies of TMGa adsorption on thin GaAs and InAs (001) Layers", J. Crystal Growth 105, 213 (1990).
3. P. D. Dapkus, S. P. DenBaars, Q. Chen, W. G. Jeong, and B. Y. Maa, "The role of surface and gas phase reactions in atomic layer epitaxy of compound semiconductors", in Mechanisms of Reactions of Organometallics Compound with Surfaces. D. J. Cole-Hamilton and J.O. Williams, eds., Proceedings of NATO Advanced Research Workshop, Vol. 198, Plenum Publishing Corp., New York (1989) pp 257-67
4. P. D. Dapkus, B. Y. Maa, Q. Chen, W. G. Jeong, and S. P. DenBaars", Atmospheric pressure atomic layer epitaxy: mechanisms and applications," Acta Polytechnica Scandinavica, 195, 39 (1990)

5. B. Y. Maa and P. D. Dapkus, "Study of Surface Reactions in Atomic Layer Epitaxy of GaAs Using Trimethylgallium by Reflectance-difference Spectroscopy and Mass Spectroscopy" *Thin Solid Film* 225, 12 (1993)
6. B. Y. Maa and P. D. Dapkus, "Reaction mechanisms of tertiarybutylarsine on GaAs(001) surfaces and its relevance to atomic layer epitaxy and chemical beam epitaxy", *J. Electron. Mater.* 20, 589 (1991)
7. B. Y. Maa and P. D. Dapkus " Reflectance difference spectroscopy of surface reactions in atomic layer epitaxy of GaAs using trimethylgallium and tertiarybutylarsine", *Appl. Phys. Letters* 58, 2261 (1991)
8. B. Y. Maa and P. D. Dapkus, "The mechanisms and kinetics of reactions of trimethylgallium on GaAs(001) surfaces and it's relevance to atomic layer epitaxy," *Proc. Mat. Res. Soc. Symp., Atomic Layer Growth and Processing*, 222, 25 (1991).

3.0 Vacuum ALE Studies

In these studies, a custom built UHV system was built to perform VALE studies on full wafers. A gas source manifold that permitted the pulsed introduction of the reactants into the chamber as a molecular beam fed the chamber. These beams impinged on the wafer which was surrounded by a leaky quartz vessel that permitted the local pressure around the wafer to rise to the 10^{-3} Torr range during the pulsed dose of reactants but which could be rapidly evacuated after the pulse was terminated. In this way the reactants were afforded the opportunity to interact with the wafer surface more than once to increase the reactant utilization.

A complete study of the growth of GaAs and related compounds using this system was completed and resulted in a publication and a PhD dissertation by Ming Yung Jow. The conclusion of this study was that it was indeed possible to achieve uniform layer by layer ALE growth of GaAs using this technique over a certain temperature range and that the surface reaction mechanisms resulted in truly atomic layer saturation and growth. It was found that only trimethylgallium (TMGa) was suitable as a saturating Ga source and that tertiarybutylarsine (TBAs) was preferable to arsine as the As source because of its lower decomposition temperature. In spite of these positive findings, a serious difficulty arose in the general use of this approach for growth of compound semiconductors. The growth rate was limited by the cycle time needed to reduce the background carrier concentration to an acceptable level. Methyl radicals on the surface can result in the incorporation of large concentrations of C in the crystal unless they are removed by exposure to TBAs. To achieve a background carrier concentration below as 10^{19} cm^{-3} required exposure times and exposure levels of TBAs that were impractical for growth of GaAs. Triethylgallium was explored for VALE growth and found to produce low carrier concentration but poor monolayer growth characteristics. The details of these studies are presented in the following two appendices to this report:

Appendix 2

Ming Y. Jow, Ben Y. Maa, Takashi Morishita and P. D. Dapkus, "Growth of GaAs by Vacuum Atomic Layer Epitaxy Using Tertiarybutylarsine" *J. Electron. Materials* 24, 25 - 29 (1994).

Appendix 3

Ming Yung Jow, "Vacuum atomic layer epitaxy of GaAs using various metalorganic precursors," Ph. D. Dissertation, University of Southern California, 1994.

4.0 Selective Area Growth Using Laser Assisted ALE and Vacuum Atomic Layer Epitaxy

Selective area growth of GaAs under laser stimulation had been studied by USC for several years prior to the start of this program. During the early stages of the program some of the final work on laser assisted growth was completed. This study emphasized the improvement of materials quality by the use of triethylgallium and tertiarybutylarsine as precursor. This work is summarized in Appendices 4 and 5:

Appendix 4

Q. Chen, C. A. Beyler, P. D. Dapkus, J. J. Alwan, and J. J. Coleman, "Use of tertiarybutylarsine in atomic layer epitaxy and laser assisted atomic layer epitaxy of device quality GaAs," *Appl. Phys. Lett.* **60**, 2418 (1992).

Appendix 5

Q. Chen and P. D. Dapkus, "Growth and characterization of device quality GaAs produced by laser assisted atomic layer epitaxy using triethylgallium," *Thin Solid Films* **225**, 115 (1993).

Selective area growth of GaAs on dielectric patterned substrates using vacuum atomic layer epitaxy was also studied. The purpose of this work was to determine the quality and morphology of GaAs grown in patterns on substrates. This work is reported in the Appendix 6:

Appendix 6

M.Y. Jow, M.H. MacDougal, N.C. Frateschi, B.Y. Maa, P.D. Dapkus, and T. Morishita, "Vacuum Atomic Layer Epitaxy - An Approach to Controlled Selective Area Epitaxy," Proc. of the Symposium on Large Area Wafer Growth and Processing for Electronic and Photonic Devices and Twentieth State-of-the-Art Program on Compound Semiconductors (SOTAPOLCS XX), Ed. by D.N. Buckley, S.A. Ringel and F. Ren, pp. 230-239, proceedings vol. 94-18, The Electrochemical Society (1995).

Finally, vacuum atomic layer epitaxy was used as a means to passivate the surfaces of laser facets formed by dry etching. It was found that (100) etched facets could be passivated to produce laser performance comparable to cleaved facets. This work is described in Appendix 7:

Appendix 7

N. C. Frateschi, M. Y. Jow, P. D. Dapkus, and A. F. J. Levi, "InGaAs/GaAs quantum well lasers with dry etched mirror passivated by vacuum atomic layer epitaxy," *Appl. Phys. Lett.* **65**, 1748 (1994).

5.0 Summary and Future Directions

Atomic layer epitaxy was studied as a potential technology to enable optoelectronic integration. In particular, vacuum atomic layer epitaxy was developed as a means to achieve large area uniform epitaxial growth. This requirement was satisfied.

Unfortunately, the residual background carrier concentration that attended the monolayer per cycle growth mode was too high to be of use in most device applications except as Ohmic contacts and surface passivation layers. The high doping is related to the use of TMGa as the Ga source, which, in turn, is required for the monolayer growth mode. Triethylgallium produces high quality material with low background concentrations of C,

but does not produce saturated monolayer per exposure cycle growth. Should a precursor be developed that can satisfy both of these criteria simultaneously, ALE and laser assisted ALE have been shown to be useful approaches to area selective growth of uniform layers. No further research in the vane of the studies performed here is warranted until such a precursor is found.

Appendix 1

B. Y. Maa, P. D. Dapkus, P. Chen, and A. Madhukar, "A Real-Time Study of the Reflection High Energy Electron Diffraction Specular Beam Intensity During Atomic Layer Epitaxy of GaAs" Appl. Phys. Lett. 62, 2551 (1993)

Real-time study of the reflection high energy electron diffraction specular beam intensity during atomic layer epitaxy of GaAs

B. Y. Maa and P. D. Dapkus

Department of Electrical Engineering and the Center for Photonic Technology, University of Southern California, Los Angeles, California 90089

P. Chen and A. Madhukar

Department of Materials Science and Engineering and the Center for Photonic Technology, University of Southern California, Los Angeles, California 90089

(Received 7 January 1993; accepted for publication 17 February 1993)

The intensity behavior of the specular beam in reflection high energy electron diffraction (RHEED) from GaAs (001) is investigated during the exposure of trimethylgallium (TMGa) and tertiarybutylarsine (TBAs) in atomic layer epitaxy (ALE) of GaAs. The temporal behavior of RHEED specular beam intensity corresponding to the transient behavior of the reflectance difference (RD) at 632.8 nm reveals several phases of surface reactions in ALE using TMGa and TBAs. RHEED specular beam intensity relaxation after short exposure to TMGa shows a longer time constant than that observed by RD, suggesting that it is the result of the overall changes in the surface atomic arrangements and morphology whereas the latter is responding to the formation/annihilation of Ga dimers.

The exploitation of atomic layer epitaxy (ALE) of III-V semiconductors has generated considerable interest due to its promise of crystal growth of layers with uniform thickness and control at the atomic level.^{1,2} Since ALE is an inherently surface controlled growth process, understanding the surface reactions involved is becoming increasingly important for optimizing the reactor design and growth conditions. Several surface science approaches have been taken to examine the chemisorption and decomposition of trimethylgallium (TMGa) in ALE of GaAs.³⁻⁸ Recently, we applied *in situ* real-time reflectance difference (RD) and transient sampled beam mass spectroscopy to investigate surface reactions and reaction rates in ALE of GaAs using TMGa and tertiarybutylarsine (TBAs) as gallium and arsenic sources, respectively.⁵⁻⁷ Combined with a mass spectroscopy study⁷ that identifies the desorbing chemical species and their time dependent behavior, several phases are unambiguously revealed in the self-limiting ALE growth of GaAs. A reaction kinetics model is thus established to account for the various phases in ALE of GaAs.

It is known that the RHEED specular beam intensity is sensitive to the surface and diffraction conditions.⁹⁻¹² Its variation contains rich information on both the surface atomic structure and morphology and hence is useful for monitoring the surface kinetics processes during growth. It should be noted that in molecular beam epitaxy (MBE) the RHEED specular beam intensity variation may be correlated directly to the surface morphology if the surface phase condition and RHEED diffraction condition are kept constant.⁹⁻¹² In ALE, by contrast, the influence of surface atomic structure must be considered since the growth surface undergoes different surface phase conditions and exhibits various surface reconstructions related to surface atomic structure.¹³ Recognizing the distinctly important impact of surface reconstructions on the surface reaction kinetics, we used RHEED previously to identify the surface reconstructions before and after ALE processes.^{5-7,14,15} Recently, Deparis *et al.* attempted to corre-

late the RHEED beam intensity with the surface stoichiometry and reconstruction by depositing Ga on GaAs As-stabilized surfaces from an elemental Ga source (MBE type).¹³ In this letter, we report the use of real-time RHEED specular beam intensity measurement to monitor the surface reaction processes in ALE of GaAs using TMGa and TBAs. The reflectance difference (RD) transient is simultaneously measured. Different time constants for the intensity variation observed in these two measurements indicate that while RD is responding to the evolution of Ga dimers, RHEED specular beam intensity is the result of the overall changes in the surface atomic arrangements and morphology.

The experiments were performed in an UHV system described previously.⁷ The samples, 10×12 mm² n-type GaAs (001) substrates, were degreased and etched in H₂SO₄:H₂O₂:H₂O=5:1:1 for about 2 min. After the sample was loaded into the chamber, it was degassed at 300 °C for 30 min and deoxidized at 610 °C where a distinct RHEED 2×4 As-stabilized pattern was observed, then a layer of GaAs~100 Å-thick was deposited by ALE. The TMGa and TBAs pressures used in the experiments were 3×10⁻⁶ and 3×10⁻⁵ Torr, respectively. For RHEED measurements, a primary electron beam of 8 keV was incident on the substrate at a grazing angle of ~1.1° along the [110] azimuth. The specular beam intensity was measured by a photodetector located in front of a TV monitor where the RHEED pattern imaged with a CCD camera was displayed. For RD measurements, the 6328 Å line of a He-Ne laser was used as the light source. At this wavelength, the RD signal monitors the formation and/or annihilation of surface Ga-Ga dimers.¹⁶ One concern in the study of surface reactions of TMGa and TBAs by RHEED is the possibility of artifacts introduced by the high energy electrons. RD transients were therefore scanned in areas exposed and unexposed to electrons and little difference in the RD response was found. We conclude that, under our experimental conditions, these high energy electrons have little influence on the surface processes.

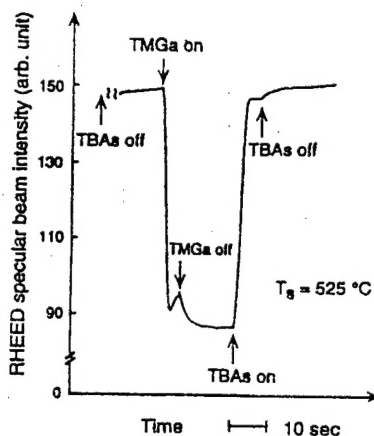


FIG. 1. The temporal RHEED specular beam intensity along [110]. A sequence of 5 s TMGa exposures followed by 15 s pumping and 7 s TBAs exposures is carried out at 525 °C.

Figure 1 shows the variation of the RHEED specular beam intensity at a substrate temperature of 525 °C with a sequence of 5 s TMGa exposure, 15 s pumping, and finally 7 s TBAs exposure. Upon TMGa exposure, the RHEED intensity decreased rapidly for 3 s and then slowly rebounded. After the termination of the TMGa exposure, the RHEED intensity gradually relaxes and saturates at a lower level. At this point the RHEED pattern exhibits a 4×6 reconstruction characteristic of a Ga-stabilized surface.¹⁷ Upon commencement of the TBAs flow, the RHEED intensity increases rapidly and saturates at an exposure of 4 s. After termination of the TBAs flow, the intensity increases again and finally saturates to the level of the starting surface. The RHEED also reverts to the As-stabilized 2×4 pattern.

In Fig. 2 are shown the temporal variations of RHEED specular beam intensity at three different substrate temperatures (T_s). The surface, initially a 2×4 reconstruction, is then exposed to four consecutive 1 s TMGa exposures with 15 s interruption between each exposure. Intensity relaxations are observed that are quite different for each different exposure stage and each T_s . During the interruption after the first exposure, more intensity relaxation is seen at 550 °C [Fig. 2(c)] than at 500 °C [Fig. 2(a)] and, at the end of the interruption, the RHEED pattern changes to a threefold for 550 °C while it remains twofold for 500 °C. By contrast, during the interruption after the second exposure, less intensity relaxation is seen at 550 °C than at 500 °C and, after the interruption, RHEED shows threefold pattern at all three T_s . Also, during the second exposure, the intensity shows small rebounds at 525 and 550 °C while it monotonically decreases at 500 °C. In the third and fourth exposures, the intensity variations at all T_s exhibit rebounds, with the lower the T_s , showing a larger rebound.

Figure 3 show the temporal variation of RD and RHEED specular beam intensity measured simultaneously at 500 °C. Again, four consecutive 1 s TMGa exposures were applied to the initial 2×4 As-stabilized surface with a 15 s interruption in between. The RHEED intensity relax-

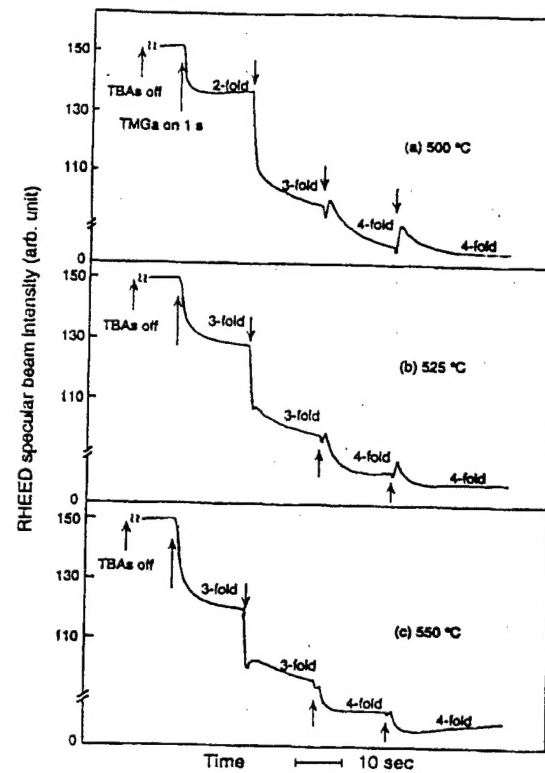


FIG. 2. The temporal RHEED specular beam intensity and its pattern along [110]. Four consecutive 1 s TMGa exposures were applied to the initial 2×4 As-stabilized surface with a 15 s interruption between each exposure at (a) 500, (b) 525, and (c) 550 °C. The arrows indicate the moment Ga exposure starts.

ation during interruption coincides with the RD signal increase upon the termination of TMGa exposure and the intensity rebound in RHEED intensity variation, to a dip in the RD signal.⁵⁻⁷ However, the RD signal saturates much faster than the RHEED intensity. In converting this Ga-stabilized surface to the As-stabilized surface, we carried out three consecutive 2 s TBAs exposures with a 15 s interruption in between. The RD signal decreases upon each exposure and saturates at the end of second TBAs exposure. The RHEED intensity shows a similar stepwise increase with a broadened twofold and a sharp narrow twofold pattern after the first and second exposure, respectively.

The observed intensity decrease when a 2×4 As-rich surface is exposed to TMGa and converted to a Ga-rich surface (as shown in Fig. 1) is similar to that observed by Déparis *et al.* on an As-stabilized surface with increasing Ga deposition in MBE.¹³ In both cases the surface goes through a reconstruction transition from 2×4 through 3×1 to 4×6 , indicating the common relation of the RHEED specular beam intensity and the surface atomic structure. A major difference in the temporal RHEED intensity using TMGa as the Ga source is the occurrence of the rebound beyond a certain TMGa exposure and a long time constant for relaxation after the TMGa exposure, indicating that surface reaction kinetic processes occurring in ALE is different from those in MBE.

As discussed in our proposed model of reaction kinet-

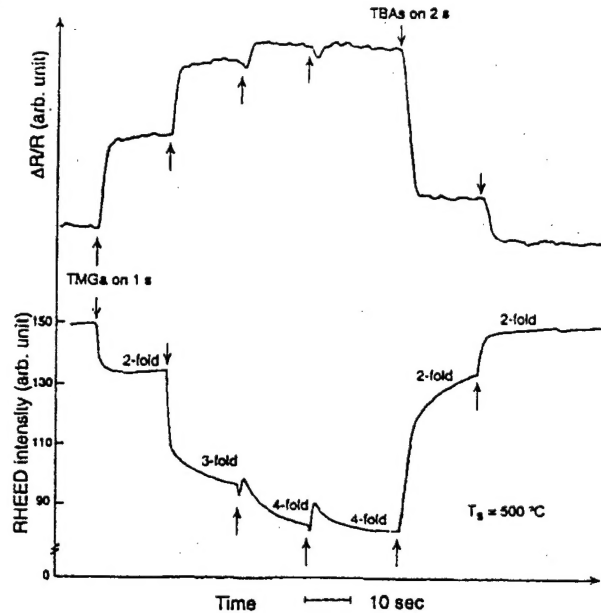


FIG. 3. RD (upper) transient and RHEED (lower) specular beam intensity variation measured simultaneously for a sequence of TMGa and TBAs exposures at 500 °C. For TMGa, four consecutive 1 s exposures with each 15 s interruption in between are applied and, for TBAs, three consecutive 2 s exposures with each 15 s interruption in between. The arrows indicate the starting of the exposures.

ics in ALE,⁵⁻⁷ TMGa is at first decomposed into GaCH₃ and two CH₃ methyl radicals. Further decomposition of GaCH₃ results in gallium atoms which tend to form Ga-Ga dimer bonds and become incorporated into GaAs. The released CH₃ methyl radicals could desorb from the surface, or attach to surface As dimers or newly formed gallium dimers by breaking the corresponding dimer bonds. After TMGa exposure is terminated, the attached CH₃ methyl radicals desorb from the surface and the Ga dimer bonds are recovered as revealed by RD measurement. These reactions are dependent on the surface reconstruction/stoichiometry and substrate temperatures. Thus, the stronger relaxation of RHEED specular beam intensity and the quicker change of the surface reconstruction to threefold at 550 °C [Fig. 2(c)] during the interruption after the surface exposure indicates that, on an initial As-stabilized 2×4 surface, the chemisorption and decomposition of TMGa proceeds faster at higher T_s . However, the relaxation after the second TMGa exposure becomes weaker at high T_s . Also, a small rebound appears at 550 °C [Fig. 2(c)] while intensity decreases monotonically at 500 °C [Fig. 2(a)]. These imply that the different surface reconstruction/stoichiometry induced by the first TMGa exposure at different T_s results in distinct reaction kinetics for impinging TMGa. The correspondence of the RHEED intensity rebound to the dip in the RD transient is shown in Fig. 3. The dip in RD signal is related to the breakdown of Ga dimer bonds due to the attachment of CH₃ radicals which becomes increasingly important as the surface becomes Ga-rich.⁵⁻⁷ Thus, the intensity rebound behavior observed at different T_s in Fig. 2 might be related to the

temperature dependence of these reactions: the weaker rebound at 550 °C indicating stronger desorption of GaCH₃ and CH₃ at high T_s , and hence the surface being less disturbed. This interpretation of the observed RHEED intensity variation is plausible and shows the usefulness of RHEED intensity in monitoring the surface reaction kinetics processes.

An exponential fit to the RHEED intensity relaxation after 4×6 Ga-rich surfaces were exposed to TMGa gives a time constant of 4.6, 1.7, and 1.4 s at 500, 525, and 550 °C, respectively. These recovery times are longer than those obtained from RD study which gives 0.9, 0.4, 0.2 s at 500, 525, and 550 °C, respectively. While the RD transient measured at He-Ne laser wavelength (632.8 nm) is sensitive to the formation/annihilation of Ga dimers, the RHEED intensity variation is the result of the overall changes in the surface atomic structure and morphology. The slower relaxation of RHEED intensity in contrast to the RD signal variation indicates that although Ga dimers are already re-established the changes on the surface, either the atomic structure or the morphology, or both, are not completed. The intensity variation behavior during the TBAs exposure is quite different from that during TMGa exposure and will be discussed elsewhere.

In summary, the study of RHEED specular beam intensity behavior on GaAs (001) in ALE of GaAs using TMGa and TBAs shows the strong dependence of intensity variation on the surface reaction kinetic processes and its usefulness in monitoring the actual growth. The difference of intensity recovery constants in RHEED intensity relaxation and RD signal transient shows that the surface recovery processes probed by these two techniques are different.

- ¹S. P. DenBaars, C. A. Beyler, A. Hariz, and P. D. Dapkus, *Appl. Phys. Lett.* **51**, 1530 (1987).
- ²K. Mori, M. Yoshida, A. Usui, and H. Terao, *Appl. Phys. Lett.* **52**, 27 (1988).
- ³U. Memmert and M. Yu, *Appl. Phys. Lett.* **56**, 1883 (1990).
- ⁴J. R. Creighton, *Surf. Sci.* **234**, 287 (1990).
- ⁵B. Y. Maa and P. D. Dapkus, *Appl. Phys. Lett.* **58**, 2261 (1991).
- ⁶B. Y. Maa and P. D. Dapkus, *Mater. Res. Soc. Symp. Proc.* **222**, 25 (1991).
- ⁷B. Y. Maa and P. D. Dapkus, *Thin Solid Films* **225**, 12 (1993).
- ⁸T. H. Chiu, J. E. Cunningham, A. Robertson, Jr., and D. L. Malm, *J. Cryst. Growth* **105**, 155 (1990).
- ⁹P. Chen, J. Y. Kim, A. Madhukar, and N. M. Cho, *J. Vac. Sci. Technol. B* **4**, 890 (1986).
- ¹⁰P. Chen, T. C. Lee, N. M. Cho, and A. Madhukar, *Proc. SPIE* **796**, 139 (1987); and references therein.
- ¹¹G. S. Petrich, P. R. Pukite, A. M. Wowchak, G. J. Whaley, P. I. Cohen, and A. S. Arrott, *J. Cryst. Growth* **95**, 23 (1989); and references therein.
- ¹²T. Shitara, D. D. Vvedensky, M. R. Wilby, J. Zhang, J. H. Neave, and B. A. Joyce, *Appl. Phys. Lett.* **60**, 1504 (1992); and references therein.
- ¹³C. Deparis and J. Massies, *J. Cryst. Growth* **108**, 157 (1991); and references therein.
- ¹⁴B. Y. Maa and P. D. Dapkus, *J. Electron. Mater.* **19**, 289 (1990).
- ¹⁵B. Y. Maa and P. D. Dapkus, *J. Cryst. Growth* **101**, 23 (1990).
- ¹⁶D. E. Aspnes, J. P. Harbison, A. A. Studna, and L. T. Florez, *J. Vac. Sci. Technol. A* **6**, 1327 (1988); D. E. Aspnes, Y. C. Chang, A. A. Studna, L. T. Florez, H. H. Farrell, and J. P. Harbison, *Phys. Rev. Lett.* **64**, 192 (1990).
- ¹⁷P. Drathen, W. Ranke, and K. Jacobi, *Surf. Sci.* **77**, L162 (1978).

Appendix 2

Ming Y. Jow, Ben Y. Maa, Takashi Morishita and P. D. Dapkus, "Growth of GaAs by Vacuum Atomic Layer Epitaxy Using Tertiarybutylarsine" J. Electron. Materials 24, 25-29 (1994)

Growth of GaAs by Vacuum Atomic Layer Epitaxy Using Tertiarybutylarsine

MING Y. JOW, BANG Y. MAA, TAKASHI MORISHITA,* and
P. DANIEL DAPKUS

Department of Materials Science and Electrical Engineering, University of
Southern California, Los Angeles, CA 90089

We report the results of GaAs grown by vacuum atomic layer epitaxy using trimethylgallium (TMGa) and tertiarybutylarsine (TBAs) as the group III and V sources. The growth rate saturates at one monolayer per cycle for a wide range of growth parameters. The temperature window for monolayer growth is as wide as 70°C. All the films are p-type with the carrier concentration depending on the exposure conditions of TMGa and TBAs.

Key words: Atomic layer epitaxy, GaAs, tertiarybutylarsine

INTRODUCTION

Atomic layer epitaxy (ALE) is an attractive crystal growth technique in which self-limited decomposition of the reactants on substrate surfaces results in a strong saturation of the growth rate. As a result, the material is grown digitally, atomic layer by atomic layer. This property enables ALE to control the layer thickness and impurity doping at the atomic level.¹⁻¹⁰ Atomic layer epitaxy has also been used to demonstrate selective area and side wall growth which are important for the integration of optical and electronic devices in optoelectronic integrated circuits (OEICs).⁴⁻⁶ Although ALE technology is in infancy, it has already shown great potential for future applications.

When the first demonstrations of saturated monolayer growth of GaAs were performed under UHV

conditions, the poor saturation, high carrier concentration, and long cycle times observed led to more extensive ALE studies at near atmospheric pressure.²⁻⁸ To investigate the cause of these initial UHV limitations and to develop a suitable ALE process, we have been motivated to re-examine a UHV based ALE process. Since the self-limiting mechanism of ALE is a surface reaction process, the suppression of gas phase decomposition of the reactants is a critical issue for successful ALE growth. Vacuum atomic layer epitaxy (VALE) avoids gas phase reaction and is expected to have wider ALE growth window and potentially better film quality.

In this paper, we present a VALE reactor design and results on growth rate and background impurity incorporation observed in the VALE growth of GaAs using trimethylgallium (TMGa) and tertiarybutylarsine (TBAs). We demonstrate saturated monolayer growth over a wide range of conditions and also demonstrate the dependence of carrier concentration on these conditions.

*Central Laboratory, ASAHI Chemical Industry Co. Ltd., 2-1 Samajima, Fuji City, Shizuoka, 416 Japan.
(Received October 12, 1993; revised September 16, 1994)

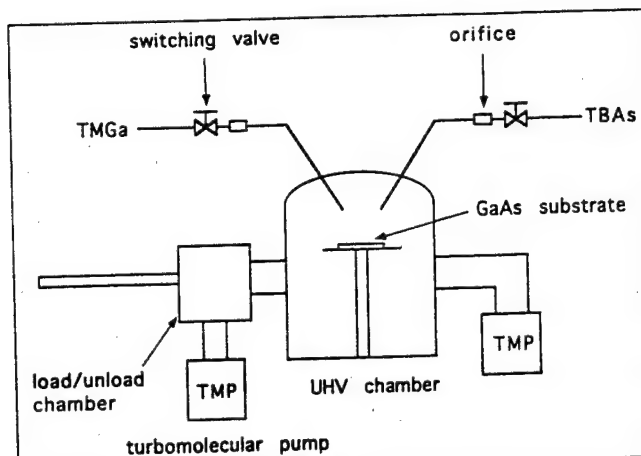
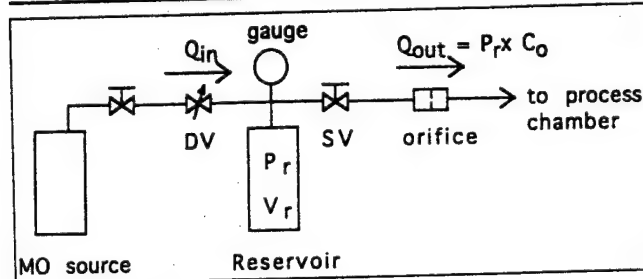
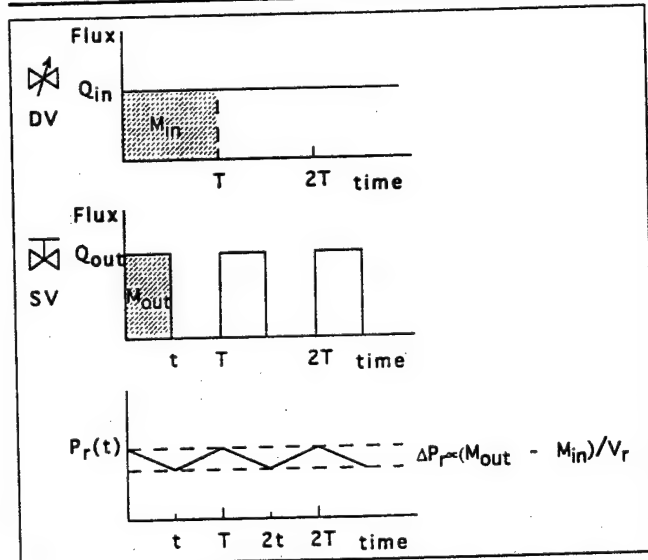


Fig. 1. The schematic of VALE reactor.

Fig. 2. The gas handling system. DV is the dosing valve; SV is the switching valve; C_0 is the conductance of the orifice, and P_r is the pressure in the reservoir.Fig. 3. The illustration of the operating principle of the gas handling system. The upper two graphs show the operation of the dosing valve and the switching valve. The bottom one shows the variation of the pressure, P_r , during the growth.

EXPERIMENTAL

The VALE reactor consists of a UHV process chamber, a sample entry chamber, and gas handling systems. Both chambers are pumped with turbomolecular pumps and show base pressures of 10^{-9} and 10^{-7} Torr, respectively. Figure 1 shows the schematic drawing of the VALE reactor. The pressure during growth is between 10^{-5} to 10^{-4} Torr depending on the exposure

level of the sources. The substrates are indium-bonded to a molybdenum block and loaded through the sample entry chamber into the process chamber by a transfer rod. The substrate is heated by a boron nitride encapsulated graphite heater and the temperature is monitored with a calibrated pyrometer. On the top of the UHV chamber, source injectors are connected to the gas handling system as shown in Fig. 2. The gas handling system needs no carrier gases and is not a "vent/run" design. Without the carrier gases, the gas manifold is simplified and easily maintained. The usage of the sources is only 5 to 50% of the usage of a normal vent/run system.

The exposure level or flow rate in the experiment is controlled by the product of the conductance of the orifice and the pressure in the reservoir; the exposure time is the open duration of the switching valves. The function of the reservoir is to reduce the pressure variation at the orifice and provide a nearly constant flow during the exposure. The dosing valves control the flow of the source materials into the reservoir.

The operating principle of the gas handling system is illustrated in Fig. 3. During the ALE growth, the switching valve is switched ON and OFF in a preset sequence to inject the source into the process chamber, but the dosing valve is continuously open and manually adjusted to maintain a constant input equal to the average output flow. Although the reservoir's pressure drops while the switching valve is open, it charges to the original value at the end of each cycle, and the exposure level is the same for the next exposure. In our design, the pressure variation is maintained at 5% during the exposure by using a large volume (~2 liter) reservoir. This is acceptable for ALE growth.

The source materials for gallium atoms and arsenic atoms are trimethylgallium and tertiarybutylarsine. The substrates are either undoped GaAs (100) or n^+ GaAs (100) with 5000\AA $\text{Al}_{0.5}\text{Ga}_{0.5}\text{As}$ and 100\AA GaAs cap layer on the top. The grown GaAs sample is patterned and selectively etched to create a step for thickness (growth rate) measurement. The carrier concentration was measured by Hall effect and electrochemical C-V profiling.

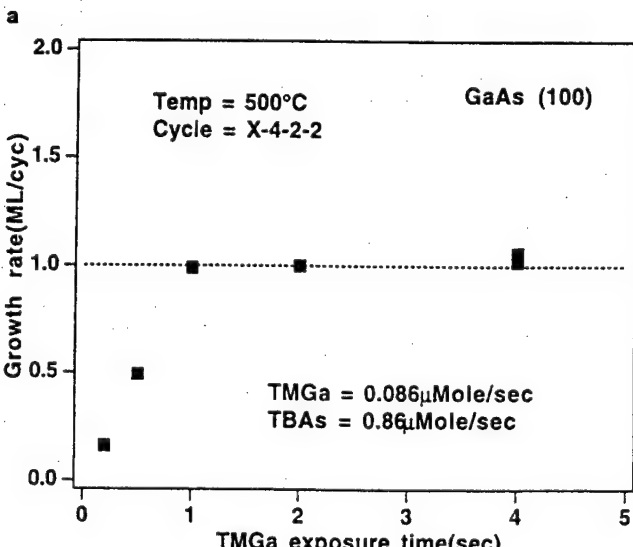
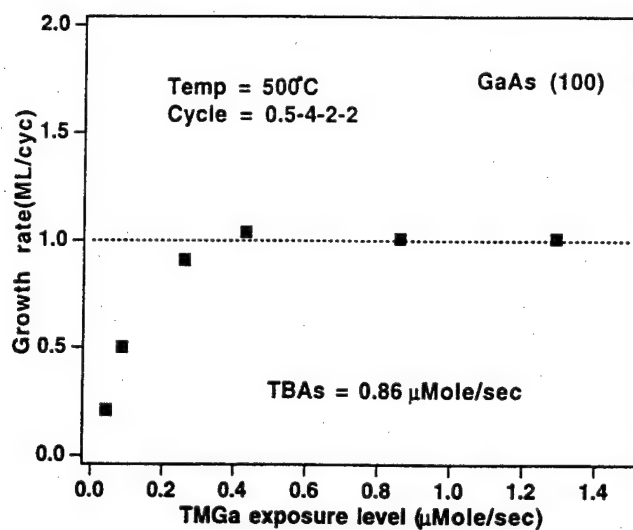
RESULTS AND DISCUSSION

Figures 4a and 4b show strong saturation of the growth rate with respect to the TMGa exposure level and exposure time. Each cycle includes the following sequence: TMGa exposure, evacuation, TBAs exposure and evacuation. For example, "Cycle = 0.5-4-2-2" means 0.5 s TMGa exposure, 4 s pumping, 2 s TBAs exposure, and 2 s pumping. At a constant TMGa exposure level of $0.086 \mu\text{Mole/s}$, the growth rate increases with increasing exposure time up to one second exposure, after which the growth rate is saturated at one monolayer per cycle for times up to four seconds. The distinct saturation is also shown with the variation of the TMGa exposure level. These data indicate a clear self-limiting decomposition of TMGa and also show that the control of the growth thickness

at the atomic scale can be achieved in VALE. Possible mechanisms for the saturated growth have been discussed in another paper.¹¹ The strong saturation observed here is in marked contrast to the work of Nishizawa et al. which showed a rather weak saturation of the growth rate.¹

The surface morphology of VALE grown GaAs is mirror-like and no gallium droplets are found even for long TMGa exposure times or high exposure levels. These observations imply that homogeneous decomposition of TMGa is nonexistent, and that surface reactions are the dominant processes in VALE. The short exposure time of TMGa is the result of fast switching of the gas handling system. This capability allows the VALE to achieve higher growth rates than other high vacuum ALE systems.^{1,9,10} Growth rates as high as 1 $\mu\text{m}/\text{h}$ can be achieved with shorter exposure and evacuation times by increasing the substrate temperature and the reactant exposure level.

The effect of TBAs exposure on growth rate is

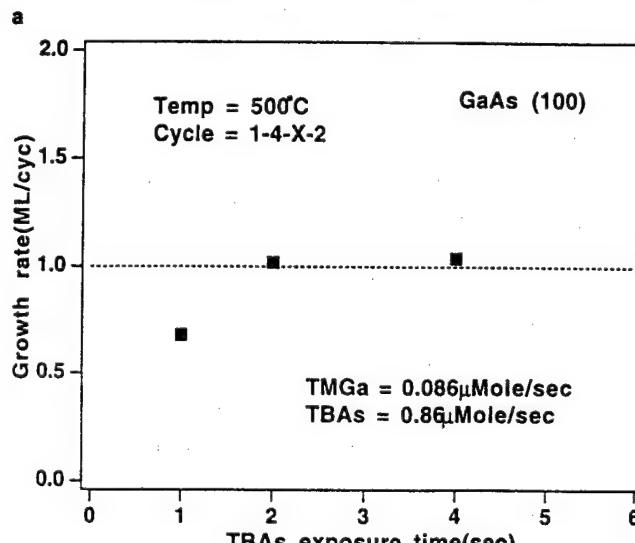
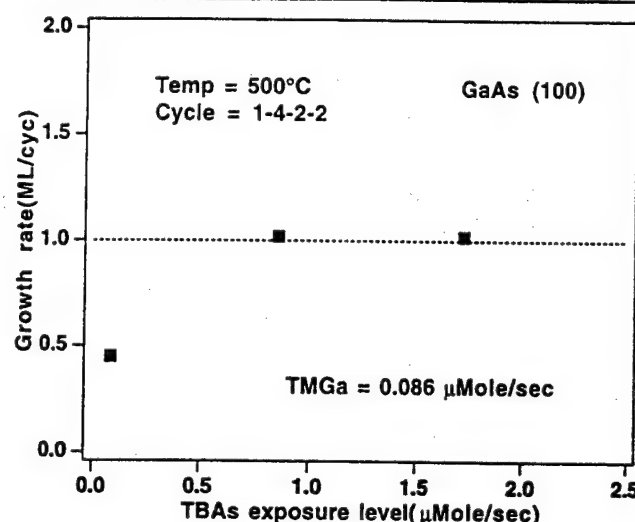


b

Fig. 4. The dependence of the growth rate on (a) TMGa exposure level and (b) exposure time.

shown in Figs. 5a and 5b. These figures also show distinct self-limiting decomposition of TBAs in terms of the exposure level and exposure time. The TBAs exposure level for monolayer growth is ten times of that of TMGa exposure, which implies that the reaction of TBAs on Ga-rich surfaces is slower than TMGa on As-rich surfaces. The mechanism of the self-limiting decomposition of TBAs is probably due to the low sticking coefficient of As on As-rich surfaces.¹² The required exposure time of TBAs for monolayer growth is much shorter than the reported value for AsH_3 under similar conditions.¹ Besides being safer to handle than AsH_3 , TBAs is also more efficient than AsH_3 when used in VALE as demonstrated by the shorter exposure time.

Figure 6 shows the saturation of the growth rate at different temperatures. These data indicate that increasing substrate temperature only enhances the growth in the unsaturated growth regime. Based on our previous work, this results from an increased TMGa decomposition rate on GaAs surfaces at higher



b

Fig. 5. The dependence of the growth rate on (a) TBAs exposure level and (b) exposure time.

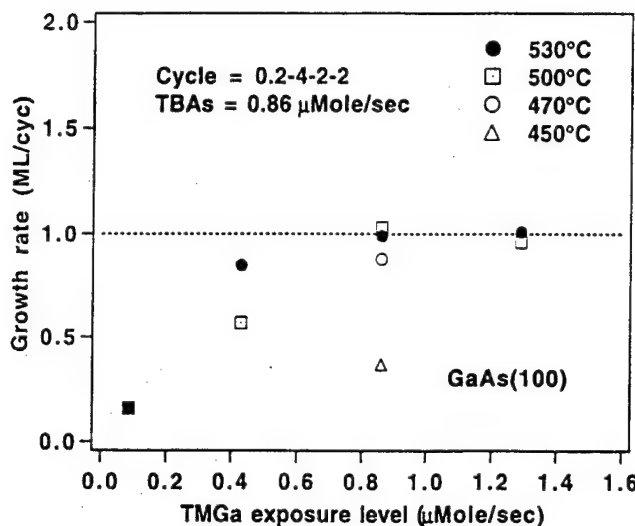


Fig. 6. The dependence of the growth rate on TMGa exposure level at different temperatures.

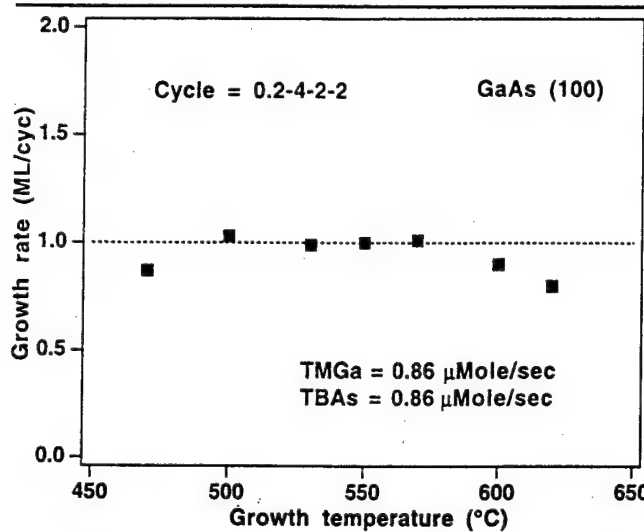


Fig. 7. The dependence of the growth rate on substrate temperature.

temperatures.¹¹ Once the growth rate reaches one monolayer per cycle, the self-limiting mechanism takes place, and the growth rate no longer increases.

The temperature window of the monolayer growth is also an important issue for ALE growth. Figure 7 shows the widest temperature window reported in high vacuum ALE growth. The growth rate is less than monolayer per cycle when the temperature is less than 500°C or higher than 570°C. The decrease of the growth rate at low temperature may be due to the slow decomposition rate of TMGa molecules and, at high temperatures, to the desorption of As atoms from the surface.

All of the grown films are p-type, and the carrier concentration varies from 10^{17} to 10^{19} cm^{-3} . The likely impurity is carbon originating from TMGa exposure. Carbon incorporation has been reported in both ALE and CBE growth.^{1,13,14} The detailed mechanism is still under investigation, but several groups have suggested that the methyl radicals, supplied by decomposed TMGa on the GaAs surface, may play an important role in the carbon incorporation.^{15,16}

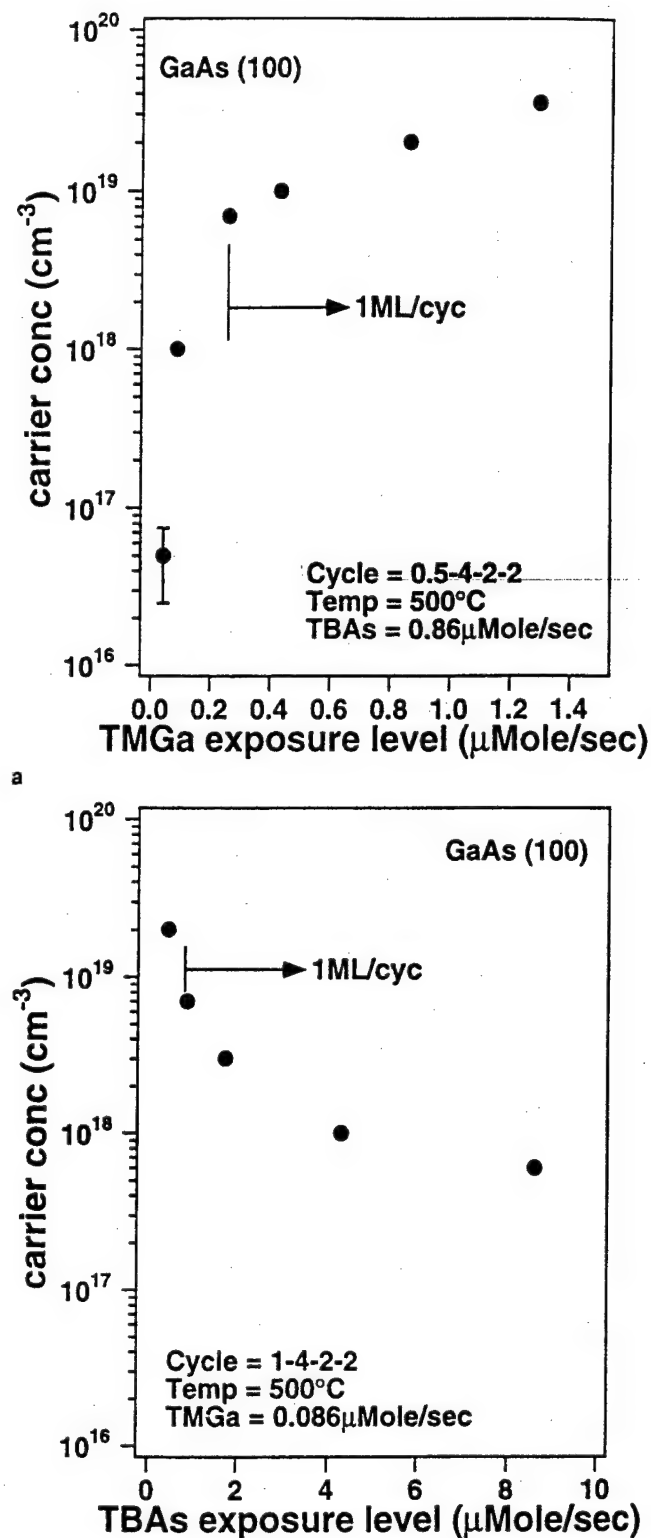


Fig. 8. The dependence of the carrier concentration on (a) TMGa and (b) TBAs exposure level.

In VALE growth, the hole concentration varies with the growth conditions, especially with TMGa exposure. Figures 8a and 8b show the dependence of the hole carrier concentration on TMGa and TBAs exposure level. In Fig. 8a, the hole concentration saturates when the TMGa exposure level is more than

enough for monolayer growth. However, for less than monolayer growth, the hole concentration decreases dramatically as the TMGa exposure level decreases. These two different behaviors indicate that the carbon incorporation is related to the population of carbon species on the GaAs surface during TMGa exposure. For TBAs, the behavior is opposite. As TBAs exposure increases, the hole concentration decreases. This observation indicates that TBAs helps reduce the carbon incorporation presumably by transporting H containing radicals that can react with the methyl radicals to produce volatile species. The growth of the lowest hole concentration samples under monolayer growth conditions, $6 \times 10^{17} \text{ cm}^{-3}$, is achieved by using small TMGa exposure and large TBAs exposure.

Background As species are always present during VALE growth. We believe that the species are As_2 or As_4 , which come from the deposits near the heater assembly. The background As species hit the substrate surface continuously and can be considered as an unintentional As source in our chamber. Since the sticking coefficient of As_2 or As_4 on As-rich surface is close to zero, there is no reaction during the TBAs exposure cycle. However, during the TMGa exposure cycle, the background As species can react with TMGa and cause more than monolayer growth. We find that the ALE window becomes narrower after more and more growths. Figure 9 shows the loss of the saturation of the growth rate due to the background As incorporation. By etching the heater assembly, the growth rate reduces to one monolayer per cycle even for the four second TMGa exposure. This fact indicates that most of the As species desorbs from the heater assembly because it is hot during the growth. In our system, serious As backgrounds appear after $\sim 20 \mu\text{m}$ of GaAs growth. Of course, this will depend on the exposure conditions used in the various runs. Since the background As species, As_2 or As_4 , do not provide hydrogen atoms to remove methyl radicals on the substrate surface, they may cause the carbon species to incorporate into the films. In order to suppress the background As incorporation and study the carbon incorporation, the installation of a liquid nitrogen shroud is necessary.

CONCLUSION

GaAs growth by VALE has been studied for various growth parameters. The distinct self-limiting of the growth rate indicates the homogeneous decomposition of TMGa is suppressed successfully in VALE. A unique gas handling system has been incorporated, which enhances the utilization of the source materials significantly. Tertiarybutylarsine is a promising As source material in VALE application. The carbon incorporation problem is serious in VALE using TMGa and TBAs and the mechanism needs more investigations. The low carbon concentration films can be grown by decreasing the TMGa exposure and increas-

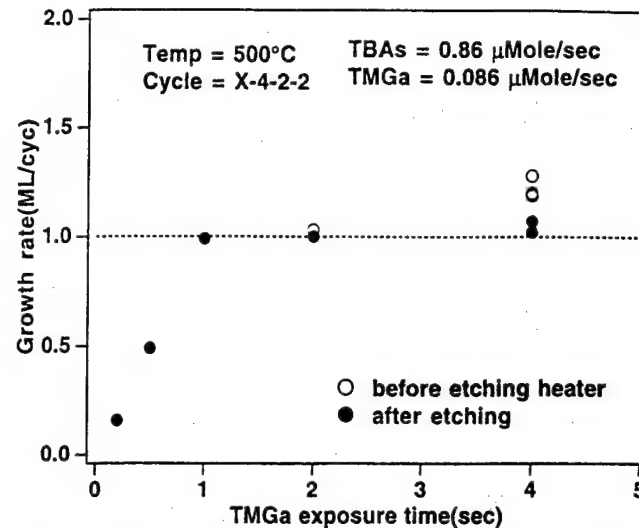


Fig. 9. The effect of the background As incorporation on ALE growth.

ing the TBAs exposure. Background As incorporation affects the ALE window and may also influence the carbon incorporation in VALE.

ACKNOWLEDGMENTS

The authors gratefully acknowledge the program support of the U.S. Office of Naval Research and National Renewable Energy Laboratory. Substrate materials provided by M.H. MacDougal are also appreciated.

REFERENCES

1. J. Nishizawa, H. Abe and T. Kurabayashi, *J. Electrochem. Soc.* 132, 1197 (1985).
2. S.P. DenBaars, P.D. Dapkus, C.A. Beyler, A. Hariz and K.M. Dzurko, *J. Cryst. Growth* 93, 195 (1988).
3. T. Takanohashi, K. Mochizuki and M. Ozeki, *Proc. Gallium Arsenide and Related Compounds, Inst. Phys. Conf. Ser.* No 106 Karuizawa, Japan, 1989, p. 39.
4. M. Ozeki, N. Ohtsuka, Y. Sakuma and K. Kodama, *J. Cryst. Growth* 107, 102 (1991).
5. A. Usui, H. Sunakawa, F.J. Stutzler and K. Ishida, *Appl. Phys. Lett.* 56, 289 (1990).
6. Y. Ide, B.T. McDermott, M. Hashemi and S.M. Bedair, *Appl. Phys. Lett.* 53, 2314 (1988).
7. E. Colas, R. Bhat and B.J. Skromme, *Appl. Phys. Lett.* 55, 2769 (1989).
8. K. Mori, M. Yoshida, A. Usui and H. Terao, *Appl. Phys. Lett.* 52, 27 (1988).
9. T.H. Chiu, J.E. Cunningham, A. Robertson, Jr. and D.L. Malm, *J. Cryst. Growth* 105, 155 (1990).
10. K. Fujii, I. Suemune, T. Kou and M. Yamanishi, *Appl. Phys. Lett.* 60, 1498 (1992).
11. B.Y. Maa and P.D. Dapkus, *Thin Solid Films* 225, 12 (1993).
12. J.Y. Tsao, T.M. Brennan and B.E. Hammons, *Appl. Phys. Lett.* 53, 288 (1988).
13. K. Mochizuki, M. Ozeki, K. Kodama and N. Ohtsuka, *J. Cryst. Growth* 93, 557 (1988).
14. M. Gotoda, S. Maruno, Y. Morishita, Y. Nomura, H. Ogata, K. Kuramoto and H. Kuroki, *J. Cryst. Growth* 100, 5 (1990).
15. L.Q. Liu, B.B. Huang, H.W. Ren and M.H. Jiang, *J. Cryst. Growth* 115, 83 (1991).
16. J.R. Creighton and B.A. Bansenauer, *J. Vac. Sci. Technol. A11*, 876 (1993).

Appendix 3

**Ming Yung Jow, "Vacuum atomic layer epitaxy of GaAs using various metalorganic precursors," Ph.D. Dissertation,
University of Southern California, 1994**

VACUUM ATOMIC LAYER EPITAXY OF GALLIUM
ARSENIDE USING VARIOUS METALORGANIC
PRECURSORS

by

Ming-Yung Jow

A Dissertation Presented to the
FACULTY OF THE GRADUATE SCHOOL
UNIVERSITY OF SOUTHERN CALIFORNIA

In Partial Fulfillment of the
Requirements for the Degree
DOCTOR OF PHILOSOPHY
(Materials Science)

December 1994

Copyright 1994 Ming-Yung Jow

UNIVERSITY OF SOUTHERN CALIFORNIA
THE GRADUATE SCHOOL
UNIVERSITY PARK
LOS ANGELES, CALIFORNIA 90007

This dissertation, written by

Ming-Yung Jow

under the direction of his Dissertation Committee, and approved by all its members, has been presented to and accepted by The Graduate School, in partial fulfillment of requirements for the degree of

DOCTOR OF PHILOSOPHY

Alice C. Parker

Dean of Graduate Studies

Date November 28, 1994

DISSERTATION COMMITTEE

P. Daniel Gaffney
Chairperson

Wm. J. Jow
William J. Steer

DEDICATION

*To my wife, Shwu-Fen,
and my parents*

ACKNOWLEDGEMENTS

I would like to express my special thanks to my thesis advisor, Dr. P. Daniel Dapkus, for his constant support and inspiration during my graduate studies at University of Southern California. I am also very appreciative of his warm and friendly personality. My sincere thanks are also owed to Dr. W. H. Steier and Dr. M. Gershenson for serving as committee members and for the excellent classes they teach.

I also appreciate the help from my colleagues and friends from other groups. I would like to thank Dr. Bang Yann Maa for introducing me to the ALE technology. I also want to thanks Michael H. MacDougal and T. Morishita for their kindly help.

I greatly thank my lovely wife, Shwu-Fen, and my parents for all the support and encouragement.

TABLE OF CONTENTS

DEDICATION	ii
ACKNOWLEDGEMENTS	iii
LIST OF FIGURES	vii
LIST OF TABLE	ix
ABSTRACT.....	x
CHAPTER 1 INTRODUCTION	1
1.1 Motivation	1
1.2 Introduction of MOCVD, MBE and CBE	4
1.3 Background Review of ALE of III-V Compounds.....	5
1.4 Thesis Organization	7
CHAPTER 2 THE VACUUM ATOMIC LAYER EPITAXY (VALE) APPROACH	9
2.1 Introduction.....	9
2.2 VALE Reactor Design and Set-up	9
2.2.1 Vacuum System	9
2.2.2 Gas Handling System.....	12
2.3 Conclusions	16
CHAPTER 3 ATOMIC LAYER EPITAXY OF GaAs BY VALE USING TMGA AND TBAS.....	18
3.1 Introduction.....	18
3.2 Experimental Procedure	19
3.3 Growth Results and Discussion	20

3.3.1 Growth Rate Study	20
3.3.2 Discussion of Self-limiting Mechanism of TMGa ..	26
3.3.3 Electrical Properties Characterization	29
3.4 Background As incorporation	34
3.5 Conclusions	38

CHAPTER 4. STUDY OF CARBON INCORPORATION IN GaAs BY VALE.....	41
4.1 Introduction.....	41
4.2 Carbon Incorporation in GaAs using TMGa	42
4.3 Reduction of Carbon Incorporation Through the Use of Alternative Ga and As Sources.....	47
4.3.1 VALE Growth with TEGa and TBAs Sources	47
4.3.2 VALE Growth with TMGa and TDMAAs Sources	52
4.3.3 VALE Growth with TEGa and TDMAAs Sources	53
4.4 Influence of Ga Atom Coverage on Carbon Incorporation using TMGa	55
4.5 Proposed Carbon Incorporation Model for VALE GaAs using TMGa	62
4.6 Conclusions	67

CHAPTER 5. SELECTIVE AREA EPITAXY(SAE) OF GaAs BY VALE.....	72
5.1 Introduction.....	72
5.2 Sample Preparation	73
5.3 Growth Results and Discussion	74
5.3.1 Selective Area Epitaxy on SiNx Masked Substrate	74

5.3.2 Selective Area Epitaxy in Trenches	80
5.3.3 Selective Area Epitaxy on Vertical Sidewalls	83
5.4 Conclusions	86

CHAPTER 6. CONCLUSIONS AND RECOMMENDATIONS FOR FUTURE WORK 89

6.1 Conclusions from this Work	89
6.2 Recommendations for Future Work	91

LIST OF FIGURES

- Fig. 2.1 Schematic drawing of the V-ALE reactor
- Fig. 2.2 Schematic of the gas manifold.
- Fig. 2.3 The operating principle of the gas handling system.
- Fig. 2.4 The pressure fluctuation of the TBAs reservoir during VALE growth with a cycle of 1-1-2-1.
- Fig. 3.1. The dependence of the growth rate on (a) TMGa exposure time and (b) exposure level.
- Fig. 3.2. The dependence of the growth rate on (a) TBAs exposure level and (b) exposure time.
- Fig. 3.3. The dependence of the growth rate on TMGa exposure level at different temperatures.
- Fig. 3.4. The dependence of the growth rate on substrate temperature.
- Fig. 3.5. The dependence of the carrier concentration on (a) TMGa level, (b) TMGa exposure time and (c) TBAs exposure level.
- Fig. 3.6 RDS transients of background As incorporation.
- Fig 3.7 RDS transients on (100) GaAs for initiation of TMGa and TBAs exposures.(after Maa, 1991)
- Fig. 3.8. The effect of the background As incorporation on ALE growth.
- Fig. 4.1 The effect of LN₂ baffle's temperature on carrier concentration.

Fig. 4.2 The effect of LN₂ baffle's temperature on growth rate.

Fig. 4.3 Dependence of the carrier concentration of GaAs grown by VALE on TEGa exposure levels.

Fig. 4.4 PL spectrum of GaAs growth with TEGa and TBAs.

Fig. 4.5 PL spectrum of GaAs growth with TMGa and TBAs.

Fig. 4.6 The linear dependence of GaAs growth rate on TEGa exposure level.

Fig. 4.7 The effect of substrate temperature on VALE growth.

Fig. 4.8 PL spectra of VALE and CBE grown GaAs films.

Fig. 4.9 Dependence of the growth rate on TEGa exposure level with TDMAAs as the As source. The exposure sequence is 0.2-1-2-1 at 470°C and 1-1-2-1 at 360°C.

Fig. 4.10 The effect of Ga atom coverage on carbon incorporation with respect to the variation of (a) TMGa exposure level and (b) TMGa exposure time.

Fig. 4.11 Arrhenius plot of the carrier concentration of layers grown on 75% Ga coverage surface at growth rate in the monolayer regime.

Fig. 4.12 Dependence of substrate temperature on carrier concentration of layers grown in monolayer regime.

Fig. 5.1 Selective area epitaxy of GaAs by VALE.

Fig. 5.2 Thickness profile of GaAs stripe after removing SiNx.

Fig. 5.3 SEM cross section of GaAs SAE using CBE mode.

Fig. 5.4 Cross section of stripes along $<01\bar{1}>$ with the openings of
(a) $3\mu\text{m}$ (b) $6.3\mu\text{m}$.

Fig. 5.5 SEM cross section of $<011>$ stripe.

Fig. 5.6 SEM view of $<010>$ strip cleaved along $<01\bar{1}>$ direction.

Fig. 5.7 SEM cross section of SAE by CBE in $<011>$ trenches.

Fig. 5.8 SEM cross section of SAE by VALE in trenches along (a)
 $<01\bar{1}>$ (b) $<011>$.

Fig. 5.9 SEM view of the $(00\bar{1})$ sidewall growth by VALE. The
sample was cleaved along $<011>$ direction.

Fig. 5.10 The surface morphologies of the regrowth on (a) $(00\bar{1})$ (b)
 (011) ECR etched mirrors.

LIST OF TABLES

Table 1. Summary of the facet formation of different direction of
stripes.

ABSTRACT

Atomic layer epitaxy is a promising technology to meet the challenges of crystal growth for the application to optoelectronic devices. The approach of vacuum atomic layer epitaxy (VALE) has the potential for a wider window of growth parameters to achieve saturated monolayer growth owing to the suppression of gas phase decomposition of the reactants under the high vacuum conditions. High quality GaAs grown by VALE is also expected.

In this work, GaAs grown by VALE using various metalorganic precursors is demonstrated. The Ga sources are trimethylgallium (TMGa) and triethylgallium (TEGa); the As sources are tertiarybutylarsine (TBAs) and trisdimethylaminoarsine (TDMAAs). Through the growth of GaAs with different combinations of Ga and As sources, we study the chemistry of the ALE growth and impurity incorporation.

VALE growth of GaAs with TMGa and TBAs shows strong saturation of growth rate over wide range of growth parameters. The temperature window is from 500°C to 570°C. The grown layers show high carbon incorporation. The carbon incorporation is likely an intrinsic property of the TMGa reaction on (100) GaAs surface.

Saturation of the VALE growth rate of GaAs with TEGa and TBAs or TDMAAs is not observed. However, the material shows very low carbon incorporation and intense photoluminescence. This indicates that the ALE mechanism and carbon incorporation

is related to the surface chemistry of the reactants on (100) GaAs surfaces. The discussion of carbon incorporation and self-limiting decomposition of TMGa is presented.

Selective area epitaxy (SAE) of GaAs on silicon nitride masked substrates by VALE is also demonstrated. The SAE growth shows flat, uniform top surface morphologies with growth rates of one monolayer per cycle. The monolayer growth rate is also independent of the mask/window area ratio. The SAE growth in trenches and on vertical sidewalls is also presented in this work.

Chapter 1

Introduction

1.1 MOTIVATION

Since the invention of the first semiconductor transistor, silicon materials have dominated the semiconductor industry. Several reasons contribute to the success of the silicon technology. First, silicon is a single element material and its chemical and physical properties are simpler than compound semiconductors. Second, high quality dielectric layers, e.g. SiO_2 , are available for silicon technology. Third, the silicon device has only one epitaxial material involved, compared with the compound semiconductor devices fabricated from multilayer epitaxial structures involving different material systems. However, silicon is an indirect bandgap material with very poor luminescence properties, and has not been successfully used as a light emitting material.

In contrast, many of the compound semiconductors are direct bandgap materials, and are good candidates for the application to optoelectronic devices even though the processing technology is much more difficult than silicon. Since the optoelectronic devices always involve multilayer epitaxial structures with different material systems, the epitaxial growth of the compound semiconductors becomes the most crucial technology for making these devices[1].

Metalorganic chemical vapor deposition (MOCVD), molecular beam epitaxy (MBE) and chemical beam epitaxy (CBE) developed, in the late 1960's or 70's, have made a great impact on the preparation of epitaxial materials for optoelectronic devices. The performance of the optoelectronic devices has been improved significantly in the last two decades. However, the modern optoelectronic devices and circuits demand more complicated epitaxial structures, which are pushing the current epitaxial technologies to their limits. The major challenges of modern epitaxial growth involve the following technologies[1],

1. Selective area epitaxy
2. Absolute thickness and composition control
3. Atomic layer doping, i.e. δ -doping
4. Large area uniformity
5. High degree of reproducibility

Atomic layer epitaxy(ALE) is an attractive crystal growth technique to achieve these goals. ALE involves the sequential exposure of the substrate to reactants in which self-limited decomposition of the reactants on substrate surfaces results in a strong saturation of the growth rate at one monolayer of the compound per cycle of exposures. As a result the material is grown digitally, atomic layer by atomic layer. This property

enables ALE to control the layer thickness at the atomic scale with great uniformity on large area wafers and to effect impurity doping at the atomic level[2~6]. ALE has also been used to demonstrate selective area and side wall growth which are important for the integration of optical and electronic devices in OEIC[5,6].

When the first demonstrations of saturated monolayer growth of GaAs were performed under UHV conditions[2], the poor saturation, high carrier concentration and long cycle times observed led to more extensive ALE studies at near atmospheric pressure[3~6]. To investigate the cause of these initial UHV limitations and to develop a suitable ALE process we have been motivated to reexamine a UHV based ALE process. Since the self-limiting mechanism of ALE is a surface reaction process, the suppression of gas phase decomposition of the reactants is a critical issue for successful ALE growth. Vacuum atomic layer epitaxy(VALE) avoids gas phase reaction and is expected to have wider ALE growth window and potentially better film quality.

In this thesis, we present a VALE reactor design and results on growth rate and background impurity incorporation observed in the VALE growth of GaAs using various metalorganic reactants. We demonstrate saturated monolayer growth over a wide range of conditions and also demonstrate the dependence of carrier concentration on these conditions.

The selective area growth of GaAs by VALE also will be presented.

1.2 INTRODUCTION OF MOCVD ,MBE, AND CBE

MOCVD has been developed for more than two decades[7]. This technology has been widely accepted by the compound semiconductor industry. The capability of growing high quality materials as well as the flexibility of different material systems are the advantages of MOCVD. It shows great potential for scale up to commercial mass production applications. Several issues need to be considered for the future of the MOCVD technology. Alternative metalorganic sources for replacing the highly toxic sources, e.g. AsH₃, PH₃, are required because of the extremely high cost of the handling of the toxic waste materials and the safety concerns. Absolute thickness and composition control is demanded for the sophisticated optoelectronic devices. *In situ* growth monitoring techniques promise to achieve the critical control of crystal growth[8].

MBE has been used in many demonstrations of high quality material preparation. Excellent interface quality for the abrupt heterostructures needed in the high speed electronic devices have also been demonstrated[9]. An inherent *in situ* monitoring capability and the UHV environment make the MBE a perfect tool for studying crystal growth mechanisms on

surfaces. Near atomic layer control of the thickness by the use of these *in situ* tools enable MBE to grow quantum effect structures which are interesting for fundamental physics studies and also important for device applications. The disadvantages of MBE technology are the difficulty experienced in growing phosphorous compounds with solid sources and in scaling up the process for mass production. Recently, the development phosphorous compounds by MBE has been a very active field[10]. However, the mass production of commercial products using MBE seems more difficult to achieve.

CBE is supposed to take the advantages from both of the MOCVD and MBE, and to avoid the drawbacks of these two technologies. It shows excellent growth of InP material systems, but suffers from the serious impurity incorporation in AlGaAs growth[11]. The use of the toxic gases is also a safety problem for CBE.

1.3 BACKGROUND REVIEW OF ALE OF III-V COMPOUNDS

Nishizawa et. al. reported the first GaAs growth by ALE in 1985[2]. The saturation of the growth rate as a function of growth parameters was weak. In analyzing his approach we decided that these characteristics were due to the poor decomposition efficiency of AsH₃ in high vacuum conditions. The grown layers were heavily p-type with carrier

concentrations in the range 10^{18} cm^{-3} . Increase a AsH_3 exposure can reduce the carrier concentration.

Tischler et al. and DenBaars et al. reported the ALE growth at atmospheric pressure[3,4]. Strong saturation of the growth rate was observed. Both groups reported the growth of device quality materials and the first semiconductor laser grown by ALE was demonstrated by DenBaars[12]. The ALE material was characterized by photoluminescence, and has shown intense luminescence[13].

Low pressure ALE was reported by Ozeki et al. using a novel pulsed-jet epitaxy technology[5]. Strong saturation of growth rate over a wide range of growth parameters was observed. High quality GaAs was grown with short TMGa exposure times. The best quality GaAs showed an electron concentration of $2 \times 10^{14} \text{ cm}^{-3}$ and a mobility of $6.5 \times 10^4 \text{ cm}^2/\text{V s}$ at 77 K. The temperature window for monolayer growth was from 440°C to 560°C , which was higher than that reported with other ALE techniques.

ALE growth using hydride VPE was reported by Usui et al[6]. The strong bonding between Ga and Cl atoms contributed to the strong saturation of the growth rate, but also resulted in the slow decomposition of Ga-Cl species. Thus, it needed 40 sec. to complete one cycle and resulted in a low growth rate of $0.03 \mu\text{m}/\text{hr}$. Side wall growth of quantum wells by ALE was

achieved by hydride ALE. The growth rate on the side wall was one monolayer per cycle.

1.4 THESIS ORGANIZATION

This thesis is organized so that the next chapter describes the idea of vacuum atomic layer epitaxy and the reactor design and set-up. Chapter three provides the results of the GaAs growth using TMGa and TBAs in VALE. Chapter four discusses the carbon incorporation in GaAs grown by VALE with different metalorganic reactants. Chapter five provides the results of selective area epitaxy of GaAs by VALE. Chapter six provides future direction from this research and conclusions on the observed experimental results.

REFERENCES

- [1] I. D. Henning, *Prog. Crystal Growth and Charact.* 19, 1(1989).
- [2] J. Nishizawa, H. Abe and T. Kurabayashi, *J. Electrochem. Soc.*, 132, 1197(1985).
- [3] S. P. Denbaars, P. D. Dapkus, C. A. Beyler, A. Hariz and K. M. Dzurko, *J. Cryst. Growth* 93, 195(1988).
- [4] M. A. Tischler and S. M. Bedair, *Appl. Phys. Lett.* 48, 1961(1986).
- [5] M. Ozeki, K. Mochizuki, N. Ohtsuka and K. Kodama, *Appl. Phys. Lett.* 53, 1509(1988).
- [6] A. Usui, H. Sunakawa, F. J. Stutzler, and K. Ishida, *Appl. Phys. Lett.* 56, 289(1990).
- [7] H. M. Manasevit, *Appl. Phys. Lett.* 11, 156(1968).
- [8] N. C. Frateschi, S. G. Hummel and P. D. Dapkus, *Electron. Lett.* 27, 155(1991).
- [9] P. D. Dapkus, *J. Crystal Growth*, 68, 345(1984).
- [10] J. N. Baillargeon, A. Y. Cho, R. J. Fischer, P. J. Pearah and K. Y. Cheng, *J. Vac. Sci. Technol.* B12, 1106(1994).
- [11] C. R. Abernathy, *J. Crystal Growth*, 107, 982(1991).
- [12] S. P. DenBaars, C. A. Beyler, A. Hariz and P. D. Dapkus, *Appl. Phys. Lett.* 51, 1530(1987).
- [13] M. A. Tischler, N. G. Anderson and S. M. Bedair, *Appl. Phys. Lett.* 49, 1199(1986).

Chapter 2

The Vacuum Atomic Layer Epiatxy (VALE) Approach

2.1 INTRODUCTION

The review of atomic layer epitaxy in section 1.3 indicates that the suppression of gas phase decomposition of TMGa is a critical issue for successful ALE growth. Ozeki et. al. reported perfect monolayer growth with a pulsed jet reactor in which high speed gas streams are injected onto the substrate to prevent the TMGa from decomposing in the gas phase[1]. We expect that atomic layer epitaxy can also be achieved in an high vacuum environment in which gas phase reactions are completely suppressed.

In this chapter, we are going to discuss the design and construction of a VALE reactor. The discussion will be focused on the vacuum system and gas handling system.

2.2 VALE REACTOR DESIGN AND SET-UP

2.2.1 Vacuum System

The vacuum system includes a UHV process chamber, a sample entry chamber and pumping systems. Both chambers are constructed with stainless steel and pumped with turbomolecular pumps (TMP). The pumping speed of the TMPs is 330 liter/sec for the process chamber and 170 liter/sec for the

sample entry chamber. The pressure is monitored by nude Bayard-Alpert ion gauges with the operating range from 4×10^{-10} to 5×10^{-2} Torr. The base pressures of the process chamber and sample entry chamber are 10^{-9} Torr and 10^{-7} Torr, respectively. Fig. 2.1 shows the schematic drawing of the V-ALE reactor. The pressure during growth is between 10^{-5} to 10^{-4} Torr depending on the exposure conditions of the reactants. The mean free path of the reactant molecules corresponding to the working pressure is about 500 cm to 50 cm which is larger than the diameter of the 8 inch process chamber. The large mean free path assures molecular behaviors of the reactant molecules and minimizes gas phase reactions.

All the flanges are conflat flanges and sealed with copper gaskets. All the vacuum components are UHV compatible and bakeable to 450°C . The sample entry chamber is equipped with a transfer rod for loading the sample holder into the reaction chamber. GaAs substrates are either bonded with indium solder or held by Mo clips on the sample holder. The substrate is heated by a graphite heater with boron nitride encapsulation layers. The substrate temperature is measured through the top viewport with a calibrated IR pyrometer. The process chamber accommodates six injection ports for different sources. At present, only four ports are connected to the sources. They are trimethylgallium (TMGa), triethylgallium (TEGa), tertiarybutylarsine (TBAs) and trisdimethylaminoarsine

(TDMAAs). Each source has its own gas line and control devices. The control of the sources will be discussed in section 2.2.2.

The sources are injected into the reaction chamber by opening the switching valves. The residual gas is pumped out by the TMP and its back-up rotary pump. The exhaust gases are thermally cracked at 900°C and then adsorbed in a charcoal filter before releasing to the air. The whole reactor including the exhaust is monitored by multi-channel MDA toxic gas detectors to ensure the safety of the operation.

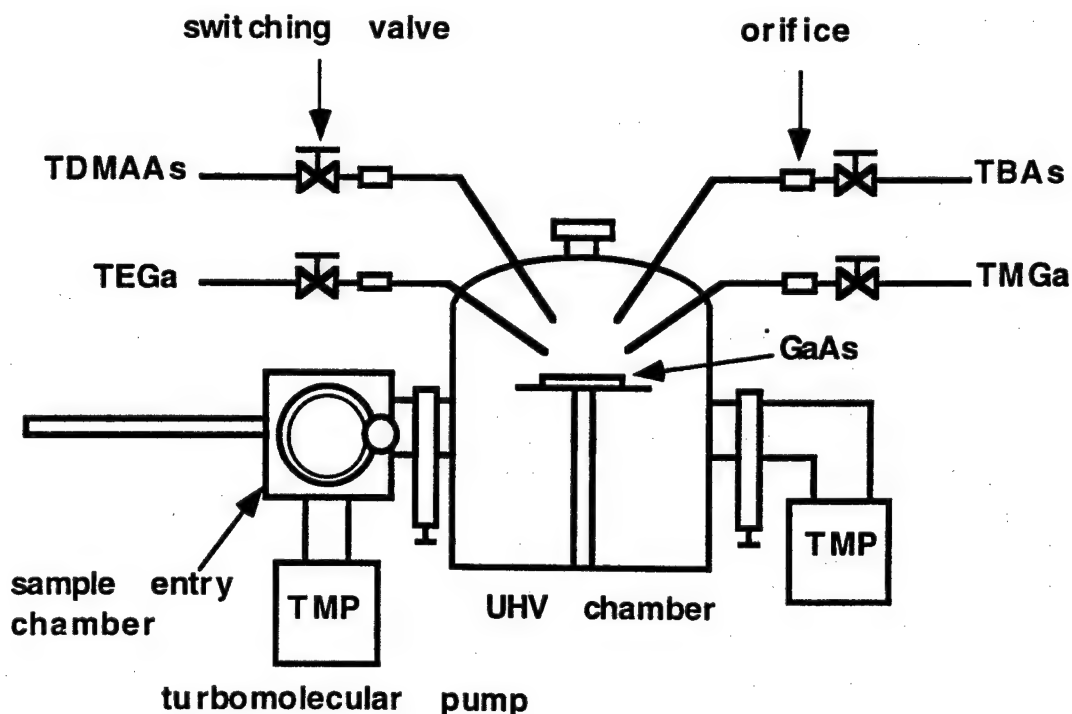


Fig. 2.1 Schematic drawing of the V-ALE reactor

2.2.2 Gas handling System

In ALE growth, the group III and V sources are injected into the reaction chamber alternately. In order to maintain a constant flow, most ALE gas handling systems use a "vent/run" design. Reactants are injected into the reaction chamber during the reactant exposure steps, but bypassed to the exhaust during the pumping or purging steps. One of the disadvantages of "vent/run" design is that it wastes too much source material to the vent. For example, suppose an ALE cycle is 1-1-1-1 which means 1 sec. TMGa exposure, 1 sec. pumping or purging, 1 sec. TBAs exposure and 1 sec. pumping. Only 1/4 of the source flows have been used for growth, and remainder are exhausted from the system. The utilization efficiency will be even lower if the purging time increases. The typical efficiency of the usage of TMGa in Ozeki's experiment is only 27%[2].

The VALE gas handling system that was used in this work is different from the "vent/run" design and can fully utilize the reactants. The system dose not require carrier gases for delivering the reactants into the reaction chamber. The fast switching manifold allows short cycle time and results in higher growth rate[3]. The schematic drawing of the gas manifold is illustrated in Fig. 2.2.

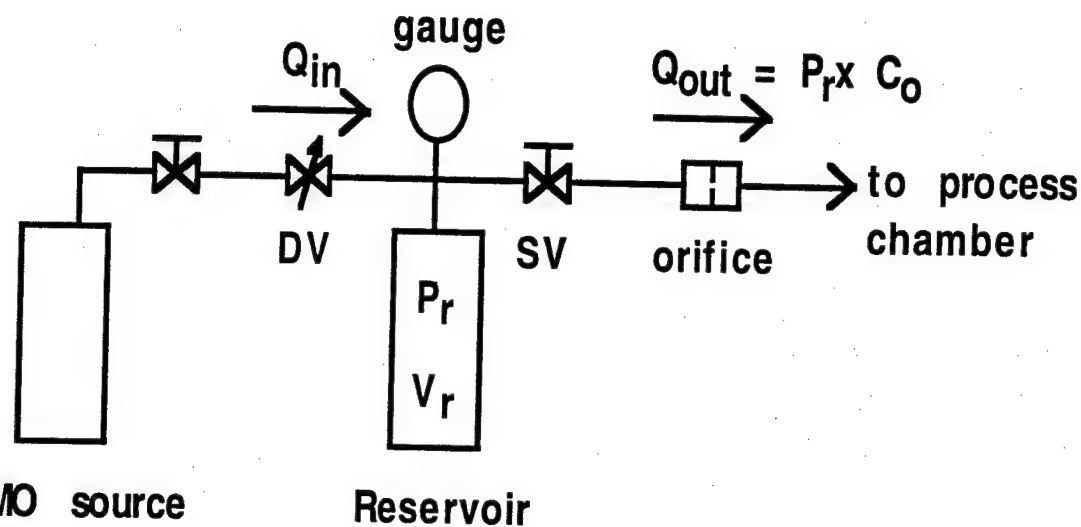


Fig. 2.2 Schematic of the gas manifold.

The gas manifold shown in Fig. 2.2 is constructed with a dosing valve (DV), a pressure gauge, a reservoir, a switching valve (SV) and an orifice. The dosing valve is a UHV leak valve with the flow range of 10 SLM to 10^{-8} SCCM, and is used to control the flow into the reservoir. The reservoir's pressure is monitored by a Baratron gauge which is an absolute pressure gauge with a usable range of 4 decades. The reservoir is an empty stainless steel vessel. The function of the reservoir is to reduce the pressure variation at the orifice and provide a nearly constant flow during the exposure. The switching valve is a Nupro air operated valve for controlling the Open/Close operation of the sources. The orifice serves as a flow element with a calibrated conductance. The exposure level or source

flux in the experiment is determined by the product of the conductance of the orifice and the pressure in the reservoir[4].

The operating principle of the gas handling system is illustrated in Fig. 2.3. During the ALE growth, the switching valve is switched ON and OFF in a preset sequence to inject the source into the process chamber but the dosing valve is continuously open and manually adjusted to maintain a constant input equal to the average output flow. Although the reservoir's pressure drops while the switching valve is open, it charges to the original value at the end of each cycle, and the exposure level is the same for the next exposure. In our design, the pressure variation is less than 5% during the exposure because of the large volume (~2 liter) reservoir. This small variation of the flow is acceptable for ALE growth. Fig. 2.4 shows the actual pressure fluctuation of the TBAs reservoir during the VALE growth with the ALE cycle of 1-1-2-1. The pressure variation is about 1%, which indicates that our design is appropriate. By using this design, an appreciable amount of the sources is conserved, and the usage of the sources is only 5% to 50% of the usage of a normal vent/run system. Without the carrier gases, the gas manifold is simplified and easily maintained.

The speed of switching the gases is determined by the time required for pumping the residual gases in the chamber after the shut off of the switching valve. The amount of sources in

the dead volume between the orifice and the switching valve plays an important role in determining the pumping time of the residual gase. In principle, the smaller the dead volume, the shorter the pumping time. Our design of the dead volume is about 0.04 c.c., and the required pumping time is less than 0.1 sec. This feature allows VALE to achieve typical growth rates of 0.3 $\mu\text{m}/\text{hr}$. which is higher than most of the other ALE techniques[1,5].

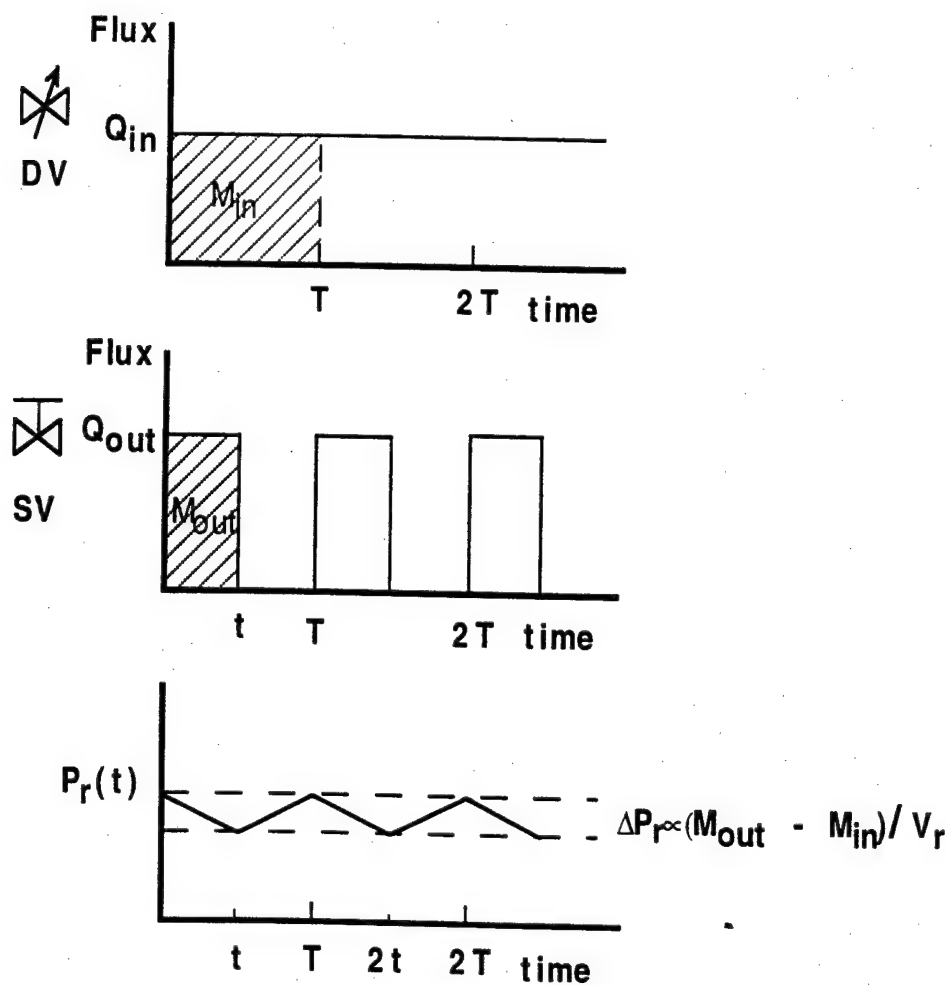


Fig. 2.3 The operating principle of the gas handling system

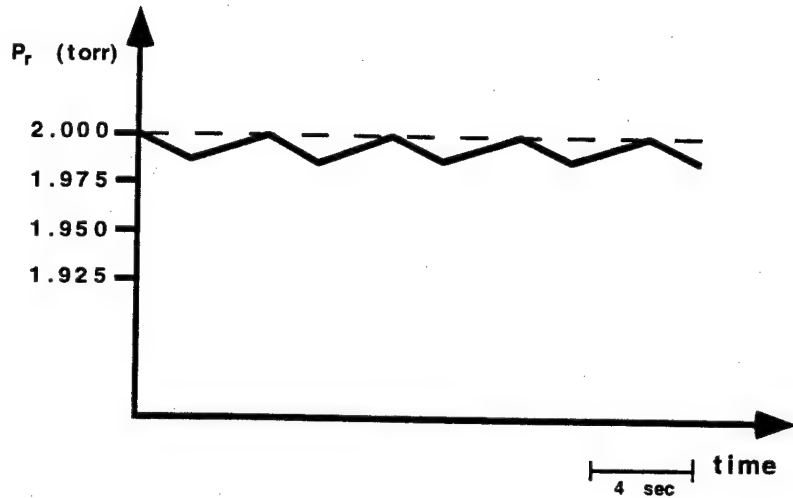


Fig. 2.4 The pressure fluctuation of the TBAs reservoir during VALE growth with a cycle of 1-1-2-1.

2.3 CONCLUSIONS

In this chapter, we have described our design of the VALE reactor focusing on the vacuum system and the gas handling system design. Stainless steel chambers and UHV compatible components are used in the construction of the vacuum system. The special design of the gas handling system improves the efficiency of the source usage appreciably. Without carrier gases, the gas manifold is simplified and easily maintained. The fast switching of the gas manifold allows VALE to reduce the cycle time and results in higher growth rates comparable to CBE and MBE.

REFERENCES

- [1] M. Ozeki, N. Ohtsuka, Y. Sakuma and K. Kodama, *J. Crystal Growth*, 107, 102(1991).
- [2] M. Ozeki, K. Mochizuki, N. Ohtsuka and K. Kodama, *Appl. Phys. Lett.* 53, 1509(1988).
- [3] M. Y. Jow, B. Y. Maa, T. Morishita and P. D. Dapkus, *J. Electron. Mater.* (to be published)
- [4] J. J. Sullivan, S. Schaffer and R. P. Jacobs, Jr., *J. Vac. Sci. Technol.* 7, 2387(1989).
- [5] J. Nishizawa, H. Abe and T. Kurabayashi, *J. Electrochem. Soc.*, 132, 1197(1985).

Chapter 3

Atomic Layer Epitaxy of GaAs by VALE using TMGa and TBAs

3.1 INTRODUCTION

As described in the previous chapters, VALE is expected to achieve wider ALE window because gas phase decomposition of reactants is suppressed. However, the work reported by Nishizawa et. al. showed poor saturation of the growth rate and long cycle times[1]. These phenomena are likely the result of the poor cracking efficiency of AsH₃ on GaAs surface under UHV conditions[2].

Tertiarybutylarsine (TBAs) has been reported as an effective As source in MOCVD. It has a convenient vapor pressure (81 torr at 10°C), and is considerably less hazardous than AsH₃. High purity GaAs grown by using TBAs and TMGa has been reported[3]. The pyrolysis of TBAs is also highly efficient compared to AsH₃ owing to the lower bond strength of As-C(CH₃)₃ as compared to the As-H bonding[4]. We expected that VALE growth using TBAs with TMGa would have better saturation of growth rate and shorter cycle times than was achieved using AsH₃.

In this chapter, we will discuss the results of experiments to measure the growth rate and background impurity incorporation observed in the VALE growth of GaAs using trimethylgallium(TMGa) and tertiarybutylarsine(TBAs). We demonstrate saturated monolayer growth over a wide range of conditions and also demonstrate the dependence of carrier concentration on these conditions.

3.2 EXPERIMENTAL PROCEDURE

Epi-ready GaAs (100) wafers or structures grown on an n⁺ GaAs (100) wafer that consist of a 5000Å Al_{0.5}Ga_{0.5}As marking layer and a 100Å GaAs cap layer grown by MOCVD are used as the substrate materials. The GaAs/AlGaAs/GaAs structure is used when selective etching is used to delineate the grown layer for growth rate measurements. The substrate is loaded into the entry chamber immediately after bonding it to a molybdenum block with indium on a hot plate. After pumping the entry chamber for 20 minutes, the substrate is loaded into the process chamber by a transfer rod and heated to 250°C by a graphite heater with boron nitride encapsulation for 20 minutes for moisture degassing. After that, the temperature is increased to 620°C for 2~5 minutes for thermal cleaning of the substrate under an arsenic over pressure provided by a 0.86 µMole/sec flux of TBAs. This is followed by cooling to the temperature for the growth. The temperature is monitored by a pyrometer

calibrated at the melting point of InSb. The pressure during growth is between 10^{-5} to 10^{-4} Torr depending on the exposure level of the sources. The source materials for gallium atoms and arsenic atoms are trimethylgallium(TMGa) and tertiarybutylarsine(TBAs).

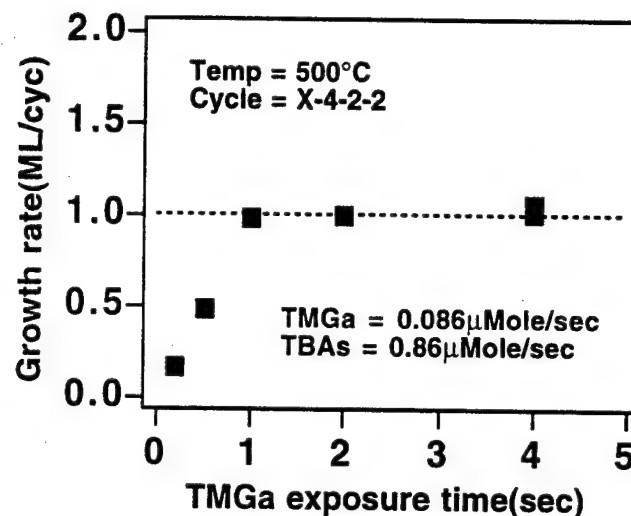
The grown GaAs sample is patterned and selectively etched to create a step for thickness (growth rate) measurements. The carrier concentration is measured by Hall effect and electrochemical C-V profiling. Photoluminescence(PL) is used for the impurity characterization. The surface morphology is examined by optical microscopy and scanning electron microscopy (SEM).

3.3 GROWTH RESULTS AND DISCUSSION

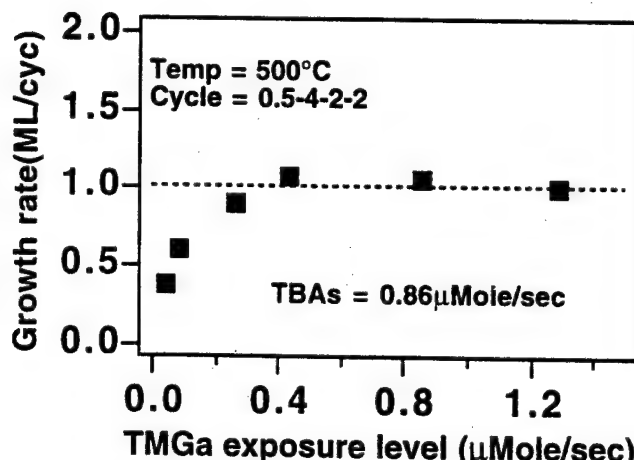
3.3.1 Growth Rate Study

Two exposure variables were found to control the saturated growth of GaAs by VALE - the TMGa flux and the TMGa exposure time. The dependence of growth rate expressed as the thickness in ML deposited per exposure cycle are plotted as a function of exposure flux and time in Fig. 3.1(a) and (b). Both of them show strong saturation of the growth rate with respect to the TMGa exposure level and exposure time. The cycle indicated in the figures represents the following sequence: TMGa exposure, evacuation, TBAs exposure and evacuation. For example, "Cycle = 0.5-4-2-2" means a 0.5 sec.

TMGa exposure followed by a 4 sec. pumping time, a 2 sec. TBAs exposure and a 2 sec. pumping. At a constant TMGa exposure level of $0.086\mu\text{Mole/sec}$, the growth rate increases with increasing exposure time up to one second exposure, after which the growth rate is saturated at one monolayer per cycle for times up to four seconds as shown in Fig. 3.1(a).



(a)



(b)

Fig. 3.1. The dependence of the growth rate on (a) TMGa exposure time and (b) exposure level.

A distinct saturation is also shown with the variation of the TMGa exposure level. These data indicate a clear self-limiting decomposition of TMGa and also show that the control of the growth thickness at the atomic scale can be achieved in VALE. Possible mechanisms for the saturated growth have been discussed by Maa and Dapkus[5]. The strong saturation observed here is in marked contrast to the work of Nishizawa *et. al.* which showed a rather weak saturation of the growth rate[1].

The surface morphology of VALE grown GaAs is mirror-like and no gallium droplets are found even for long TMGa exposure times or high exposure levels. These observations imply that homogeneous decomposition of TMGa is nonexistent, and that surface reactions are the dominant processes in VALE. The short exposure time of TMGa is the result of fast switching of the gas handling system. This capability allows the VALE to achieve higher growth rates than other high vacuum ALE systems[1,6,7]. Growth rates as high as $1\mu\text{m}/\text{hr}$ can be achieved with shorter exposure and evacuation times by increasing the substrate temperature and the reactant exposure level.

The effect of TBAs exposure on growth rate is shown in Figs. 3.2(a) and (b). These figures also show distinct self-limiting decomposition of TBAs in terms of the exposure level and exposure time. The TBAs exposure level for monolayer

growth is ten times of that of TMGa exposure, which implies that the reaction of TBAs on Ga-rich surfaces is slower than TMGa on As-rich surfaces.

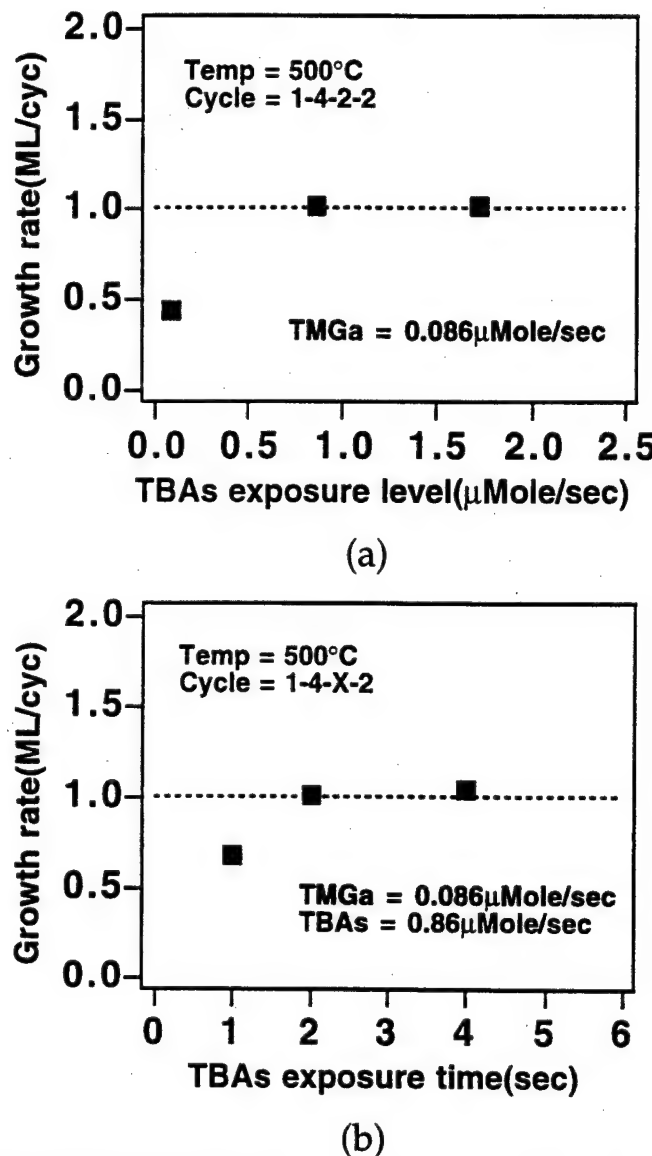


Fig. 3.2. The dependence of the growth rate on (a) TBAs exposure level and (b) exposure time.

The mechanism of the self-limiting decomposition of TBAs is probably due to the low sticking coefficient of As on As-rich surfaces at the growth temperature[8]. The required exposure time of TBAs for monolayer growth is much shorter than the reported value for AsH₃ under similar conditions[1], indicating that the pyrolysis efficiency of TBAs is higher than AsH₃. It also confirms that the weak saturation of growth rate reported by Nishizawa et. al. is due to the insufficient supply of As atoms.

Fig. 3.3 shows the saturation of the growth rate at different substrate temperatures. These data show that increasing substrate temperature enhances only the growth in the unsaturated growth regime. This indicates that the dominant reaction is a surface kinetic reaction, and not limited by the mass transfer of the sources. Based on our previous work, this results from an increased TMGa decomposition rate on GaAs surfaces at increased temperatures[5]. Once the growth rate reaches one monolayer per cycle, the self-limiting mechanism takes place, and the growth rate no longer increases.

The temperature window for the monolayer growth is also an important issue for ALE growth. Fig. 3.4 shows the widest temperature window reported in high vacuum ALE growth. The growth rate is less than monolayer per cycle when the temperature is less than 500°C or higher than 570°C. The decrease of the growth rate at low temperature may be caused

by the slow decomposition rate of TMGa molecules, and by the desorption of As atoms from the surface at high temperatures.

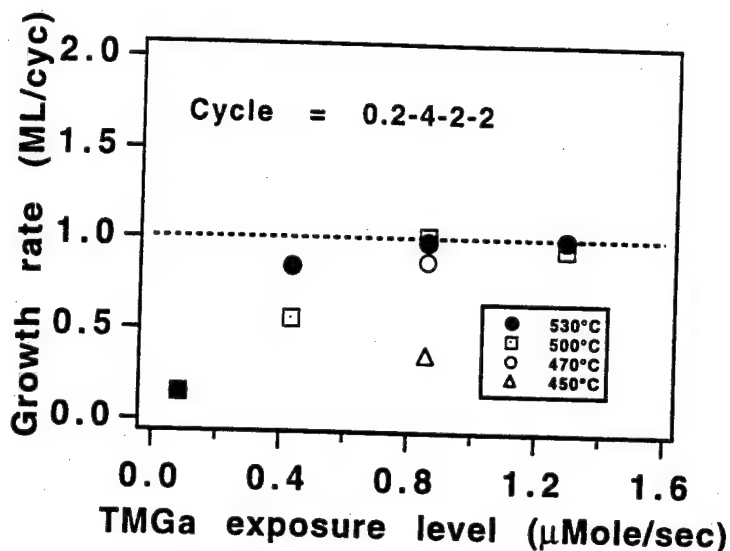


Fig. 3.3. The dependence of the growth rate on TMGa exposure level at different temperatures.

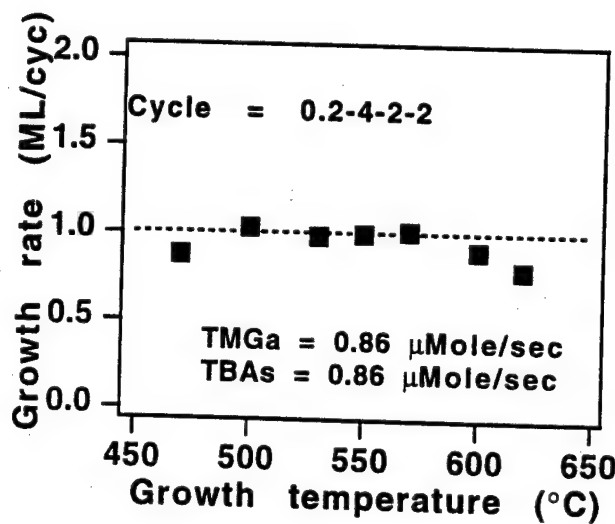


Fig. 3.4. The dependence of the growth rate on substrate temperature.

This wide temperature window is remarkably different with Nishizawa's work and other atmospheric pressure ALE (AP-ALE) studies[1,9]. As compared with AP-ALE, it strongly indicates that suppression of the gas phase decomposition of the reactants, namely TMGa, is the reason for the successful monolayer growth in VALE. It also confirms that the ALE growth results from the self-limiting deposition of TMGa on GaAs surfaces.

3.3.2 Discussion of Self-limiting Mechanism of TMGa

Since monolayer per cycle growth results from the self-limiting decomposition of TMGa on (100) GaAs surfaces, it is necessary to discuss the surface decomposition mechanisms of TMGa. There are several models proposed for the self-limiting decomposition of TMGa. One is called adsorbate inhibition mechanism proposed by Nishizawa et al[1], and the other is selective adsorption mechanism proposed by Ozeki et al[10]. Yu et. al. proposed another model called flux balance mechanism[11]. Maa and Dapkus proposed a more detailed model of the TMGa surface pyrolysis mechanism[12]. In this section, we will compare our experimental results with these models and try to find the best explanation of the ALE mechanism.

The model of adsorbate inhibition is that TMGa converts the As-rich surface to a gallium-rich surface covered with adsorbates, i.e. CH₃ radicals. The adsorbates inhibit further decomposition of TMGa. If there are no adsorbates on the Ga-rich surface, the TMGa will decompose on the surface and results the formation of Ga droplets. In reality, Ga droplets have never been found in this work in the regime of monolayer growth. Maa has also reported that no deposition of TMGa on Ga-rich surfaces from RDS and RHEED measurements[13]. In this work and in work by Ozeki, the decomposition of TMGa on partially Ga coverage surface created by TEGa deposition has been studied. It was found that the growth rate is saturated at one monolayer per cycle so long as the Ga deposited by TEGa did not exceed one monolayer[10]. If TMGa decomposed on Ga atoms, the growth rate of the above experiments would depend on the Ga coverage of the starting surface.

The key assumption of the selective adsorption model is that TMGa only adsorbs on As atoms for decomposition. Once the surface converts from As-rich surface to Ga-rich surface, the adsorption of TMGa stops and further TMGa reflects intact from the surface. This model simplifies over the dynamic properties of the GaAs surface at the ALE temperature. Actually, the Ga-rich surface is still very active to the TMGa molecules at this temperature. Maa et. al. and Yu et. al. have

reported that the TMGa can react on Ga-rich surfaces but this reaction does not lead to decomposition into Ga atoms on the surface[5,11].

The key feature of the flux balance model is that TMGa decomposes on the Ga-rich surface but a gallium-containing species, namely MMGa, leaves the surface such that no net gallium deposition occurs[11]. This model is consistent with the observation of the desorption of the MMGa species from the Ga-rich surface during TMGa exposure. The shortcoming of this model is that it does not take the surface reconstruction into account. This model has difficulty explaining transient behavior of TMGa reacting on the Ga-rich surface reported by Maa and the carbon incorporation phenomenon reported in this work[12].

We believe that the model proposed by Maa and Dapkus is most consistent with the experimental results in this study and reported elsewhere[5]. The major part of their model is that TMGa only decomposes on As atoms. When the surface is As-rich, TMGa decomposes on As atoms and leaves Ga atoms on the surface by releasing all the methyl radicals. As the surface becomes Ga-rich, the 4x6 reconstruction of the surface will expose the underlying As atoms at Ga vacancy site to the vacuum. These sites provide the TMGa adsorption and reaction sites. However, the TMGa adsorbed on these sites are not stable and will desorb as Ga-containing species. This results in no net

Ga deposition. This model has dealt with the surface reconstruction and provides a better explanation for the RDS experiments and the carbon incorporation results in this study. We will use this model in chapter 4 to discuss the carbon incorporation mechanism.

3.3.3 Electrical Property Characterization

All of the VALE grown films are p-type, and the carrier concentration varies from 10^{17} to 10^{19}cm^{-3} . The likely impurity is carbon originating from TMGa exposure. Carbon incorporation has been reported in both ALE and CBE growth[1,14,15]. Several groups have suggested that the methyl radicals, supplied by decomposed TMGa on the GaAs surface, play an important role in the carbon incorporation[16,17]. The possible mechanism of carbon incorporation will be discussed in chapter 4.

In VALE growth, the hole concentration varies with the growth conditions, especially with TMGa exposure. Figs. 3.5(a), (b) and (c) show the dependence of the hole carrier concentration on TMGa exposure level , TMGa exposure time and TBAs exposure level, respectively. In fig. 3.5(a) and 3.5(b), the dependence of the hole concentration on TMGa exposure is smaller when the TMGa exposure level or exposure time is more than enough for monolayer growth. However, for less than monolayer growth, the hole concentration decreases

dramatically as the TMGa exposure decreases. These two different behaviors indicate that the carbon incorporation is related to the population of carbon species on the GaAs surface during TMGa exposure. For TBAs, the behavior is opposite. As TBAs exposure increases, the hole concentration decreases. This observation indicates that TBAs helps reduce the carbon incorporation presumably by transporting H containing radicals that can react with the methyl radicals to produce volatile species. The growth of the lowest hole concentration samples under monolayer growth conditions, $6 \times 10^{17} \text{ cm}^{-3}$, is achieved by using small TMGa exposure and large TBAs exposure.

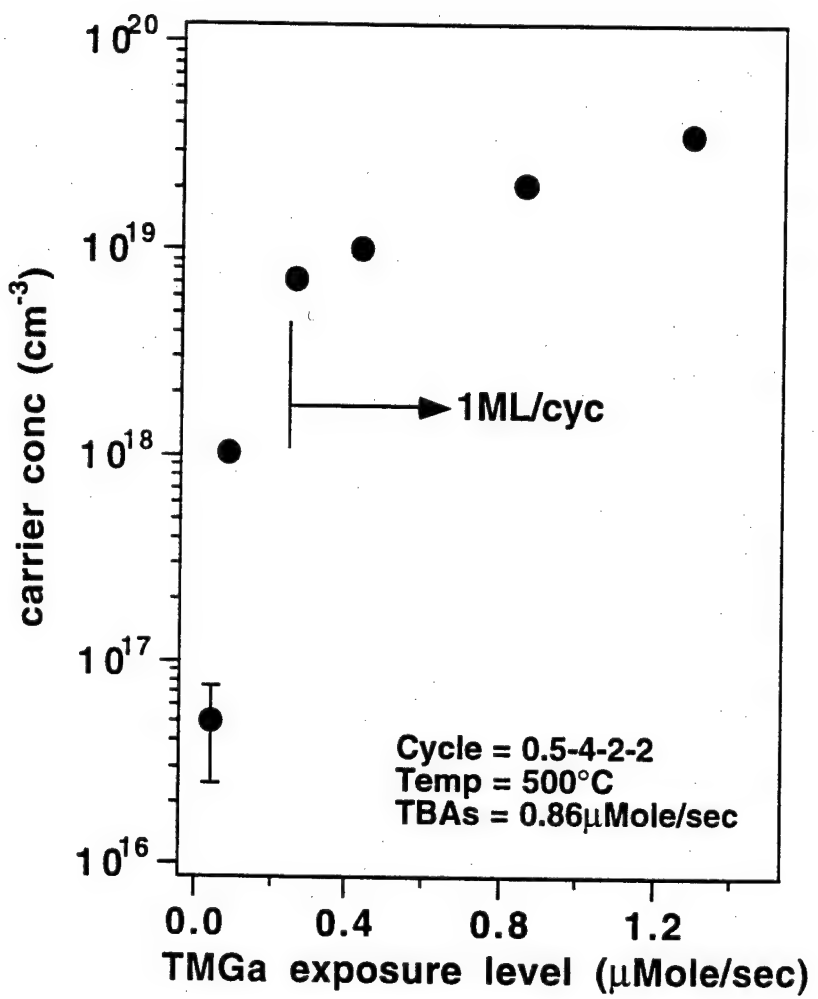


Fig. 5(a)

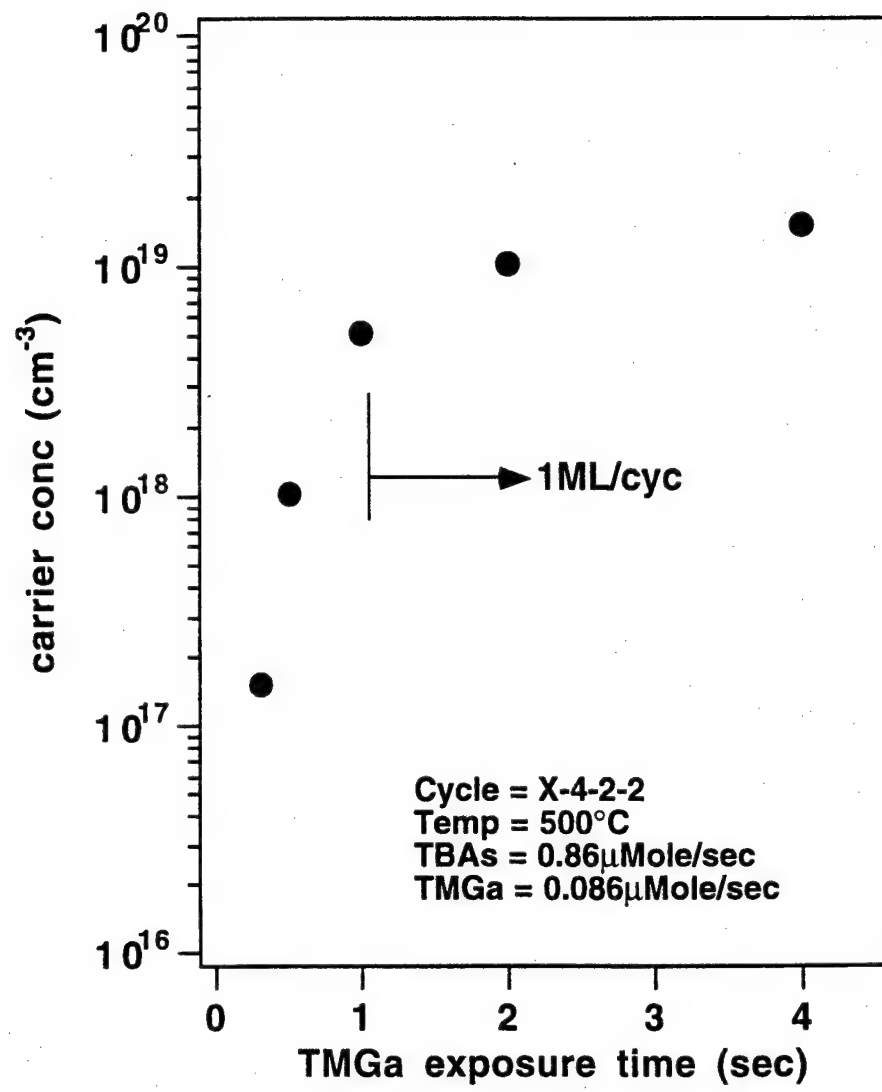
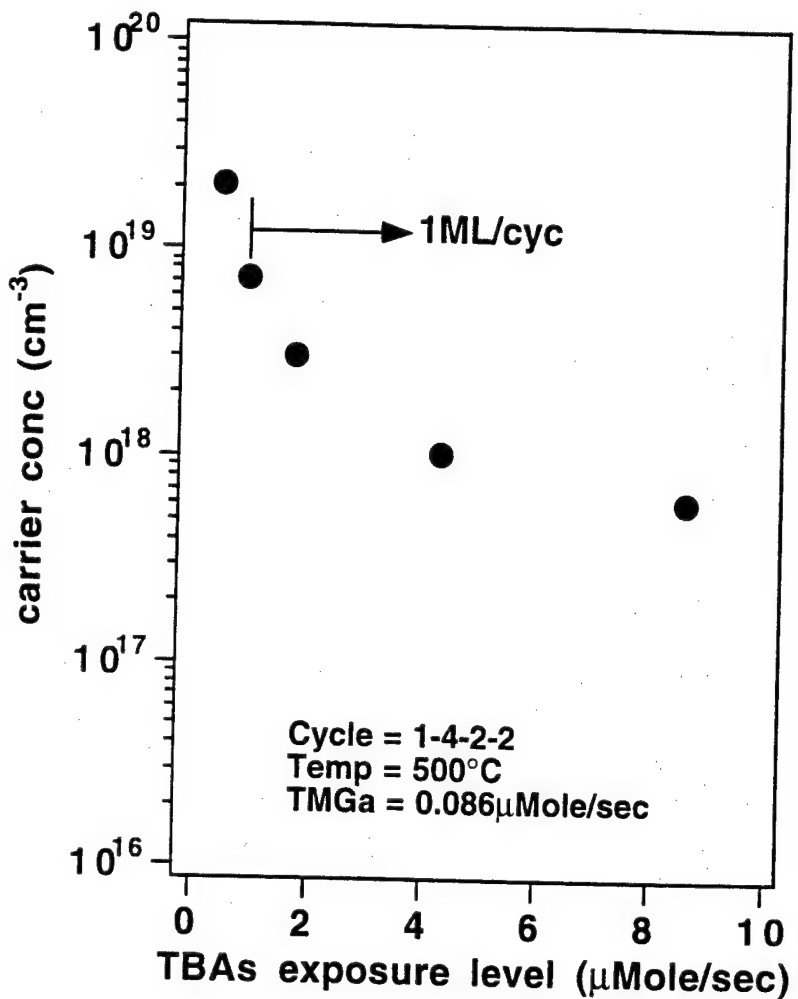


Fig. 5(b)



(c)

Fig. 3.5. The dependence of the carrier concentration on (a) TMGa level, (b) TMGa exposure time and (c) TBAs exposure level.

3.4 BACKGROUND ARSENIC INCORPORATION

Background As incorporation is detected by using Reflectance Difference Spectroscopy(RDS) in the VALE GaAs growth. The principle of RDS has been described previously[12]. Fig. 3.6 shows the decay of RDS signal due to the As incorporation. The sample is exposed to TBAs with varied exposure time from 1 sec to 5 sec, followed by 10 sec pumping, 0.2 sec TMGa exposure and 60 sec pumping. The transient of the RDS signal is due to variation of the surface reconstruction during TMGa and TBAs exposures. The signal level at the bottom represents As-stabilized surfaces. It increases to a higher level after forming a Ga-stabilized surfaces by the TMGa exposure. The background As incorporation is found during the 60 sec pumping period after the TMGa exposure. Ideally, the Ga stabilized surface should be sustained and the RDS signal level should be constant for long times as seen in Fig. 3.7. In stead of leveling off, the RDS signals start to decrease to the As stabilized surface level after stopping the TMGa exposure.

The question is: Where are these As species coming from? Are they the residual TBAs species inside the chamber or As species desorbing from the deposits on the heater assembly? The decay time of the signal is several tens of seconds which is much longer than the required time for pumping the residual TBAs species. Based on our calculations, we expect the residual

species to be pumped out within one second. In addition, the decay rate is strongly dependent on the TBAs exposure time while the exposure level is kept constant. This can not be explained by the residual TBAs incorporation. We believe that As species desorbing from the heater assembly is a more reasonable explanation for the background As species.

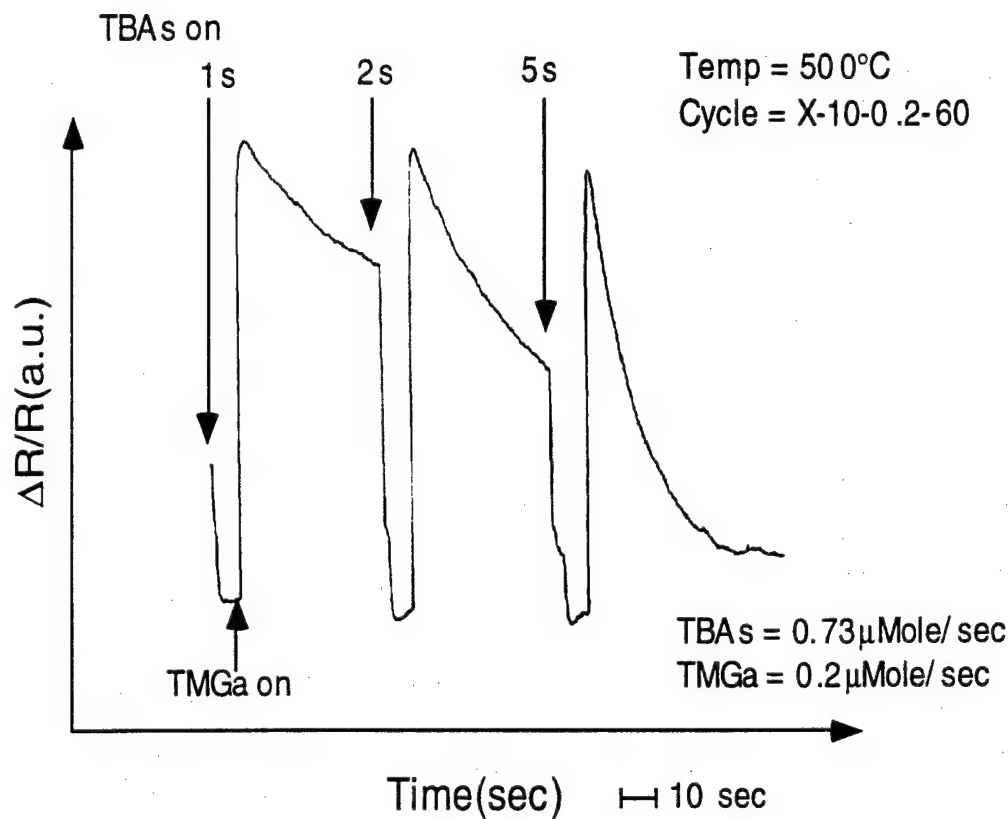


Fig. 3.6 RDS transients of background As incorporation.

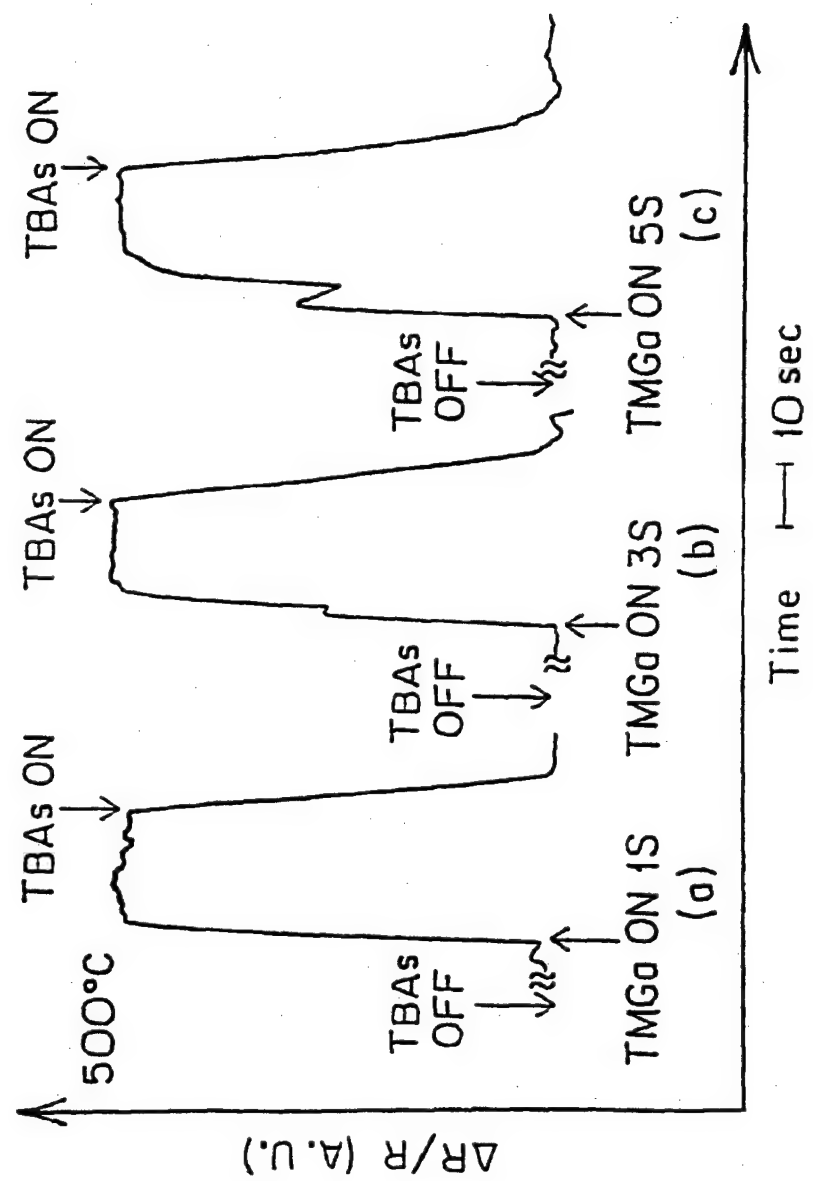


Fig 3.7 RDS transients on (100) GaAs for initiation of TMGa and TBAs exposures.(after Maa, 1991)

Background As species are always present during VALE growth. We believe that the species are As_2 or As_4 which come from the deposits near the heater assembly. The background As species hit the substrate surface continuously and can be considered as an unintentional As source in our chamber. Since the sticking coefficient of As_2 or As_4 on As-rich surface is close to zero, there is no reaction during the TBAs exposure cycle. However, during the TMGa exposure cycle, the background As species can react with TMGa and cause more than monolayer growth. We find that the ALE window becomes narrower after more and more growths. Fig. 3.8 shows the loss of the saturation of the growth rate due to the background As incorporation. By etching the heater assembly, the growth rate reduces to one monolayer per cycle even for the four second TMGa exposure. This fact indicates that most of the As species desorbs from the heater assembly because it is hot during the growth. In our system, serious As backgrounds appear after $\sim 20 \mu\text{m}$ of GaAs growth. Of course, this will depend on the exposure conditions used in the various runs. Since the background As species, As_2 or As_4 , do not provide hydrogen atoms to remove methyl radicals on the substrate surface, they may cause the carbon species to incorporate into the films. In order to suppress the background As incorporation and study the carbon incorporation, the installation of a liquid nitrogen shroud is necessary.

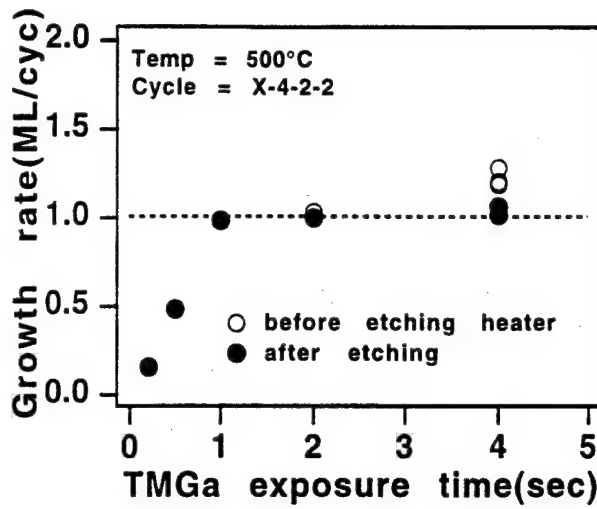


Fig. 3.8. The effect of the background As incorporation on ALE growth.

3.5 CONCLUSION

GaAs growth by VALE has been studied for various growth parameters. The distinct self-limiting of the growth rate indicates the homogeneous decomposition of TMGa is suppressed successfully in VALE. TBAs is a promising As source material in VALE application. The carbon incorporation problem is serious in VALE using TMGa and TBAs and the mechanism needs more investigations. Low carbon concentration films can be grown by decreasing the TMGa exposure and increasing the TBAs exposure. Background As incorporation affects the ALE window and may also influence the carbon incorporation in VALE.

REFERENCES

- [1] J. Nishizawa, and H. Abe, T. Kurabayashi, *J. Electrochem. Soc.* 132, 1197(1985).
- [2] A. Usui and H. Watanabe, *Annu. Rev. Mater. Sci.*, 21, 185(1991).
- [3] S. P. Watkins and G. Haacke, *Appl. Phys. Lett.* 59, 2263(1991).
- [4] A. C. Jones, *J. Crystal Growth*, 129, 728(1993).
- [5] B. Y. Maa, and P. D. Dapkus, *Thin Solid Films* 225, 12(1993).
- [6] T. H. Chiu, J. E. Cunningham, A. Robertson, Jr. and D. L. Malm, *J. Cryst. Growth* 105, 155(1990).
- [7] K. Fujii, I. Suemune, T. Kouji, and M. Yamanishi, *Appl. Phys. Lett.* 60, 1498(1992).
- [8] J. Y. Tsao, T. M. Brennan, and B. E. Hammons, *Appl. Phys. Lett.* 53, 288(1988).
- [9] S. P. Denbaars, P. D. Dapkus, C. A. Beyler, A. Hariz and K. M. Dzurko, *J. Cryst. Growth* 93, 195(1988).
- [10] M. Ozeki, N. Ohtsuka, Y. Sakuma, and K. Kodama, *J. Cryst. Growth* 107, 102(1991).
- [11] M. L. Yu, U. Memmert and T. F. Kuech, *Appl. Phys. Lett.* 55, 1011(1989).
- [12] B. Y. Maa and P. D. Dapkus, *Appl. Phys. Lett.* 58, 2261(1991)

- [13] B. Y. Maa and P. D. Dapkus, *Appl. Phys. Lett.* 62, 2551(1993)
- [14] K. Mochizuki, M. Ozeki, K. Kodama, and N. Ohtsuka, *J. Cryst. Growth* 93, 557(1988).
- [15] M. Gotoda, S. Maruno, Y. Morishita, Y. Nomura, H. Ogata, K. Kuramoto and H. Kuroki, *J. Cryst. Growth* 100, 5(1990).
- [16] L. Q. Liu, B. B. Huang, H. W. Ren, and M. H. Jiang, *J. Cryst. Growth* 115, 83(1991).
- [17] J. R. Creighton, and B. A. Bansenauer, *J. Vac. Sci. Technol.* A11, 876(1993).

Chapter 4

Study of Carbon Incorporation in GaAs by VALE

4.1 INTRODUCTION

In chapter 3, we have discussed the growth of GaAs by VALE using TMGa and TBAs. The results show that perfect monolayer growth can be achieved over wide range of growth parameters, which indicates that VALE is potentially a powerful technique for the growth of complex structures for optoelectronic devices. Although atomic level control of growth has been achieved by VALE, several obstacles still need to be overcome before this technique is widely accepted. One of the problems is the serious carbon incorporation in GaAs grown by VALE. The typical carbon concentration for monolayer growth is around $5 \times 10^{18} \text{ cm}^{-3}$, even though the carbon level can be reduced to certain level by increasing TBAs exposure. Therefore, the application of this technology will be limited, if high purity GaAs is not available by VALE. In order to reduce the carbon incorporation, it is necessary to study the incorporation mechanism of TMGa in VALE. Of course, our final goal is to achieve high purity GaAs with monolayer per cycle of growth rate.

In this chapter, different metalorganic sources are being used as Ga and As sources in VALE growth to study the mechanism of carbon incorporation, and also for the monolayer growth of low carbon GaAs. The Ga sources are TMGa and TEGa; TBAs and TDMAAs(trisdimethylaminoarsine) are used as the As source. From the different combinations of the metalorganic sources, we find that the carbon incorporation in GaAs grown with TEGa is always lower than with TMGa, whether TBAs or TDMAAs is used as the As source. However, in contrast to TMGa, self-limiting decomposition of TEGa is not found. When comparing the effect of different As sources on reducing carbon incorporation with TMGa as the Ga source, TDMAAs is more effective than TBAs.

By analyzing these results, we proposed a model for the incorporation of carbon impurities using TMGa in VALE. Monolayer growth of high purity GaAs can also be obtained by decomposing TMGa on partially Ga coverage surface created by TEGa and normal expoure level of TBAs.

4.2 CARBON INCORPORATION IN GaAs USING TMGa

The carbon incorporation of GaAs using TMGa as the gallium source has been reported in MOCVD, CBE and ALE [1~6]. The detailed microscopic mechanisms are not yet clarified. One of the main difficulties in providing such a model is that the carbon incorporation is a minor and multistep reaction on

the GaAs surface during the exposure of the reactants. The carbon concentration is usually less than 10^{16}cm^{-3} (1 ppm) in MOCVD growth, which makes the characterization of the impurity incorporation very difficult. For example, the sensitivity of secondary ion mass spectroscopy for carbon impurities is about 10^{17}cm^{-3} [8]. This low level of carbon makes chemical analysis very difficult to carry out, and the only way to characterize the carbon impurity concentration is through electrical or optical property measurements which are indirect measurements of the carbon concentration. Therefore, the interpretation of carbon incorporation in MOCVD is still controversial[1~3].

In CBE and VALE growth, the carbon concentration can be as high as 10^{20}cm^{-3} (1 at%) which is near the sensitivity of most of the surface analysis tools (e.g. XPS, UPS, AES). This suggests a good method for studying carbon incorporation of TMGa. In addition, the high vacuum environment of CBE and VALE also allows the use of the surface analysis tools to do *in situ* study of the reaction kinetics of carbon incorporation during the growth. Recently, there are several papers discussing possible models of carbon incorporation of using TMGa in CBE and the dissociation kinetics of TMGa on GaAs surfaces with the relevance of carbon incorporation[9~14]. Since these experiments were carried out under similar conditions to our

VALE growth, they will be used to interpret our results related to carbon incorporation mechanisms using TMGa.

In section 3.3.2, we have discussed the electrical property of the GaAs films characterized by electrochemical C-V profiling. The results show very high carbon incorporation, and the concentration is strongly dependent on the exposure conditions of the sources. The RDS measurement also shows strong background As incorporation in the VALE growth, as shown in Fig. 3.6. Since we believe that active H on the surface is important for reducing the carbon incorporation, we suspect the high carbon level is related to the background As present in the system. Such As species are likely to be As_2 or As_4 and are known to promote the incorporation of carbon as compared to species that contain H. Thus, VALE growths of GaAs with a LN_2 baffle near the substrate to minimize the ambient As background were carried out. Fig. 4.1 shows the effect of the LN_2 baffle's temperature on carrier concentration. Reducing the baffle's temperature from 60°C to -80°C does not affect the carrier concentration. The decreasing of the carrier concentration at -100°C is due to the condensation of the metalorganic sources on the baffle resulting less than monolayer growth. Fig. 4.2 shows less than monolayer growth at -100°C baffle. If we increase the reactants' exposure levels in order to obtain monolayer growth, the carrier concentration will increase to the level similar to that observed with higher

temperatures. The lowest baffle temperature we have achieved is about -140°C, but the carrier concentration is still high with a baffle at this temperature. At such a low temperature, most of the As species should be trapped on the baffle. The result indicates that the background As has little effect on carbon incorporation, even though it causes more than monolayer growth.

The result also raises two points regarding the carbon incorporation during TMGa exposure. First, the carbon incorporation does not come from the hydrocarbon or carbon species in the background because all the carbon species are frozen on the LN₂ baffle, but from the dissociation of absorbed carbon species on GaAs surfaces. This is consistent with Kuech et al and Creighton's results, but contrary to Mochizuki's conclusion[1,12,6]. Secondly, it is possible that TBAs is not efficient at removing the carbon species from the substrate surface. In the following section, we are going to study the influence of using different Ga and As metalorganic sources on the carbon incorporation.

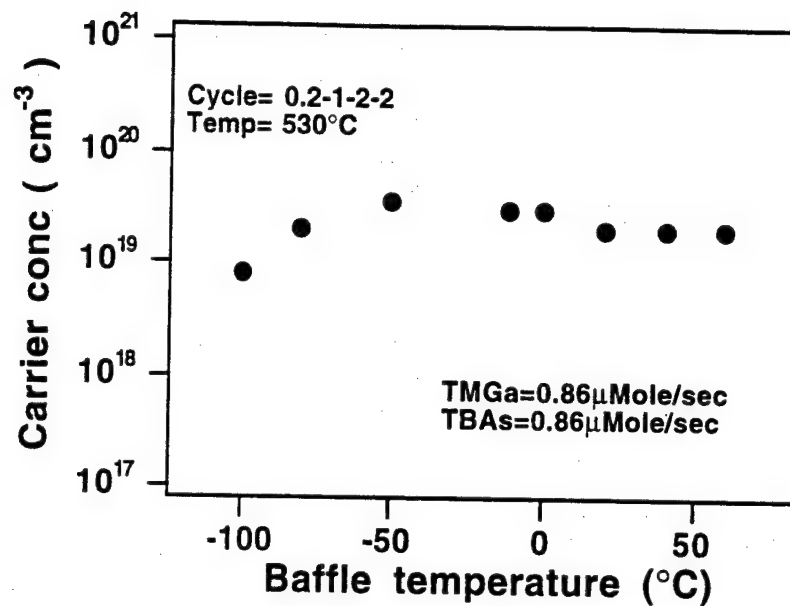


Fig. 4.1 The effect of LN₂ baffle's temperature on carrier concentration.

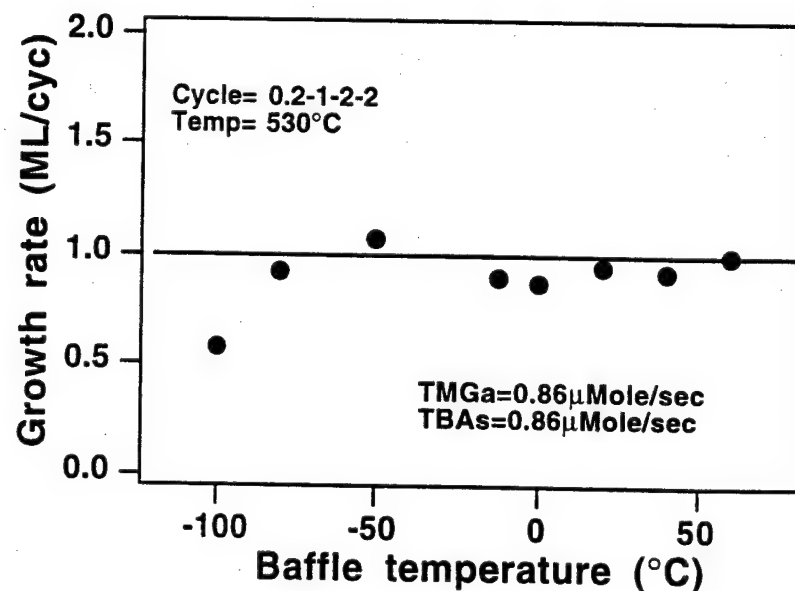


Fig. 4.2 The effect of LN₂ baffle's temperature on growth rate.

4.3 REDUCTION OF CARBON INCORPORATION THROUGH THE USE OF ALTERNATIVE Ga AND As SOURCES.

4.3.1 VALE Growth with TEGa and TBAs Sources

The growth of GaAs using TEGa has produced very low carbon level in CBE owing to the low Ga-C₂H₅ bonding energy and the dominance of the β-hydride elimination process[4,17]. The major products of TEGa decomposition on GaAs surface have been confirmed as ethylene, hydrogen and small amount of ethyl radicals in high vacuum conditions[15,16]. It is expected that the growth of GaAs with TEGa in VALE can also produce low carbon layers. Fig. 4.3 shows the dependence of carrier concentration of GaAs grown by VALE on TEGa exposure levels. The hole concentration is around 10^{16} cm^{-3} which is almost three orders lower than observed when TMGa is the Ga source. Fig. 4.4 and 4.5 are the typical PL spectra of VALE-grown GaAs with TEGa and TMGa, respectively.

In Fig. 4.4 , the peak at $\sim 8300\text{\AA}$ is related to the carbon impurity and the peak around 8200\AA is due to the band edge emission. In contrast with the well resolved peaks in Fig. 4.4, Fig. 4.5 shows a broad peak that is the result of a heavy carbon incorporation. The band edge emission peak has been reduced in relative intensity and can not be resolved. The PL data are consistent with the carrier concentration measurements and provide evidence that the carbon incorporation is greater when

TMGa is used as a source. It indicates that the methyl radicals play an important role on carbon incorporation.

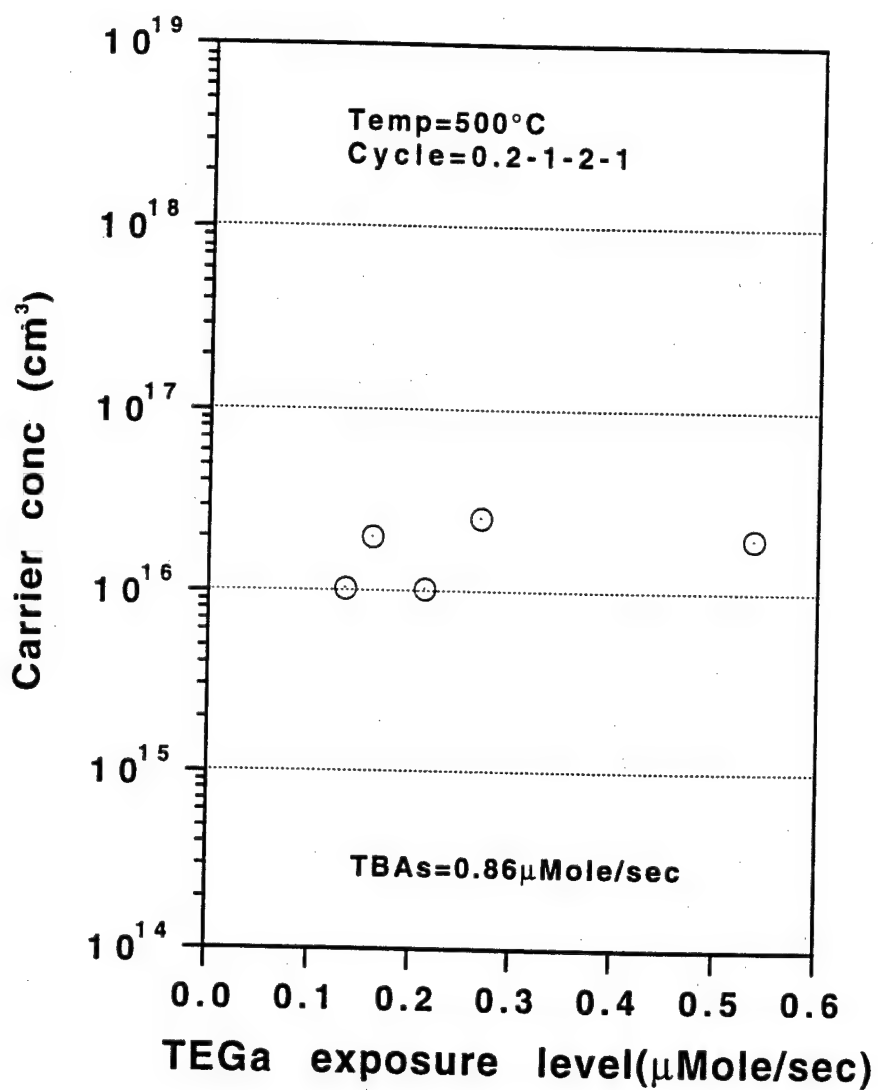


Fig. 4.3 Dependence of the carrier concentration of GaAs grown by VALE on TEGa exposure levels.

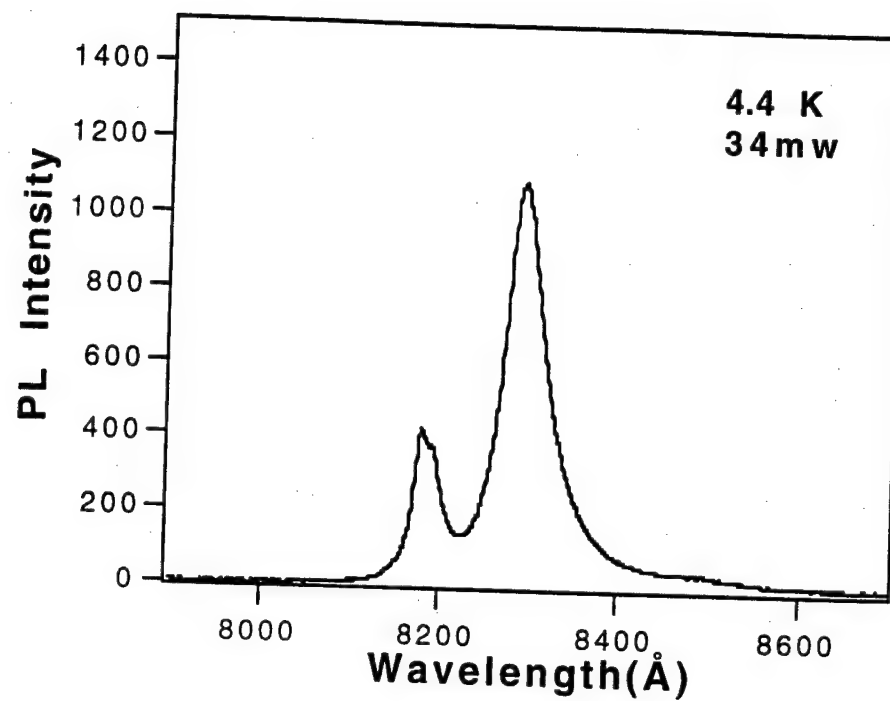


Fig. 4.4 PL spectrum of GaAs growth with TEGa and TBAs.

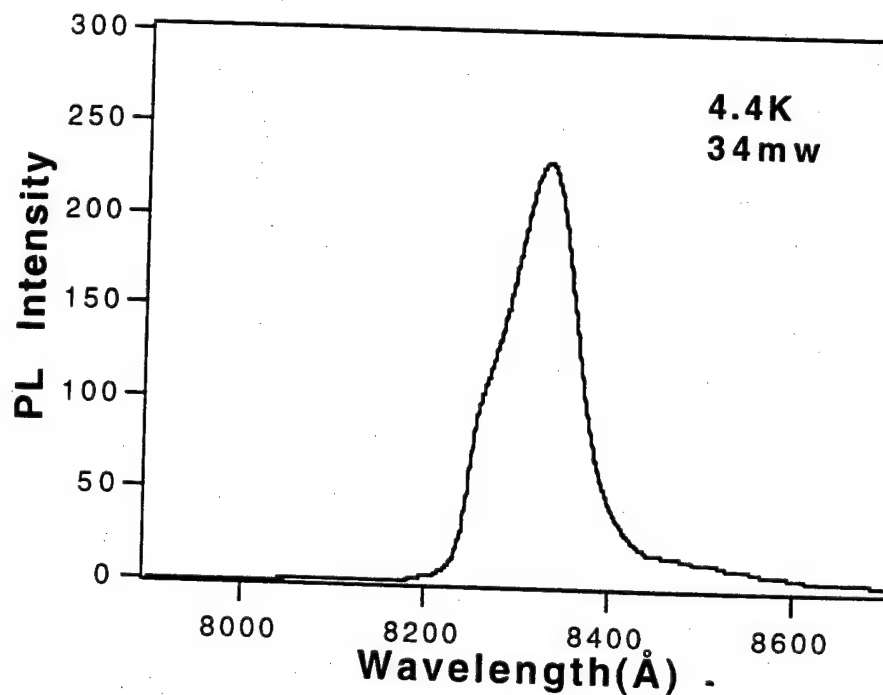


Fig. 4.5 PL spectrum of GaAs growth with TMGa and TBAs.

Since growth with TEGa results in a very low carbon incorporation, its monolayer growth window in VALE was examined. However, the result was disappointing. Self-limiting decomposition of TEGa is not observed. Fig. 4.6 shows that the growth rate is linearly dependent on TEGa exposure level. The linear dependence of the growth rate indicates that there is no self-limiting decomposition of TEGa on the GaAs surface. The sample surface even shows Ga droplets after extended TEGa exposures, which is in contrast to the case with TMGa. We have tried to lower the growth temperature to 360°C, but still find no saturation with respect to TEGa exposure level. The variation of growth rate with the substrate temperature at a fixed TEGa exposure level also shows a very weak saturation, as shown in Fig. 4.7. This lack of saturation in the growth rate under alternate exposure conditions using TEGa had also been reported previously[15,18]. However, this work, carried out in a system optimized for ALE growth and capable of very short exposures, shows that the lack of saturation is fundamental to the surface chemistry of TEGa on GaAs.

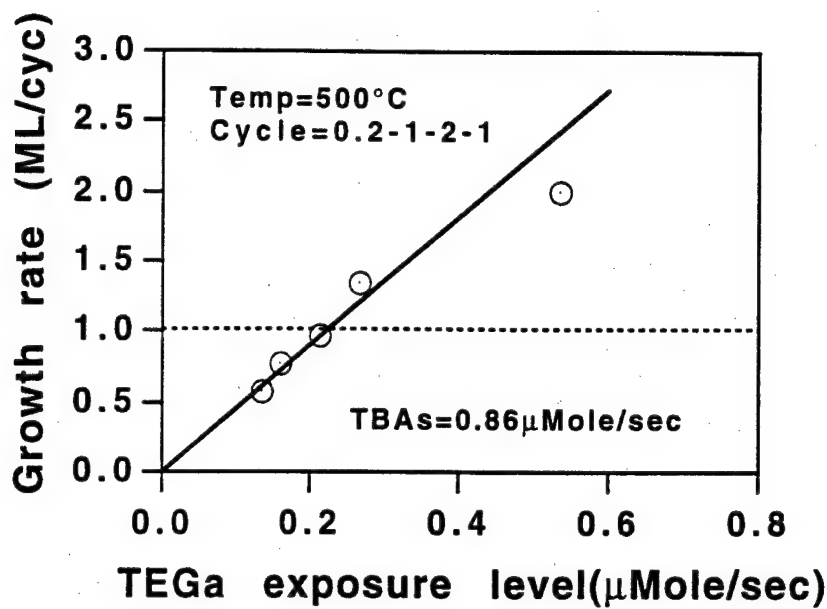


Fig. 4.6 The linear dependence of GaAs growth rate on TEGa exposure level.

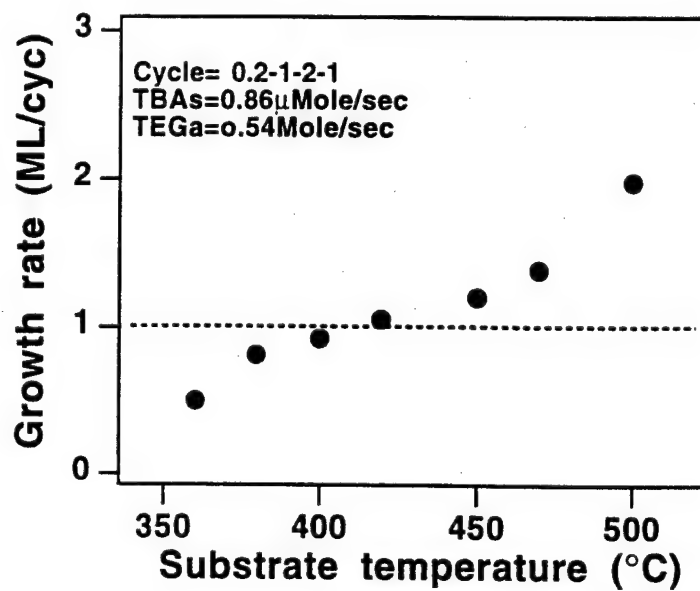


Fig. 4.7 The effect of substrate temperature on VALE growth.

4.3.2 VALE Growth with TMGa and TDMAAs Sources

Comparing VALE growth under various conditions including the use of different sources for Ga atoms and conditions where the background As is controlled in the system, it is clear that the carbon incorporation originates from the dissociation of the adsorbed CH₃ on GaAs surfaces. In order to reduce the carbon incorporation with TMGa, other alternative As sources with higher efficiency for removing carbon species than TBAs are required for the VALE growth.

Recently, CBE growth using TDMAAs has been reported to result in very low carbon level of GaAs growth with TMGa[9,19]. As a result, we investigated the use of TDMAAs in conjunction with TMGa to effect VALE growth. In contrast with the reported CBE results, the VALE growth of GaAs using TDMAAs and TMGa results in grown films with high carbon concentrations. The typical carrier concentration is around $1 \times 10^{18} \text{ cm}^{-3}$. However, the carbon incorporation is reduced dramatically when the films are grown by the CBE mode in the same reactor. The film becomes n-type with carrier concentration of $2 \times 10^{16} \text{ cm}^{-3}$. Fig. 4.8 is the comparison of the PL spectra between VALE and CBE grown films. From Fig. 4.8, the CBE film shows both the band edge emission and carbon peaks, but the VALE film has only the carbon peak due to high carbon incorporation. The PL measurement is consistent with the carrier concentration measurement and confirms that the

carbon concentration is reduced dramatically by introducing TDMAAs only in CBE mode.

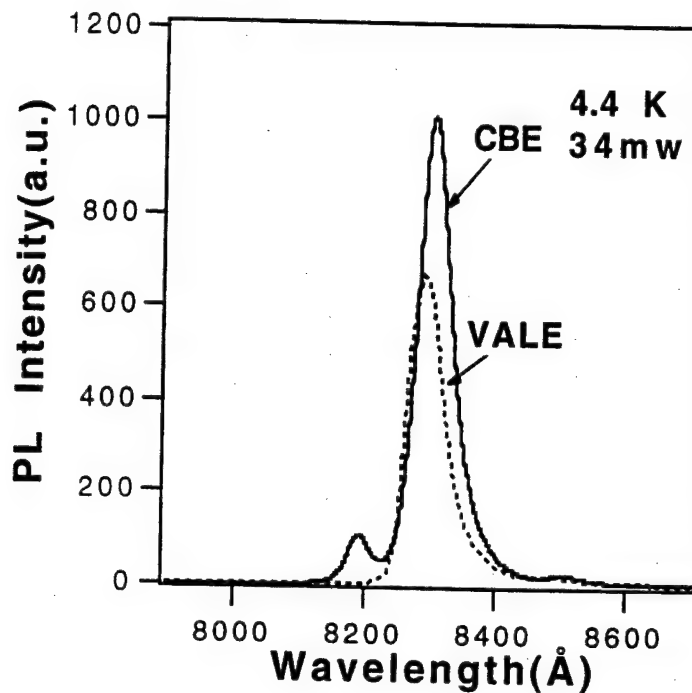


Fig. 4.8 PL spectra of VALE and CBE grown GaAs films.

This result strongly indicates that once the adsorbed CH_3 originating from TMGa initiate the processes of carbon incorporation when there is no TDMAAs molecules present on the surface, the carbon species incorporate into the film and can not be completely eliminated by the subsequent TDMAAs exposure.

4.3.3 VALE Growth with TEGa and TDMAAs Sources

Atomic layer epitaxy of GaAs using TEGa and TDMAAs has been reported by Fujii et al.[20]. They proposed that the

monomethylamino(MMA) radical from decomposition of TDMAAs adhere to both the As and Ga terminated surfaces. They further propose that this radical transfers from As surfaces to Ga surfaces during TEGa exposures and serves to block adsorption of TEGa after a monolayer is formed leading to monolayer growth. Since we were unable to observe saturation of growth rate with TEGa and TBAs sources, their hypothesis and observations strongly argue that the As source can also promote saturated growth. A study was undertaken to grow GaAs using TDMAAs with TEGa to verify Fujii's self-limiting model.

Fig. 4.9 shows the VALE growth rate with respect to the variation of TEGa exposure levels at 360°C and 470°C. At both of the growth temperatures, the growth rates are linearly proportional to the TEGa exposure level, which is similar with the case of TEGa and TBAs. The grown films are p-type, and the typical carrier concentration is around $1 \times 10^{16} \text{ cm}^{-3}$. Therefore, the results reported by Fujii are not confirmed in our study.

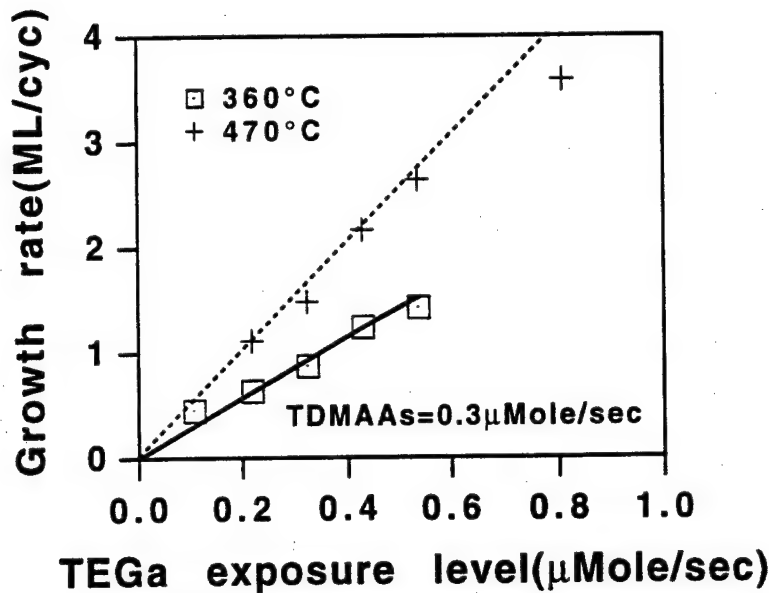


Fig. 4.9 Dependence of the growth rate on TEGa exposure level with TDMAAs as the As source. The exposure sequence is 0.2-1-2-1 at 470°C and 1-1-2-1 at 360°C.

4.4 INFLUENCE OF Ga ATOM COVERAGE ON CARBON INCORPORATION USING TMGa

VALE growth using different Ga and As sources resulted in saturated growth only for one Ga source, TMGa. This source, in turn, results in rather high carrier concentrations that seem to be related to the surface chemistry of CH_3 radicals on (100) GaAs surfaces. In this section, we will focus on the carbon incorporation mechanism associated with the decomposition of adsorbed TMGa molecules on GaAs surfaces.

The carrier concentration measurements as described in Fig. 3.5(a) and (b) show a sharp transition from low to high carbon incorporation as the exposure of TMGa is close the level

necessary for a 1ML/cyc growth rate. In the monolayer regime, the carbon incorporation increases linearly with increases of the TMGa exposure. However, in the submonolayer regime, the carbon incorporation increases more rapidly with the TMGa exposure. This sharp transition of carbon incorporation can not be explained by a simple model of carbon species population with respect to the TMGa exposure. We suspect that the carbon incorporation mechanism is related to carbon species adsorbed on specific sites which are suitable for carbon incorporation. Since the carbon impurity needs to occupy an As site and bonds to Ga atoms in order to act as an acceptor, it is reasonable to assume that the Ga atom surface coverage will have an influence on the carbon incorporation.

In order to study the effect of the Ga atom surface coverage on carbon incorporation, we performed the following experiments. Several starting GaAs surfaces with various degrees of Ga atom coverage are prepared using TEGa prior to the exposure of TMGa. Since the Ga surface created by TEGa contains a low carbon incorporation, it will not affect the carbon incorporation caused by TMGa. Fig. 4.10(a) and (b) show the effects of Ga coverage on carbon incorporation.

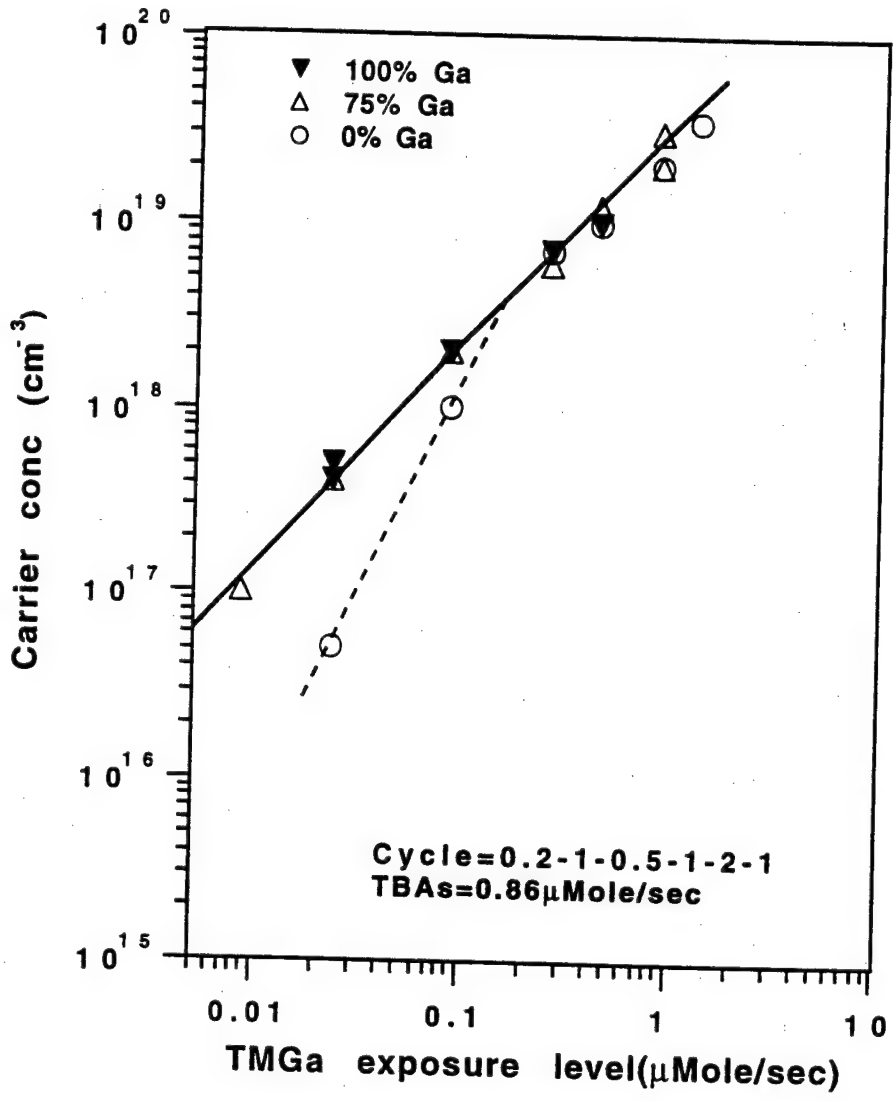
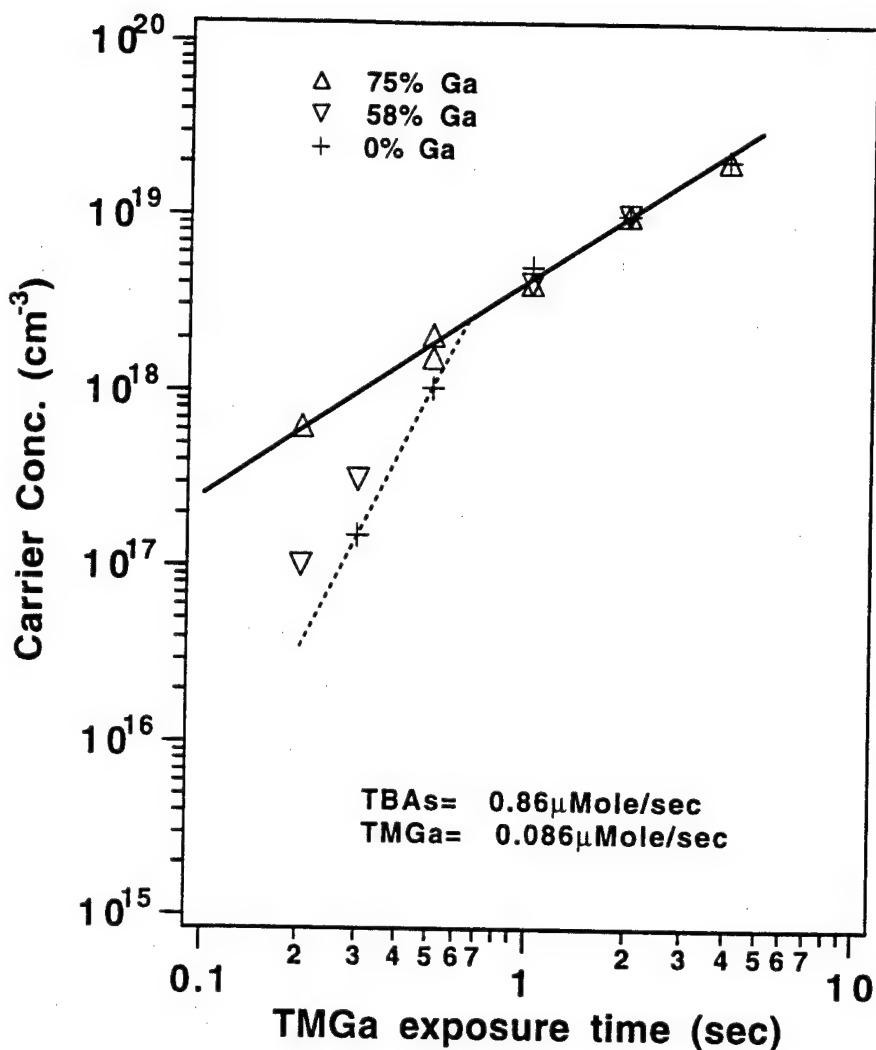


Fig. 4.10(a)



(b)

Fig 4.10 The effect of Ga atom coverage on carbon incorporation with respect to the variation of (a) TMGa exposure level and (b) TMGa exposure time.

Fig 4.10(a) shows the variation of carrier concentration of GaAs as a function of the TMGa exposure level with three Ga coverages at 0%, 75% and 100%. The 0% Ga coverage means that the surface fully covered with As atoms when the TMGa

exposure takes place. For growth at 0% Ga coverage, the carrier concentration continuously increases with TMGa exposure level. A change of slope in the increase occurs when the TMGa exposure level exceeds the level sufficient for a monolayer per cycle growth rate. This suggests that the carbon incorporation kinetics in the saturated regime differ from that submonolayer regime. For growth at 75% and 100% Ga coverage, all of the growth rate are monolayer per cycle such that the transition behavior in the increase of carrier concentration is not observed. In both cases, the dependence is the same as for growth on the 0% Ga coverage at exposures in the monolayer growth rate regime.

A similar dependence of carbon incorporation on TMGa exposure time is shown in Fig.4.10(b). For growth at 0% Ga coverage, the carrier concentration increases more rapidly with the exposure time in the submonolayer regime. All the growths at 75% Ga coverage are monolayer growth and the carrier concentration is linearly dependent on TMGa exposure times. However, the growth at 58% Ga coverage shows a change of the slope when the exposure time is close to that required to achieve monolayer growth. In the submonolayer regime, the measured carrier concentration for growth at 58% Ga coverage is higher than on an As-terminated surface with same amount of TMGa exposure. The results indicates that the carbon incorporation is dependent on the Ga coverages of the surfaces.

It seems that the carbon incorporation in GaAs grown by VALE using TMGa is an intrinsic property.

In order to estimate which species or process play an important role in carbon incorporation, the dependence of carrier concentration on substrate temperature was investigated. Fig. 4.11 shows the Arrhenius plot of the carrier concentration of layers grown on 75% Ga coverage surface at exposures in the monolayer regime. The data shows an activation energy of 35kcal/mol. The carrier concentration decreases with the increase of the substrate temperature.

For a comparison, the temperature dependence of the carrier concentration of layers grown on As-terminated surface in the monolayer growth regime is shown in Fig. 4.12. The carrier concentration is independent of substrate temperature. The layers grown in the submonolayer regime on As-terminated surfaces also show no effects of the substrate temperature as shown in Fig. 4.12. The difference in activation energy for carbon incorporation on surface with 75% Ga coverage and As-terminated surfaces suggests that the carbon incorporation mechanism is a multistep reaction and the rate limiting step is affected by the surface Ga/As stoichiometry.

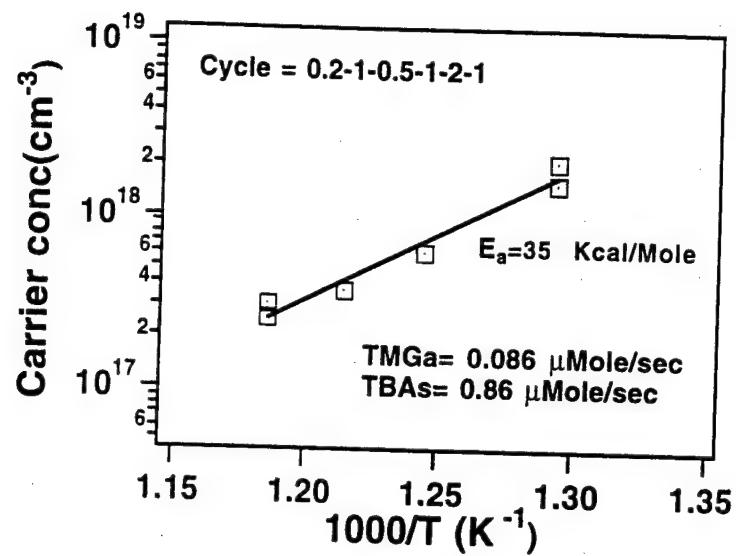


Fig. 4.11 Arrhenius plot of the carrier concentration of layers grown on 75% Ga coverage surface at growth rate in the monolayer regime.

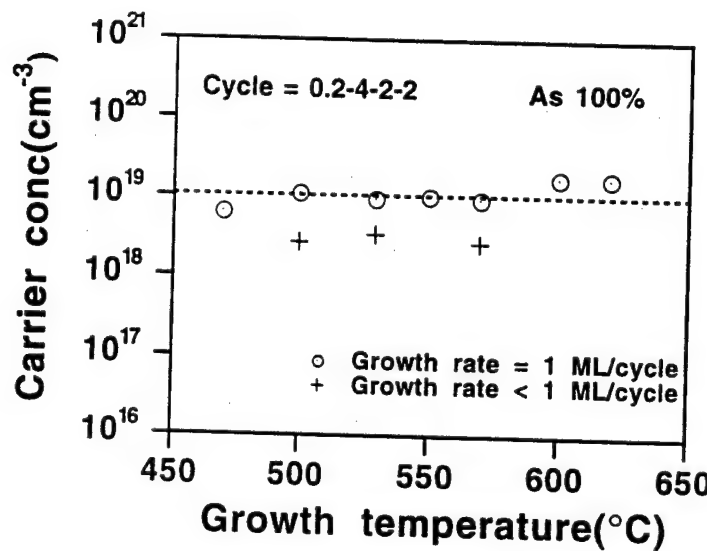


Fig. 4.12 Dependence of substrate temperature on carrier concentration of layers grown in monolayer and submonolayer regimes.

4.5 PROPOSED CARBON INCORPORATION MODEL FOR VALE GaAs USING TMGa

A model for the carbon incorporation into VALE grown GaAs must take into account several observations presented in this chapter. First, the independence of the carrier concentration on the background As and carbon species concentration, as indicated by the LN₂ baffle growth study, indicates that the carbon incorporation is due to the dissociation of the adsorbed carbon species on the surface. Secondly, the CH₃ radical originating from TMGa plays an important role on carbon incorporation. Third, the initial step of the carbon incorporation process happens quickly during the TMGa exposure cycle. However, the whole process may take a long time to complete. Fourth, the sharp transition of the rate of carbon incorporation between the monolayer and the submonolayer regimes indicates that the carbon incorporation is a site-related process in the submonolayer regime, and is supported by the dependence of carbon incorporation on Ga surface coverage. Fifth, the rate limiting step of carbon incorporation is affected by the surface stoichiometry, as indicated by the difference in activation energy of growths on 75% Ga coverage and As terminated surfaces.

The most likely surface carbon species responsible for the incorporation are CH₃ radicals adsorbed on Ga atoms during TMGa exposure. There are two types of CH₃ attached to Ga on

the surface. One is the CH₃ which is transferred from the TMGa molecule to a neighbor Ga atom during the TMGa dissociation. The other is the undissociated TMGa fragments, like Ga(CH₃)₂ (DMGa) or GaCH₃ (MMGa). The MMGa species have been reported as the dominant product species of TMGa fragmentation on a GaAs surface in the VALE temperature range [21,22,23].

We suspect the CH₃ transferred from the dissociated TMGa molecules is not the major source of carbon incorporation. This CH₃ forms a bond with the Ga atom by attacking the Ga-Ga dimer bond. The bonding is weak and unstable at high temperature[21]. It may desorb rather than undergo further dehydrogenation. The life time of this CH₃ radical is less than 1 sec at 500°C[21,24]. The incorporation of this CH₃ radical can not explain the dependence of carbon incorporation on different substrate orientations[1,5]. Nishizawa et al. have reported that the carbon incorporation of GaAs grown on (111)Ga substrate is much lower than on (100) surface even though (111)Ga surface has higher density of Ga atoms than (100) surface[5]. Buchan et al. have also reported that the CH₃ radical has no effects on carbon doping in MOCVD growth[25]. We speculate that the undissociated MMGa on the specific sites of the reconstructed GaAs surface, i.e. Ga vacancy, is the source of carbon incorporation.

The site related model of carbon incorporation is consistent with the time dependent mass spectroscopy data of Maa et al. who observed that the desorption kinetics for CH₃ and MMGa were strongly dependent on the Ga surface coverage[14]. They observed that the desorption rate of CH₃ decreased and the rate of MMGa increased as the surface approached monolayer Ga coverage. The TMGa molecules on the surface are thought to decompose to MMGa by releasing two CH₃ radicals by direct reaction on As atoms. The MMGa species decomposes further to Ga atoms and form Ga-Ga dimers. When the surface is largely covered with As atoms during the initial TMGa exposure, the desorbing species detected by mass spectrometer is CH₃. As the surface approaches a Ga-rich surface, CH₃ desorption decreases and MMGa desorption increases. At the same time, the surface was observed to approach the 4x6 Ga-rich reconstruction. Maa et. al. suggested that this behavior could be explained by the fact that the 4x6 Ga-rich surface was at equilibrium when there was a 3/4 ML Ga coverage comprised of three Ga dimer pairs and a pair of Ga vacancies. The 4x6 Ga surface reconstruction has Ga vacancies occupying 1/4 of the top surface lattice sites[26,27]. At these vacancies, the underlying As atoms are exposed to vacuum. If the reaction of impinging TMGa occurs predominantly on Ga vacancies sites, the only sites for reaction on a 4x6 surface would be those sites that on an equilibrium surface are vacant. As a result, the

complete decomposition of TMGa to Ga on those sites is unfavorable and desorption of the last CH_3 is unlikely[28]. The more favorable desorption species is MMGa. Yu et al. has also reported the similar tendency for MMGa desorption on Ga-rich surfaces[15].

Creighton et al. have reported that the major methyl groups on the surface desorb intact but small numbers of them may undergo dehydrogenation above 400°C [12]. They have proposed that the path for carbon incorporation involves the dehydrogenation of CH_3 on the surface and have presented mass spectroscopic data to support this mechanism. A model that incorporates all of these studies and the data in this chapter is proposed here.

We propose that the dominant mechanism for incorporation of carbon into GaAs during TMGa exposure in VALE is the dehydrogenation of MMGa at the Ga sites that would be vacant on an equilibrium surface reconstruction. At these "unfavorable" sites, complete decomposition of MMGa is unlikely and the reduced tendency for desorption of the last CH_3 leads to an increased probability of dehydrogenation and incorporation. The CH_3 dehydrogenates and forms CH_2 , CH , and C . These species create Ga-CH_2 , Ga-CH , Ga-C bonds. The gallium-carbon bond of these species is more stable than that of GaCH_3 . The number of dehydrogenated species from MMGa will be proportional to the product of the MMGa population

and the number of unfavorable sites. The further the dehydrogenation reaction undergoes, the less likely would be the reverse reaction hydrogenating these species back to CH_3 . The resulting Ga-C configuration would result in the incorporation of C on the As sites as acceptors and the p-type behavior we observed.

The number of dehydrogenated species related to carbon incorporation such as CH_2 , CH , C is small in submonolayer regimes where the population of MMGa is small and the number of unfavorable sites is limited. As the Ga surface coverage increases with TMGa exposures, the population of MMGa increases and the number of unfavorable sites increases, too. This increases the likelihood of the dehydrogenation process causing carbon incorporation. In the monolayer regime, the number of unfavorable sites is constant, but the population of MMGa increases with increased TMGa exposures, leading to increase carbon concentration. The carbon concentration can be expressed as a function of the density of the unfavorable sites and TMGa flux in submonolayer regime and as a function of TMGa flux alone in monolayer regime owing to the constant number of unfavorable sites. This model is consistent with both the observation of increased carbon incorporation with Ga surface coverage in the submonolayer exposure regime and with the similar dependence on TMGa exposure for Ga-rich surfaces regardless of the source of Ga on the surface. The

higher carrier concentration in the ALE mode than in CBE mode with TMGa and TDMAAs indicates that the initial step of MMGa dehydrogenation happens rapidly.

The temperature dependence of carbon incorporation on 75% Ga coverage surface is related to MMGa desorption from the unfavorable sites. The activation energy is 35 kcal/mole which is close to the value of 31 kcal/mole reported by Creighton[29]. The rate limiting step of carbon incorporation of growth on As terminated surface is different from on 75% Ga surface, as indicated by the decreased dependence on the substrate temperature. It is possible that the incorporation process is limited by the adsorption of MMGa on the unfavorable sites because of the number of unfavorable site is limited on As terminated surface.

4.6 CONCLUSIONS

The mechanism of carbon incorporation has been studied using a LN₂ baffle to minimize the background As and CH₃ concentration and various Ga and As metalorganic sources. The carbon concentration is independent of the temperature of LN₂ baffle. The growth of GaAs with TMGa and TDMAAs shows higher carbon concentration in the ALE mode than in CBE mode. The carbon concentration on a surface partially covered with Ga atom is higher than on As-terminated surface in submonolayer regime. The growth on 75% Ga coverage shows

strong temperature dependence with the activation energy of 35 kcal/mole which is related to the desorption of MMGa from the surface. However, the growth on As-terminated surface shows no dependence of substrate temperature. MMGa adsorbed on the unfavorable vacancy site in a reconstructed Ga-rich surface is the dominant species responsible for the carbon incorporation.

REFERENCES

- [1] T. F. Kuech and E. Veuhoff, *J. Crystal Growth* 68, 148(1984).
- [2] M. Masi, H. Simka, K. F. Jensen, T. F. Kuech and R. Potemski, *J. Crystal Growth*, 124, 483(1992).
- [3] T. Mountziaris and K. F. Jensen, *J. Electrochem Soc.*, 138, 2426(1991).
- [4] N. Pütz, H. Heinecke, M. Heyen, P. Balk, M. Weyers and H. Lüth, *J. Crystal Growth*, 74, 292(1986).
- [5] J. Nishizawa, H. Abe and T. Kurabayashi, *J. Electrochem Soc.*, 132, 1197(1985).
- [6] K. Mochizuki, M. Ozeki, K. Kodama and N. Ohtsuka, *J. Crystal Growth*, 93, 557(1988).
- [7] M. Y. Jow, B. Y. Maa, T. Morishita and P. D. Dapkus, *J. Electron. Mater.* (to be published)
- [8] R. M. Lum, J. K. Klingert, D. W. Kisker, S. M. Abys and F. A. Stevie, *J. Crystal Growth*, 93, 120(1988).
- [9] K. Ishikura, A. Takeuchi, M. Kurihara, H. Machida and F. Hasegawa, *Jpn. J. Appl. Phys.* 33, L495(1994).
- [10] M. Mashita, M. Sasaki, Y. Kawakyu and H. Ishikawa, *J. Crystal Growth*, 131, 61(1993).
- [11] C. R. Abernathy, *J. Crystal Growth*, 107, 982(1991).
- [12] J. R. Creighton, B. A. Bansenauer, T. Huett and J. M. White, *J. Vac. Sci. Technol. A11*, 876(1993).

- [13] M. L. Yu, U. Memmert and T. F. Kuech, *Appl. Phys. Lett.* 55, 1011(1989).
- [14] B. Y. Maa and P. D. Dapkus, *Thin Solid Films*, 225, 12(1993).
- [15] M. L. Yu, *J. Appl. Phys.* 73, 716(1993).
- [16] B. A. Banse and J. R. Creighton, *Surf. Sci.* 257, 221(1991).
- [17] T. H. Chiu, W. T. Tsang, E. F. Schubert and E. Agyekum, *Appl. Phys. Lett.* 51, 1109(1987).
- [18] Y. Sakuma, M. Ozeki, N. Ohtsuka and K. Kodama, *J. Appl. Phys.* 68, 5660(1990).
- [19] C. R. Abernathy, P. W. Wisk, S. J. Pearton, F. Ren, D. A. Bohling and G. T. Muhr, *J. Crystal Growth*, 124, 64(1992).
- [20] K. Fujii, I. Suemune, T. Kou and M. Yamanishi, *Appl. Phys. lett.* 60, 1498(1992).
- [21] U. Memmert and M. L. Yu, *Appl. Phys. Lett.* 56, 1883(1990).
- [22] J. R. Creighton, *Surf. Sci.* 234, 287(1990).
- [23] L. Q. Liu, B. B. Huang, H. W. Ren and M. H. Jiang, *J. Crystal Growth*, 115, 83(1991).
- [24] B. Y. Maa and P. D. Dapkus, *Appl. Phys. Lett.* 58, 2261(1991).
- [25] N. I. Buchan, T. F. Kuech, D. Beach, G. Scilla and F. Cardone, *J. Appl. Phys.* 69, 2156(1991).

- [26] D. J. Frankel, C. Yu, J. P. Harbison and H. H. Farrel, *J. Vac. Sci. Technol.* B5, 1113(1987).
- [27] D. J. Chadi, *Ultramicroscopy*, 31, 1(1989).
- [28] H. H. Farrel, J. P. Harbison and L. D. Peterson, *J. Vac. Sci. Technol.* B5, 1482(1987).
- [29] J. R. Creighton, *J. Vac. Sci. Technol.* A9, 2895(1991).

Chapter 5

Selective Area Epitaxy of GaAs by VALE

5.1 INTRODUCTION

In contrast to silicon integrated circuit technology in which there is only one epitaxial material, optoelectronic integrated circuit(OEIC) components are comprised of multilayer epitaxial structures involving different materials[1]. Selective area epitaxy(SAE) of the device structures is a promising approach to the integration of disparate electronic and optoelectronic devices. In principle, the materials for optical and electronic devices can be grown selectively on different areas of the wafer using dielectric masks to inhibit growth in certain regions. Selective area epitaxy by conventional epitaxial techniques, like MBE, MOCVD and CBE, typically exhibit nonuniformities of growth rate and composition in the grown regions[2~6]. The reactants adsorbed on the mask areas tend to diffuse into the opening , which results in a concentration gradient at the edge of the opening and a strong dependence of the growth on the aspect ratio, defined as masked to unmasked area ratio. The concentration gradient causes composition nonuniformity across the opening and raised features at the edges, which limits the useful area in the opening. The strong influence of the aspect ratio causes difficulties in controlling the composition

and growth rate in various size openings on the wafer and will add more restrictions on the design of the mask layout.

The unique characteristic of surface-controlled, self-limiting decomposition of reactants inherent to vacuum atomic layer epitaxy(VALE) make it a promising approach to control selective area growth. The decomposition of reactants are controlled by low temperature surface reactions and self-limited at one monolayer per cycle of reactant exposure. In this way, it is possible to achieve perfectly selective epitaxy and control of the deposits in the openings on an atomic scale with no aspect ratio effects. In this chapter, the characteristics of selective area growth of GaAs by VALE in dielectric openings oriented in various directions on (100) GaAs wafers are discussed in section 5.3.1. The selective area growth in trenches and on vertical sidewalls will also be discussed in sections 5.3.2 and 5.3.3, respectively.

5.2 SAMPLE PREPARATION

The GaAs(100) substrates are coated with 2000Å SiN_X with plasma enhanced chemical vapor deposition(PECVD) and patterned with stripes along various directions using photolithography. Then the dielectric layers are removed by reactive ion etching(RIE) to form the openings. The orientations of the stripes are along <011>, <01 $\bar{1}$ > and <010>. The size of the openings are varied from 3μm to 100μm, while the spacings

between stripes are kept constant. The samples for selective area epitaxy in trenches are prepared with $H_2SO_4:H_2O_2:H_2O$ (1:15:15) etching solution to create (111)A trench sidewalls. The trenches are oriented in $<011>$ and $<01\bar{1}>$ directions. In addition, the samples for vertical sidewall growth are oriented along $<010>$ and $<011>$ directions. The growth temperature is chosen to be $530^\circ C$ taking advantage of the wide ALE window ($500^\circ C \sim 570^\circ C$) so that the SAE has a large temperature tolerance. During VALE growth, the substrate is exposed to TMGa for 0.2 sec and TBAs for 2 sec alternatively with a 1 sec pumping period in between to prevent gas intermixing, and the exposure levels (flow rates) of TMGa and TBAs are $0.86\mu Mole/sec$. The grown samples are examined by optical microscope, scanning electron microscope(SEM) and Dektak surface profiler.

5.3 GROWTH RESULTS AND DISCUSSION

5.3.1 Selective area epitaxy(SAE) on SiN_x masked substrate.

Fig. 5.1 shows the top view of selective area epitaxy of GaAs by VALE. There are no deposits on the mask area, and the surface morphology of the growth in the opening is specular. The Dektak profile in Fig. 5.2 shows flat-topped surfaces with no raised features at the edges and a growth rate equal to one monolayer per cycle.

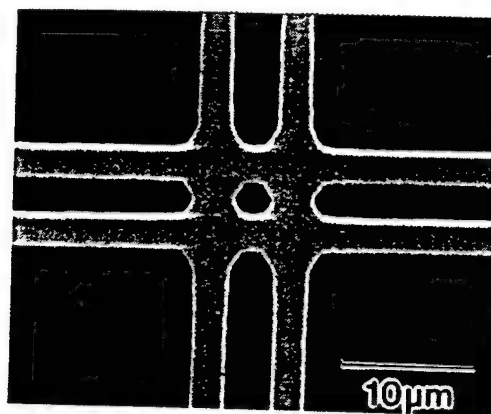


Fig. 5.1 Selective area epitaxy of GaAs by VALE.

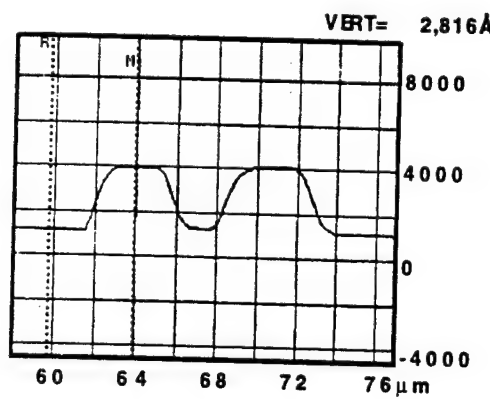


Fig. 5.2 Thickness profile of GaAs stripe after removing SiNx.

These results indicate that the mechanisms of SAE using VALE are different from MOCVD and CBE growth[4,7,8]. In MOCVD or CBE, decomposition of reactants on the masked regions causes several undesirable characteristics in the epitaxial region. The most common phenomena are raised features at the window boundaries and the strong dependence of the growth rate and composition on the aspect ratio. This property is due to the gas phase diffusion and surface

migration from the dielectric to the opening and surface migration of the materials on side facets[9]. Fig. 5.3 is a typical SEM cross section of SAE using the CBE mode in the same reactor. It shows raised features at the edges and a curved thickness profile across the opening, which results from the migration of species from the dielectric and side facets to the top surface.

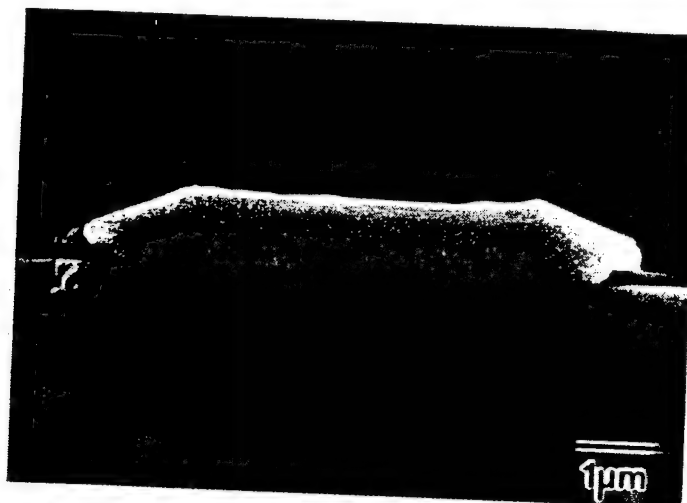


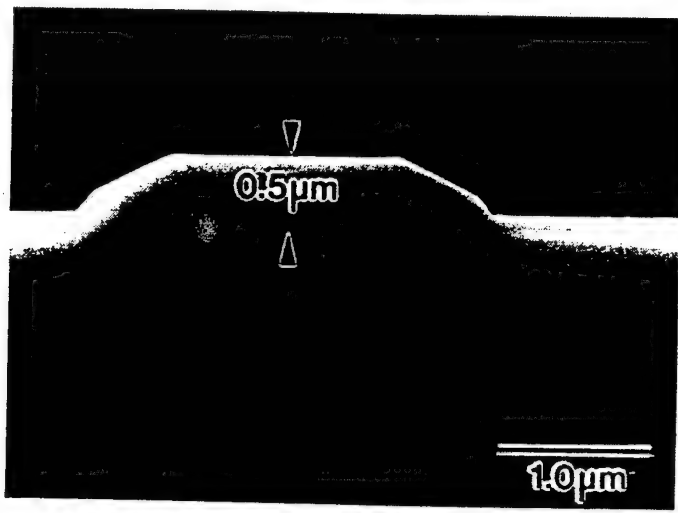
Fig. 5.3 SEM cross section of GaAs SAE using CBE mode.

For VALE growth, the SEM cross section in Fig. 5.4 shows flat-topped surfaces, as expected from thickness profiles, which is caused by the self-limiting decomposition of the reactant species. The adsorbed species on the dielectric and on the side facets will desorb before they decompose or migrate to the fast growing top surface plane. Adsorbed species which do migrate to the top surface cannot decompose there if the surface is already saturated. Thus, once the top surfaces are covered with

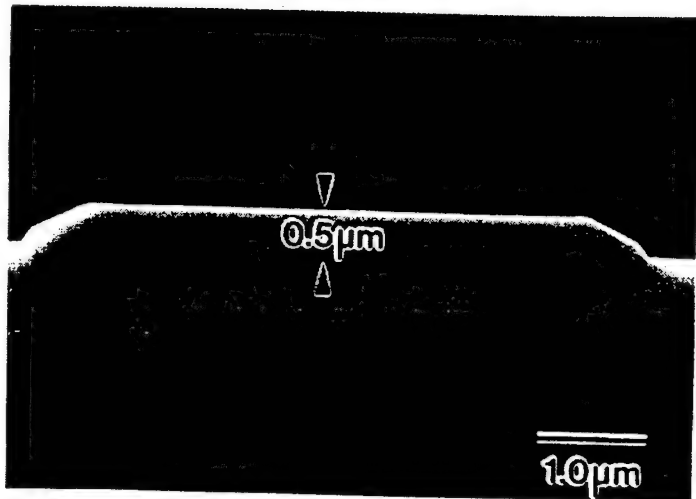
the reactants, the surface reaction stops. Therefore, although reactants' arrival rate at the edges is larger than at the center of the opening, there is only one monolayer of the reactants decomposed. This results in a uniform deposition across the opening. By the same principle, the self-limiting decomposition also eliminates the aspect-ratio-induced-enhancement of the growth rate in the opening. As shown in Fig. 5.4(a) and (b), the GaAs thickness is independent of the size of the openings, and the growth rate is one monolayer per cycle -- the same as on unmasked substrates. The achievement of flat-topped surfaces and atomically controlled thickness in the opening makes VALE an important tool for the integration of electronic and optical devices.

Another important issue seen in Fig. 5.4 is facet formation. From the cross section view, the stripe has developed (311) facets closed to the top surface and (111) facets at the bottom. The formation of these facets is caused by the low growth rate of those facets[9,10,11]. Isshiki et al. reported that the low growth rate is due to the desorption of As species[11]. Since, in VALE growth, there is a pumping period after TBAs exposure, the desorption of As species is enhanced and results in better defined facet formation than using CBE as in Fig. 5.3. The stable development of the facets during growth will benefit the fabrication of nanostructure quantum-sized devices, like quantum wires and quantum dots. The uniformity and atomic

scale controllability of the thickness makes VALE a viable technique to make quantum wire and quantum dot arrays which are still very difficult tasks for conventional techniques[12,13].



(a)



(b)

Fig. 5.4 Cross section of stripes along $<01\bar{1}>$ with the openings of (a) $3\mu\text{m}$ (b) $6.3\mu\text{m}$.

The dependence of facet formation on the direction of the stripes has also been studied. Fig. 5.5 and Fig. 5.6 show the cross section view of $<011>$ stripe and tilted view of $<010>$ stripe cleaved along $<01\bar{1}>$, respectively. The facets of $<011>$ oriented stripes are $(3\bar{1}1)$ and $(0\bar{1}1)$, and (101) facets are formed on $<010>$ stripes. Table 1 is the summary of the facet formation observed in this study. In Fig. 5.6, the (101) facets are very smooth and are tilted 45° with respect to (100) substrate, suggesting that these facets could possibly be used as 45° mirrors for surface emitting laser diodes. The optical quality of the VALE grown mirror should be better than a mirror created by dry etching because dry etch processes always cause a certain degree of damage and roughness on the mirror surface[14].

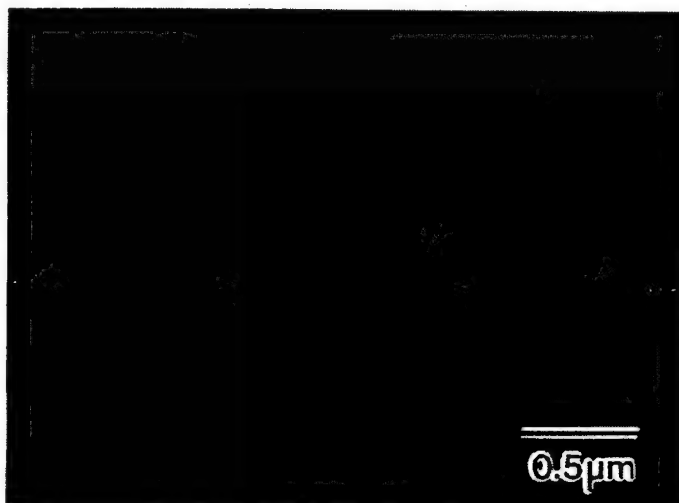


Fig. 5.5 SEM cross section of $<011>$ stripe.

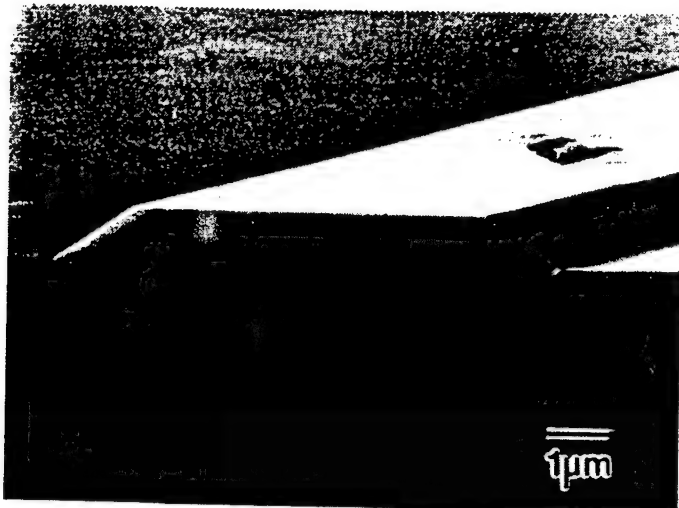


Fig. 5.6 SEM view of $<010>$ strip cleaved along $<0\bar{1}\bar{1}>$ direction.

Table 1. Summary of the facet formation of different direction of stripes.

Stripes	Facet formation
$<0\bar{1}\bar{1}>$	(311), (111)A
$<011>$	(3 $\bar{1}$ 1), (0 $\bar{1}$ 1)
$<010>$	(101)

5.3.2 Slective area epitaxy in trenches

So far, most of the selective area growths have been done on planar dielectric openings. However, it is realized that an important application of SAE lies with growth in trenches to achieve planarization[1]. In order to integrate optical devices and electronic devices on the same wafer with a surface suitable for fine line lithography, the optical devices need to be grown

in trenches. However, SAE in trenches is more complex and difficult because various crystal planes are involved. Fig. 5.7 is the SEM cross section of SAE in trenches using CBE mode in our reactor. The trench is oriented along $<011>$ and etched with $\text{H}_2\text{SO}_4:\text{H}_2\text{O}_2:\text{H}_2\text{O}$ (1:15:15) to create (111)A sidewalls. The figure shows that there is a void under the edge of the SiN_x layer, which is the result of shadowing effects of the dielectric layer overhang and the inconsistency of the growth rate on (111)A and (100) planes. These voids will cause current leakage, light scattering and interface defects, which are not acceptable for device applications.

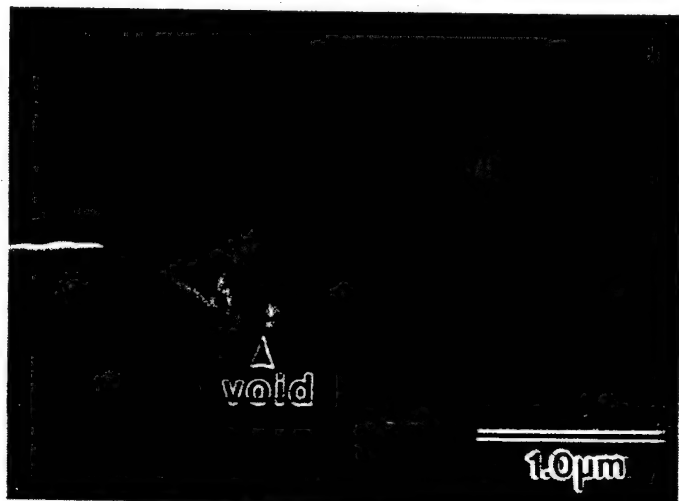


Fig. 5.7 SEM cross section of SAE by CBE in $<011>$ trenches.

On the contrary, no voids are observed under the dielectric layer in the VALE growth, as seen in Fig. 5.8(a) and (b). The trenches are completely refilled by VALE GaAs with a growth rate of one monolayer per cycle, and with good surface morphology. The interfaces between (111)A sidewalls and the grown layers are free of any detectable defects under SEM examination.

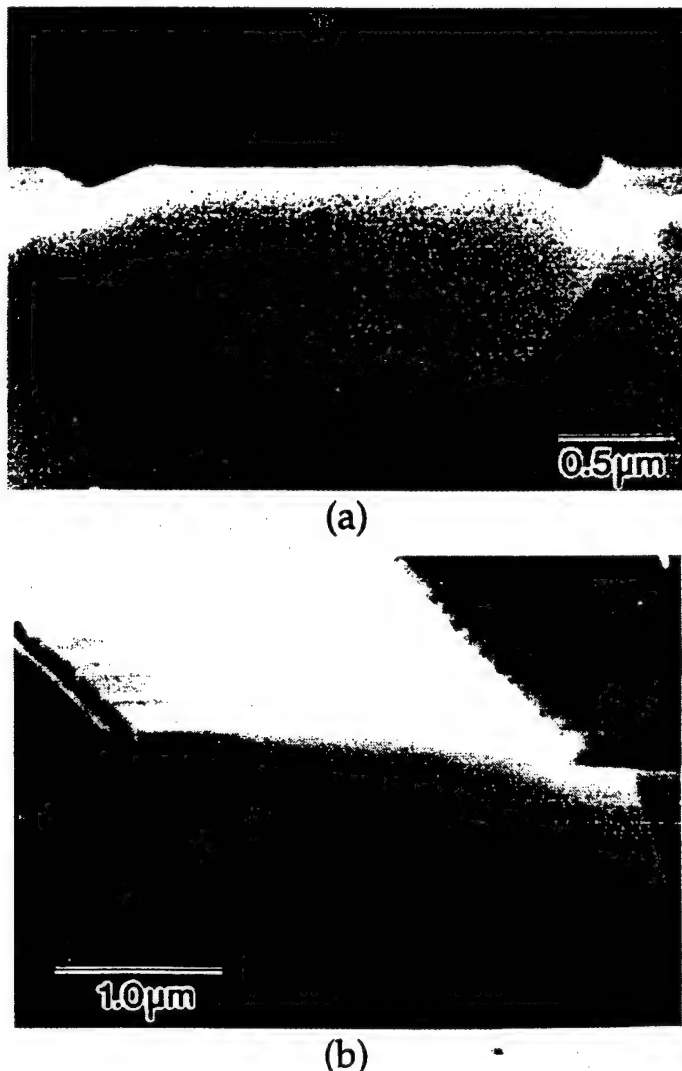


Fig. 5.8 SEM cross section of SAE by VALE in trenches along (a) $<01\bar{1}>$ (b) $<011>$.

This result can be explained by the self-limiting deposition that occurs on the (100) plane and the smaller growth rate that occurs on (111)A facets. Nishizawa et. al. and Isshiki et. al. both found that the ALE growth was strongly dependent on the substrate orientation[10,11]. They reported the growth rate of (111)A was only 0.1 monolayer per cycle at 530°C, and close to zero at higher temperatures. Therefore, in our case, layer-by-layer growth only occurs on the (100) plane, but little or no growth occurs on the (111)A sidewall such that the growth can refill the trench completely.

5.3.3 Selective area epitaxy on vertical sidewall

In addition to SAE in trenches, vertical sidewall growth is also an important technology for making high density circuits and nanostructure devices[15]. Fig. 5.9 shows the VALE growth on the (00 $\bar{1}$) sidewall. The substrate was patterned along <010> direction and then deep etched to create (00 $\bar{1}$) facets on the sidewall prior to the SAE growth. The figure shows the grown layers on the (100) plane and the (00 $\bar{1}$) sidewall are uniform, and the growth rate is one monolayer per cycle. The presence of the dielectric layer overhang does not affect the growth on the bottom and on the sidewall, owing to the self-limiting deposition by VALE. This indicates that VALE can achieve good uniformity and precise control for vertical sidewall growth.

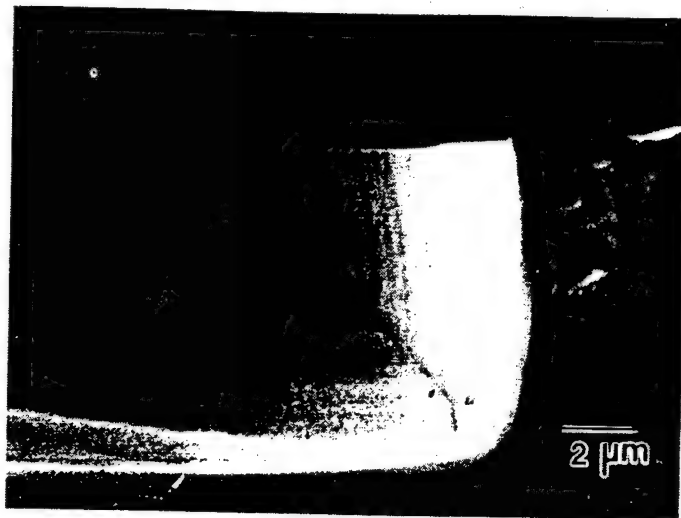


Fig. 5.9 SEM view of the $(00\bar{1})$ sidewall growth by VALE. The sample was cleaved along $\langle 011 \rangle$ direction.

The achievement of the $(00\bar{1})$ sidewall growth by VALE has generated interest in using such growth for applications. One of the ideas is the passivation of the ECR etched mirrors using VALE sidewall growth of GaAs. We found that the surface morphology of (011) and $(00\bar{1})$ facets after regrowth shows different behavior. The $(00\bar{1})$ facet is smooth and specular after the regrowth but the (011) facet becomes rough. Fig. 5.10 (a) and (b) shows the difference. This is probably due to the very low growth rate of GaAs on (011) facets by ALE[10,11]. Since the ECR etched (011) surface is a terraced plane which contains facets between two (011) steps. The growth may occur on these facets but not on the (011) plane resulting in three dimensional growth and surface roughness. The situation on $(00\bar{1})$ surface contrasts with that of the (011) surface. There is monolayer growth on the $(00\bar{1})$ surface but no growth on the side facets.

Recently, we have compared the quality of the ECR etched mirrors with sidewall passivation by characterizing the properties of edge emitting laser diodes. The results confirm that the passivation of ECR etched $(00\bar{1})$ mirrors can improve the quality of the mirrors and reduce the threshold current of the laser diode by 50%, but the regrowth on (011) sidewall deteriorates the mirrors' quality[14].

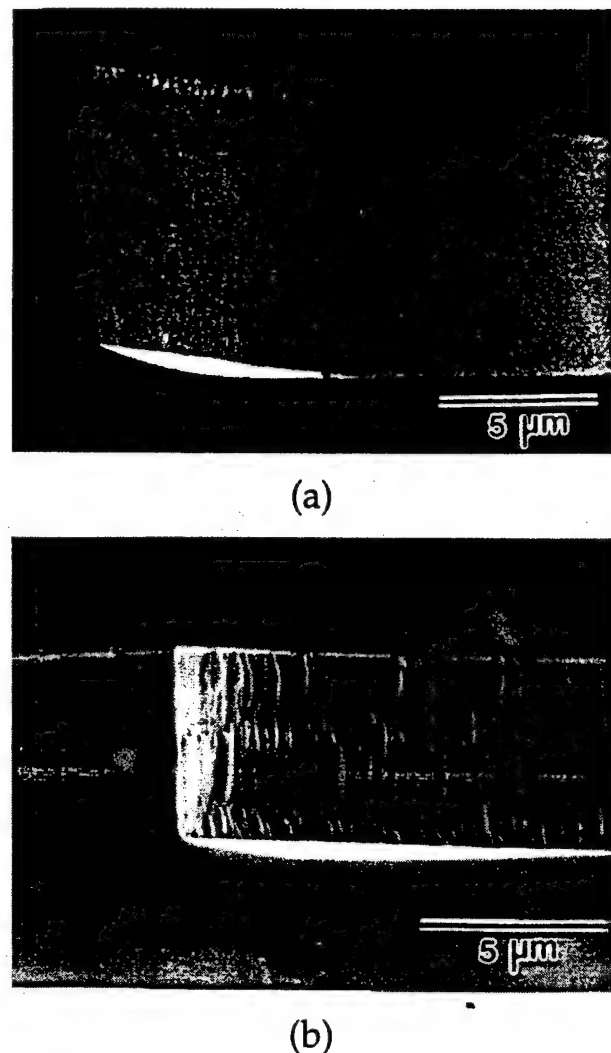


Fig. 5.10 The surface morphologies of the regrowth on (a) $(00\bar{1})$ (b) (011) ECR etched mirrors.

5.4 CONCLUSION

We have reported SAE of GaAs on SiN_x masked substrates using VALE. SAE results in flat-topped surfaces, and the growth rate in the opening is one monolayer per cycle. The growth is independent of the aspect ratio. These achievements are due to the self-limiting deposition of VALE. SAE on different orientation stripes results in different facet formation depending on the orientation of the stripes. In addition, the SAE in trenches shows complete refilling of the trench without any voids. Vertical $(00\bar{1})$ sidewall growth is achieved by VALE with perfect uniformity and atomic level control. The quality of the ECR etched $(00\bar{1})$ mirrors is improved by VALE regrowth.

REFERENCES

- [1] I. D. Henning, *Prog. Crystal Growth and Charact.* 19 (1989) 1.
- [2] G. J. Davies, W. J. Duncan, P. J. Skevington, C. L. French and J. S. Foord, *Mater. Sci. Eng. B9* (1991) 93.
- [3] R. Bhat, *J. Crystal Growth*, 120 (1992) 362.
- [4] H. Heinecke, A. Milde, B. Baur and R. Matz, *Semicond. Sci. Technol.* 8 (1993) 1023.
- [5] W. T. Tsang, *Semicond. Sci. Technol.* 8 (1993) 1016.
- [6] A. Okamoto, *Semicond. Sci. Technol.* 8 (1993) 1011.
- [7] T. Sasaki, M. Kitamura and I. Mito, *J. Crystal Growth*, 132 (1993) 435.
- [8] O. Kayser, R. Westphalen, B. Opitz and P. Balk, *J. Crystal Growth*, 112 (1991) 111 .
- [9] T. F. Kuech, *J. Crystal Growth*, 115 (1991) 52 .
- [10] J. Nishizawa, T. Kurabayashi, H. Abe and A. Nozoe, *Surface Sci.* 185 (1987) 249.
- [11] H. Isshiki, Y. Aoyagi, T. Sugano, S. Iwai and T. Meguro, *Appl. Phys. Lett.* 63(11) (1993) 1528.
- [12] M. López, T. Ishikawa and Y. Nomura, *Jpn. J. Appl. Phys.* 32 (1993) L1051.
- [13] Y. Nagamune, M. Nishioka, S. Tsukamoto and Y. Arakawa, *Appl. Phys. Lett.* 64(19) (1994) 2495.

- [14] N. C. Frateschi, M. Y. Jow, P. D. Dapkus and A. F. J. Levi,
Appl. Phys. Lett. to be published.
- [15] A. Usui, H. Sunakawa, F. J. Stützler and K. Ishida,
Appl. Phys. Lett. 56(3) (1990) 289.

Chapter 6

Conclusions and Recommendations for Future Work

6.1 CONCLUSIONS FROM THIS WORK

In this work, a vacuum atomic layer epitaxy (VALE) reactor has been designed, constructed and used to grow GaAs by VALE and chemical beam epitaxy (CBE). The reservoir design of the gas handling system allows VALE to fully utilize the reactants, and the fast switching of the valves enables higher growth rate than other reported UHV ALE.

Monolayer growth by VALE is achieved over a wide range of growth parameters. The temperature window is from 500°C to 570°C which is the widest temperature range ever been reported by UHV ALE and also wider than most of the atmospheric pressure ALE processes. The success in monolayer growth of GaAs by VALE indicates that the suppression of the gas phase decomposition of TMGa is the key issue for achieving monolayer growth. TBAs is an efficient As source in VALE, as indicated by the short exposure time required for monolayer growth. Background As species desorbing from the heater assembly causes the loss of monolayer growth when not adequately controlled.

Serious carbon incorporation is observed in GaAs grown by VALE using TMGa as the Ga source. The study in chapter 4 indicates several aspects of the carbon incorporation mechanism. First, the carbon incorporation is due to the dehydrogenation of the adsorbed MMGa on unfavorable Ga vacancy sites. Second, the initial step of the incorporation process happens very fast during TMGa exposure, but the whole process may take several seconds to complete. Third, the carbon incorporation is an intrinsic property of TMGa decomposition on (100) GaAs surface, as indicated by the dependence of carbon concentration on Ga coverage surface. Fourth, the rate limiting step of the carbon incorporation depends on the surface Ga/As stoichiometry.

Selective area growth of GaAs is successfully achieved by VALE. The GaAs selective growths show flat-topped surfaces, and the growth rate in the unmasked area is one monolayer per cycle, independent of the aspect ratio. The facets formed on the selectively grown island depend on the orientation of the mask opening. Selective area epitaxy in trenches shows complete refilling of the trench without any voids. Vertical $(00\bar{1})$ sidewall growth is achieved by VALE with perfect uniformity and atomic level control.

6.2 RECOMMENDATIONS FOR FUTURE WORK

Atomic layer epitaxy by VALE has demonstrated several unique properties of GaAs growth including atomic level control of the thickness and excellent selective area epitaxy. Carbon incorporation is the current major difficulty for VALE. It seems the carbon incorporation is an intrinsic property of TMGa on the GaAs surface. Since the self-limiting decomposition and carbon incorporation is related to the surface chemistry of TMGa on the surface, it is possible to find a novel Ga metalorganic source with proper radical which can accomplish the satisfaction of monolayer growth as well as low carbon concentration. The use of foreign chemical species or energized particles, e.g. photon, electron and ion, flowing with TMGa to prevent the carbon incorporation process is also an interesting topic for the future. Of course, the study of the surface kinetics of these reactions will also be very interesting. The growth of InP material system by VALE may be interesting because carbon does not incorporate as an acceptor. The study of heterostructure interfaces by using VALE in concert with CBE is also an interesting topic.

Appendix 4

Q. Chen, C. A. Beyler, P. D. Dapkus, J. J. Alwan, and J. J. Coleman, "Use of tertiarybutylarsine in atomic layer epitaxy and laser assisted atomic layer epitaxy of device quality GaAs," Appl. Phys. Lett. 60, 2418 (1992)

Use of tertiarybutylarsine in atomic layer epitaxy and laser-assisted atomic layer epitaxy of device quality GaAs

Q. Chen, C. A. Beyler, and P. D. Dapkus

National Center for Integrated Photonic Technology, Departments of Materials Science and Electrical Engineering/Electrophysics, University of Southern California, Los Angeles, California 90089-0483

J. J. Alwan and J. J. Coleman

Microelectronics Laboratory, Materials Research Laboratory, Department of Electrical and Computer Engineering, University of Illinois, Urbana, Illinois 61801

(Received 3 October 1991; accepted for publication 4 March 1992)

The use of trimethylgallium (TMGa) and tertiarybutylarsine (TBAs) in atomic layer epitaxy (ALE) and laser-assisted atomic layer epitaxy (LALE) of GaAs is studied for the first time. TBAs is found to be a direct and suitable replacement for arsine (AsH_3) in achieving monolayer self-limiting growth. Carbon contamination in the GaAs films grown by LALE using TMGa and TBAs is greatly reduced relative to those using TMGa and AsH_3 . Laser structures with single GaAs quantum wells grown by ALE and LALE using TBAs exhibit threshold current densities as low as 300 and 520 A/cm^2 , respectively.

Atomic layer epitaxy (ALE) employing metal alkyl and hydride sources is attracting increased attention as an approach for the growth of III-V semiconductors because it offers several unique processing capabilities.¹⁻⁸ However, the reduction of the carbon background impurity levels that are believed to result from the incomplete decomposition of metal alkyls on the surface is a persistent problem in low temperature ALE and LALE growth involving an organometallic precursor. With regards to this problem, we present the first study of the use of tertiarybutylarsine (TBAs) as an arsenic source in ALE and LALE growth of high-quality GaAs materials. TBAs was chosen for the study because it is known to decompose at lower temperature than AsH_3 ,⁹⁻¹² is believed to remove CH_3 from the surface more efficiently than AsH_3 ,¹³ and has been used in conventional MOCVD growth of GaAs and AlGaAs to produce high-quality bulk materials and devices.¹⁴

The ALE and LALE work described here was carried out in a conventional atmospheric pressure MOCVD system outfitted with a specially designed quartz tube.¹⁵ The reactor tube is a horizontal laminar flow-type reactor with a flat window for optical access. The window is flushed by a separate stream of H_2 . The SiC-coated graphite susceptor is inductively heated and the temperature monitored with a thermocouple. The uniqueness of our reactor design lies in its full compatibility with conventional MOCVD, permitting the growth of double heterostructures (DHs) and quantum wells (QWs) with the GaAs region grown by ALE or LALE and the $\text{Al}_x\text{Ga}_{1-x}\text{As}$ cladding layers by MOCVD.

Alternate exposure of the substrate to TMGa and TBAs (or AsH_3) is achieved by the temporal switching of TMGa and TBAs into the main H_2 carrier flow. An exposure mode of 1 s of TMGa exposure, 4 s of H_2 purge, 4 s of TBAs exposure, and another H_2 purge of 4 s will be designated as a 1-4-4-4 exposure mode. ALE is performed at 480 °C and LALE at 380 °C. The 514.5 nm line of an Ar ion laser is used for all LALE growths in this letter. The laser beam is first expanded and then focused with a cylindrical lens to obtain suitable intensity over a narrow line of

typical dimensions as 300 μm wide and 4 mm long. A shutter consisting of a beam stop and a stepper motor is employed to control the timing of the laser illumination, i.e., both with respect to the duration of the illumination and to the initiation of the TMGa exposure. The optical pulse is typically 0.1 s duration.

To characterize material quality several types of structures were produced. For PL measurements, DHs and QWs with ALE- or LALE-grown GaAs sandwiched between MOCVD $\text{Al}_{0.3}\text{Ga}_{0.7}\text{As}$ cladding layers were formed. Capacitance-voltage ($C-V$) measurements with a Schottky junction formed by a Au or Ag dot used similar DHs as well as samples with a thick (0.5 μm) top GaAs layer grown by LALE. For secondary ion mass spectrometry (SIMS) profiling, multiple layer DHs with each ~700 Å thick GaAs layer using a different combination of precursors were produced. As a means of testing the quality of the material for device applications, GRINSCH QW laser structures were formed with the single GaAs QW (100 Å) grown by ALE or LALE.

For ALE study, suitable exposure modes obtained from previous growth using TMGa and AsH_3 were used directly in the experiments using TBAs. QWs and DH structures were grown with the central GaAs region by ALE using TBAs at nominal V/III ratios of 3 and 3.6. It is more reasonable to use a V/III ratio pertaining to the ALE mode of operation, i.e., $(V/\text{III})_{\text{ALE}} = (\text{moles of group V injected in a cycle}) / (\text{moles of group III injected in a cycle})$. The corresponding $(V/\text{III})_{\text{ALE}}$ ratios at a 1-4-4-4 mode are 12 for the QWs and 14.4 for the DH.

The final surface morphology of the QWs and DH with the central GaAs region 200 monolayers thick (565 Å) grown by ALE are featureless as viewed by the naked eye and under $\times 1000$ optical microscope, indicating perfect layer-by-layer growth. Room-temperature PL can be observed from these QWs and DH at moderate excitation, as is shown by the dashed trace in Fig. 1 for a DH structure. The observation of intense room-temperature luminescence suggests that the materials and interfaces are of reasonably good quality.

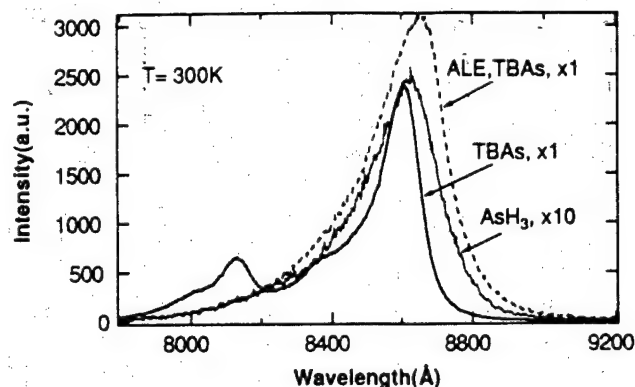


FIG. 1. Photoluminescence spectra from DHs grown by ALE (dashed line) and LALE (solid line) using TMGa and TBAs and by LALE using TMGa and AsH_3 (dotted line). Note that the samples grown using TBAs have $\sim 10\times$ higher PL efficiency.

The samples grown by LALE using TMGa and TBAs are specular on and off the LALE stripe for typical flow conditions which correspond to a nominal V/III ratio of ~ 0.64 if the TMGa and the TBAs were to be injected simultaneously into the reactor and a $(\text{V}/\text{III})_{\text{ALE}}$ as low as 2.5. This result is in accord with the results from MOCVD using TMGa and TBAs where a V/III of approximately unity could be used to obtain GaAs layers of good morphology.^{9,16}

Self-limiting LALE growth using TBAs occurs over a similar range of laser intensities as those using AsH_3 , specifically from $\sim 750 \text{ W/cm}^2$ up to 1 kW/cm^2 on bare N^+ GaAs oriented 2° off (100) and thus is a direct replacement for AsH_3 . Thin GaAs layers ($\sim 565 \text{ \AA}$) grown by LALE using TBAs show intense photoluminescence emission at room temperature. The solid and dotted lines in Fig. 1 compare typical PL spectra from DHs grown using TBAs and AsH_3 , respectively. For both cases, the exposure modes are 1-5-5-4 and the laser illumination durations are 0.1 s. GaAs layers using TMGa and TBAs show about ~ 7 - 10 -fold higher PL efficiency than films grown using TMGa and AsH_3 . In addition, the whole $\text{Al}_{0.3}\text{Ga}_{0.7}\text{As}/\text{GaAs}/\text{Al}_{0.3}\text{Ga}_{0.7}\text{As}$ structure for the TBAs case exhibits a much lower rate of nonradiative recombination, as evidenced by the QW peak on the short wavelength side of the main peak. This peak originates from the excess carriers diffusing through the $\sim 1.7 \mu\text{m}$ isolation layer, and being captured by the conventional MOCVD QW deliberately imbedded in the lower part of these DH structures. This is a result of a low nonradiative recombination rate either in the LALE GaAs or at the interfaces or both. Complete isolation was possible when the $\text{Al}_{0.3}\text{Ga}_{0.7}\text{As}$ layer thickness was increased to about $2.5 \mu\text{m}$.

Figure 2 shows the results of C-V measurements. In Fig. 2(a), the carrier concentration profile from a DH with the central GaAs layer grown by LALE using TBAs is compared to one with the GaAs layer grown using AsH_3 . In the first case, no acceptor related impurity is detected above the background level of the conventionally grown $\text{Al}_{0.3}\text{Ga}_{0.7}\text{As}$, i.e., $p \sim 3 \times 10^{15} \text{ cm}^{-3}$. This is in contrast to

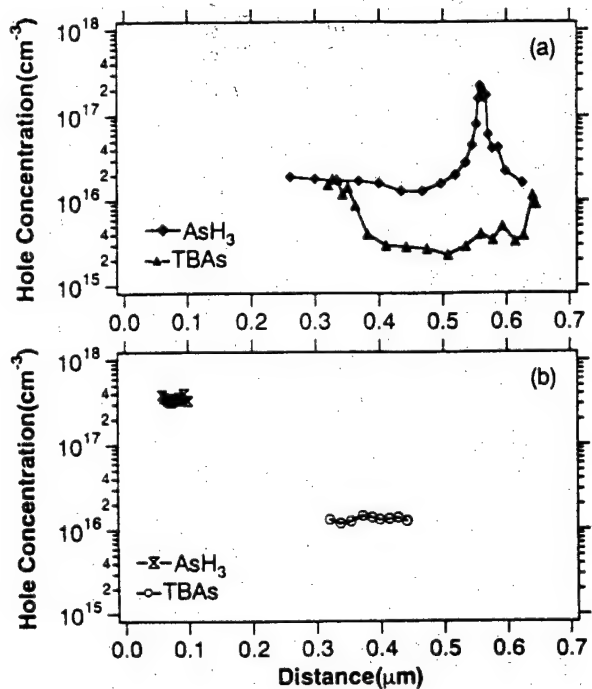


FIG. 2. C-V profiles of (a) the DH structures with GaAs grown by LALE using TMGa and TBAs and TMGa and AsH_3 , and (b) $0.5\text{-}\mu\text{m}$ -thick GaAs grown by LALE using TMGa and TBAs and TMGa and AsH_3 .

the appreciable amount of acceptors in the GaAs grown using TMGa and AsH_3 . The C-V data from the measurements performed directly on the $0.5\text{-}\mu\text{m}$ -thick LALE grown GaAs are included in Fig. 2(b). The hole concentration is $3\text{-}4 \times 10^{17} \text{ cm}^{-3}$ for the material grown using TMGa and AsH_3 and between 1 and $2 \times 10^{16} \text{ cm}^{-3}$ using TMGa and TBAs.

This low-carbon contamination in the GaAs grown by LALE using TMGa and TBAs is further confirmed by SIMS measurements. Figure 3(a) shows the C, Al, and H traces of SIMS profiles on a three-layer DH where the drawing over the traces is meant to locate the approximate boundaries of each layer. Only the GaAs layer grown by LALE using TMGa and AsH_3 , layer (III), shows appreciable amounts of carbon relative to the background level in the MOCVD grown $\text{Al}_{0.3}\text{Ga}_{0.7}\text{As}$ layers. The GaAs layer grown by LALE using TMGa and TBAs, layer (II), contains, at most, a level of carbon within the background of the conventional MOCVD $\text{Al}_{0.3}\text{Ga}_{0.7}\text{As}$ layer on which the LALE is performed. The smearing at the GaAs/AlGaAs interfaces is believed to be a measurement artifact because of the high acceleration potential of the primary Cs beam that enhances ion-beam mixing yet is necessary for sensitive carbon detection. In addition, the sputtered area is larger than the dimension of the LALE stripe. In a separate measurement of a sample grown by LALE using TMGa and AsH_3 at different TMGa flow rates, Fig. 3(b), an appreciable amount of carbon above the background level is clearly seen while no interface carbon accumulation is observed. The observed reduction in carbon contamination with the use of TBAs may be attributed to the abundance of species like AsH_x on the growing surface from the

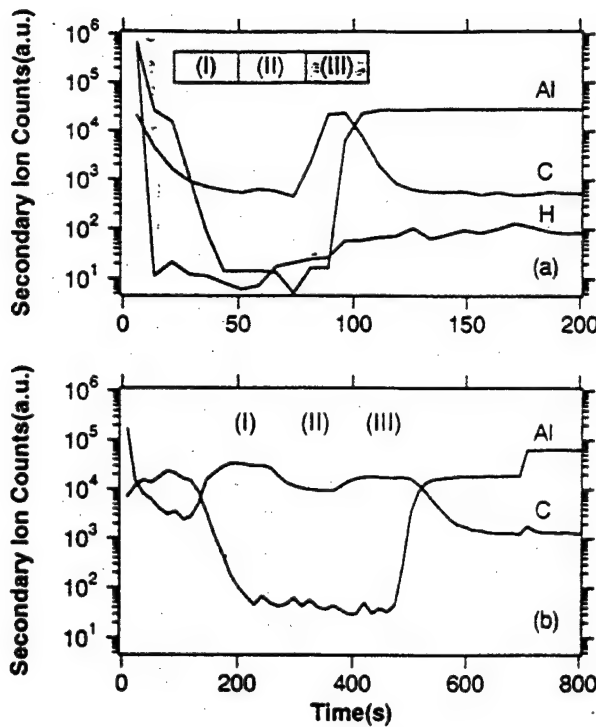


FIG. 3. (a) SIMS profiles of a GaAs multilayer structure grown by LALE using (I) TEGa and AsH_x, (II) TMGa and TBAs, and (III) TMGa and AsH_x; and (b) C and Al traces of a GaAs multilayer structure grown by LALE using TMGa and AsH_x under TMGa mole fractions of (I) 4.0×10^{-4} , (II) 3.3×10^{-4} , and (III) 1.0×10^{-4} .

decomposition of TBAs.^{17,18} Unsaturated carbon-containing species are saturated through reacting with the AsH_x and largely removed as stable and volatile molecules.

Broad area laser diodes have been successfully fabricated from structures grown by ALE and LALE using TBAs. Threshold current densities as low as 300 A/cm^2 (cavity length $744 \mu\text{m}$) were obtained for ALE-grown materials under pulsed testing conditions at a 10 kHz repetition rate. For LALE-grown materials, the threshold current densities were 520 A/cm^2 (cavity length $675 \mu\text{m}$). These are the lowest values reported for lasers with the GaAs QW grown by ALE and LALE and also the first demonstration of the device quality of GaAs grown by ALE and LALE using TBAs. A similar structure grown entirely by conventional MOCVD in the same reactor and fabricated in parallel gives a threshold current density as low as 225 A/cm^2 for a $1010\text{-}\mu\text{m-long}$ device.

In conclusion, TBAs is observed to be a direct and efficient replacement for AsH_x in ALE and LALE. GaAs material grown by LALE using TBAs exhibits low carbon

contamination as is evidenced by *C-V* and SIMS measurements. Intense room-temperature photoluminescence response is observable from DHs grown by ALE and LALE, indicating good optical quality and suitable interfaces between the ALE- or LALE-grown GaAs and the MOCVD-grown Al_{0.3}Ga_{0.7}As layers for device applications. Broad area lasers are fabricated from GRIN-SCH structures with the single QW grown by ALE and LALE using TMGa and TBAs. Low-threshold current densities of 300 and 520 A/cm^2 are obtained for cases of ALE and LALE, respectively.

The USC authors wish to acknowledge partial support from the Strategic Defense Initiative (SDIO/IST) program monitored by ARO and from DARPA through the National Center for Integrated Photonics Technology. The Illinois authors wish to acknowledge support from the National Science Foundation (ECD 89-43166 and DMR 89-20538). J. J. Alwan is supported in part by an Amoco Fellowship.

- ¹J. Nishizawa, H. Abe, T. Kurabayashi, and N. Sakurai, *J. Vac. Sci. Technol. A* **4**, 706 (1986).
- ²Y. Sakuma, M. Ozeki, N. Ohtsuka, and K. Kodama, *J. Appl. Phys.* **68**, 5660 (1990).
- ³A. Doi, Y. Aoyagi, and S. Namba, *Appl. Phys. Lett.* **49**, 785 (1986).
- ⁴N. H. Karam, H. Liu, I. Yoshida, and S. M. Bedair, *Appl. Phys. Lett.* **52**, 1144 (1988).
- ⁵Y. Aoyagi, A. Doi, S. Iwai, and S. Namba, *J. Vac. Sci. Technol. B* **5**, 1460 (1987).
- ⁶T. Meguro, T. Suzuki, K. Ozaki, Y. Okano, A. Hirata, Y. Yamamoto, S. Iwai, Y. Aoyagi, and S. Namba, *J. Cryst. Growth* **93**, 190 (1988).
- ⁷S. D. DenBaars and P. D. Dapkus, *J. Cryst. Growth* **98**, 195 (1989).
- ⁸Q. Chen, J. S. Osinski, and P. D. Dapkus, *Appl. Phys. Lett.* **57**, 1437 (1990).
- ⁹C. H. Chen, C. A. Larsen, and G. B. Stringfellow, *Appl. Phys. Lett.* **50**, 218 (1987).
- ¹⁰J. Nishizawa and T. Kurabayashi, *J. Electrochem. Soc.* **130**, 413 (1983).
- ¹¹S. D. DenBaars, B. Y. Maa, P. D. Dapkus, A. D. Danner, and H. C. Lee, *J. Cryst. Growth* **77**, 188 (1986).
- ¹²M. R. Leys, *Chemtronics* **2**, 155 (1987).
- ¹³B. Y. Maa and P. D. Dapkus, *J. Electron. Mater.* **20**, 589 (1991).
- ¹⁴S. G. Hunnemel, C. A. Beyler, Y. Zou, P. Grodzinski, and P. D. Dapkus, *Appl. Phys. Lett.* **57**, 695 (1990).
- ¹⁵Q. Chen, J. S. Osinski, C. A. Beyler, M. Cao, P. D. Dapkus, J. J. Alwan, and J. J. Coleman, presented in the MRS Spring Meeting, April 29, 1991, Anaheim, CA, Symposium D. [Full paper in *Atomic Layer Growth and Processing*, Mater. Res. Soc. Symp. Proc. **222**, 109 (1991)].
- ¹⁶G. B. Stringfellow, *J. Electron. Mater.* **17**, 327 (1988).
- ¹⁷C. A. Larsen, N. I. Buchan, S. H. Li, and G. B. Stringfellow, *J. Cryst. Growth* **93**, 15 (1988).
- ¹⁸A. V. Annapragada, S. Salim, and K. F. Jensen, presented in the 1991 Spring Materials Research Society Meeting, April 17–May 1, Anaheim, CA, Symposium D. [Full paper in *Atomic Layer Growth and Processing*, Mater. Res. Soc. Symp. Proc. **222**, 81 (1991)].

Appendix 5

Q. Chen and P. D. Dapkus, "Growth and characterization of device quality GaAs produced by laser-assisted atomic layer epitaxy using triethylgallium," Thin Solid Films 225, 115 (1993)

Growth and characterization of device quality GaAs produced by laser-assisted atomic layer epitaxy using triethylgallium

Q. Chen and P. D. Dapkus

National Center for Integrated Photonic Technology, Departments of Materials Science and Electrical Engineering, University of Southern California, Los Angeles, CA 90089-0483 (USA)

Abstract

Triethylgallium is used in combination with arsine in selective area deposition of GaAs by laser-assisted atomic layer epitaxy with the 514.5 nm line of an Ar ion laser. In addition to the much lower laser intensity required to achieve monolayer self-limiting growth than that using trimethylgallium, an intense room temperature photoluminescence response is observable from the double heterostructures of $\text{Al}_{0.3}\text{Ga}_{0.7}\text{As}/\text{GaAs}$ with the central GaAs grown by this technique, indicating good quality of the GaAs material and interfaces. The GaAs also exhibits low C contamination levels as is evidenced by capacitance-voltage and secondary ion mass spectrometry measurements. GaAs and Zn-doped p-GaAs grown by laser-assisted atomic layer epitaxy are incorporated in broad area laser devices for the first time. A threshold current density as low as 544 A cm^{-2} is obtained on a $570 \mu\text{m}$ long device under pulsed testing conditions at a 10 kHz repetition rate.

1. Introduction

Selective area growth by laser-assisted atomic layer epitaxy (LALE) is an attractive technique for realizing complex layer structures in optoelectronic integration. Both trimethylgallium (TMGa) and triethylgallium (TEGa) have been used in LALE studies [1-4]. A systematic LALE study undertaken by us [5] has led to the growth of device quality GaAs by LALE using TMGa and AsH_3 . The need for further reduction in C contamination in the epilayers was also indicated. C contamination is not uncommon to the growth techniques involving the use of metal-organics at reduced temperature. This may be the consequence of incomplete decomposition of the group III metal-organics and/or the inefficiency of the group V hydrides at low growth temperatures. Although it has been shown that the growth conditions can be optimized to produce device quality GaAs by LALE using TMGa and AsH_3 [5], further improvement of the material quality is expected only from a change in the growth chemistry by using different precursors.

In this paper, the use of TEGa as the group III precursor in combination with AsH_3 as the group V precursor in LALE of GaAs is reported. The low C contamination obtainable from metal-organic chemical vapor deposition (MOCVD) [6] and metal-organic molecular beam epitaxy [7, 8] using TEGa makes it a first candidate in the study aimed at reducing the background impurity levels in the GaAs grown by LALE. Photoluminescence (PL) spectroscopy, capaci-

tance-voltage $C-V$ measurement, and secondary ion mass spectrometry (SIMS) have been utilized to assess the quality of GaAs grown by LALE using TEGa. Through a correlation of the results from material characterization and the growth control parameters, suitable conditions for achieving monolayer self-limiting LALE growth with device quality GaAs are established.

2. Experimental procedures

The LALE growth is performed in a switched flow horizontal reactor operated at atmospheric pressure. The schematics of the set-up and the sequence of ALE operation are shown in Fig. 1. The alternate exposure

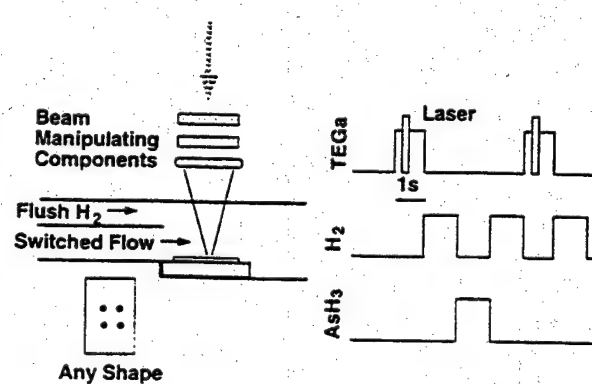


Fig. 1. The schematics of the LALE experimental set-up and the sequence of LALE operations.

of substrates to TEGa and AsH₃, is achieved by temporal switching of the TEGa and AsH₃ into a main carrier H₂ that is flowing continuously through the main chamber of the reactor. The gas handling system and the reactor tube are so designed that both conventional MOCVD and LALE can be performed in a single run of hybridized growth. The optical access is provided by a quartz window situated above the susceptor. A separate stream of H₂ is used to protect the window from fogging. The laser beam from the 514.5 nm line of an Ar ion laser is first expanded and then refocused with a cylindrical lens producing typical beam dimensions of about 10 mm long and about 300 μm wide. A chopper mechanism consisting of a beam stop and a computerized stepper motor is utilized to control the timing of laser illumination. Laser pulse durations from 0.03 s to 1 s have been used. It was found previously [9] that the overlap between group III injection and the laser pulse was necessary to obtain monolayer self-limiting growth.

For growth studies, a narrow line is deposited with 300 LALE cycles and the thickness is measured by a stylus profilometer. PL, C-V, and SIMS measurements are used to characterize the optical quality and the C contamination. The samples for PL measurement are double heterostructures (DHs) with the central GaAs region (570 Å) grown by LALE using TEGa and the barrier layers grown by conventional MOCVD using TMGa, trimethylaluminum, and AsH₃. C-V measurement was performed with the Schottky contacts formed directly on top of the 0.5 μm thick GaAs grown by LALE on either the bare n⁻-GaAs(100) substrates or on the buffer layer of Al_{0.3}Ga_{0.7}As grown by MOCVD on such substrates. A similar DH structure is used also for SIMS measurement whereby multiple GaAs layers are grown by LALE using a different combination of precursors and the C contamination is studied. LALE was carried out at a substrate bias temperature of about 330 °C. The TEGa source is kept at 20 °C. The accompanying conventional MOCVD growths were carried out at 750 °C.

3. Experimental results

Shown in Fig. 2 is the laser intensity dependence of LALE growth rate (in monolayers (MLs) per cycle) for different illumination times. For a given illumination time, the LALE growth rate will depend on the laser intensity at low intensity range before it reaches 1 ML cycle⁻¹. At very high laser intensity, on the contrary, LALE growth tends to result in rough morphology with the formation of a polycrystalline deposit. There exists a range of laser intensities with which 1 ML cycle⁻¹ of LALE growth can be obtained. The onset of the monolayer growth defines a threshold

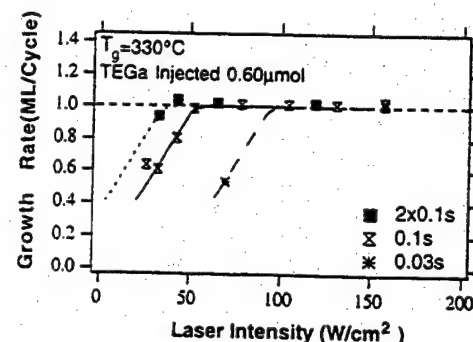


Fig. 2. Laser intensity dependence of LALE growth rate for different illumination times. The lines are drawn to aid the eyes.

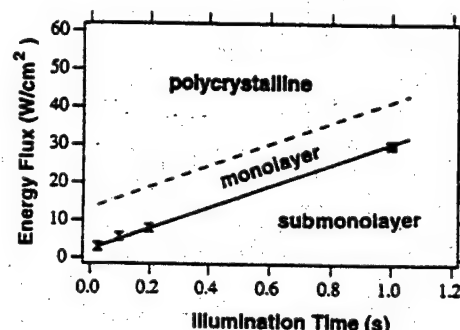


Fig. 3. The illumination for monolayer self-limiting LALE growth. The phase of monolayer LALE operation is obtainable only in the area bounded by the two lines.

intensity for monolayer self-limiting LALE growth at the specific illumination duration. The product of this threshold intensity and the illumination time gives a threshold energy deposit for each LALE cycle (in joules per square centimeter per cycle). Such energy flux for different illumination times is plotted in Fig. 3. The approximate upper bound of LALE monolayer growth is also given by the broken line based on the 0.1 s illumination data in Fig. 2. The point labeled with the square is from work by Meguro and Aoyagi [10]. The plot given in Fig. 3 defines a "phase boundary" of LALE operation within which monolayer LALE growth can be obtained.

Because of the much lower intensity required to achieve monolayer LALE growth in this case than in the case using TMGa, heating effects are greatly reduced. As a result, the lateral definition of the LALE deposit is more abrupt as is shown in Fig. 4 by the full line of the typical cross-sectional profile across LALE stripes as compared with the profile obtained from a stripe grown

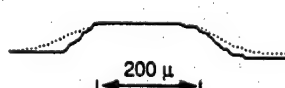


Fig. 4. Typical thickness profiles across LALE stripes grown using TEGa (—) and TMGa (···).

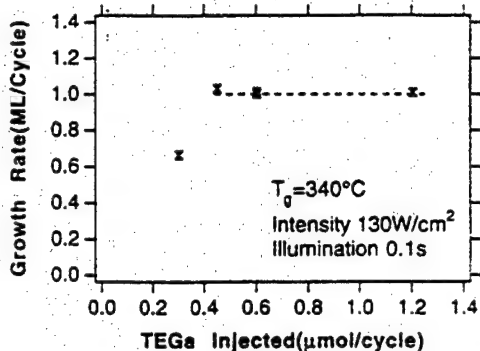


Fig. 5. LALE growth rate as a function of TEGa flux, showing self-limiting growth with respect to TEGa exposure.

using TMGa. This is one of the advantages in using TEGa as the source material.

The LALE growth rate (in monolayers per cycle) as a function of TEGa flux per cycle for the same TEGa exposure time of 1.5 s is plotted in Fig. 5. In contrast to thermal ALE using TEGa where no self-limiting is observable, monolayer self-limiting growth is observed in LALE with respect to TEGa input. This is a strong argument that LALE is not simply the result of localized heating.

Typical room temperature PL spectra from DHs with the central GaAs grown by LALE are shown in Fig. 6 for samples grown using TEGa and TMGa. The intense PL response at room temperature under moderate excitation indicates good quality of the GaAs material and the interfaces. Better PL efficiency is generally obtained in the case of using TEGa despite the lower substrate bias temperature of 330°C as compared with 380°C in the case of using TMGa.

In addition, LALE GaAs layers grown to thicknesses up to $0.5\text{ }\mu\text{m}$ were depleted through even at zero bias. A low zero bias capacitance (5 pF) allows us to estimate the background carrier concentration to be $p \leq 4 \times 10^{15}\text{ cm}^{-3}$ using a built-in potential of 1.4 V . This low

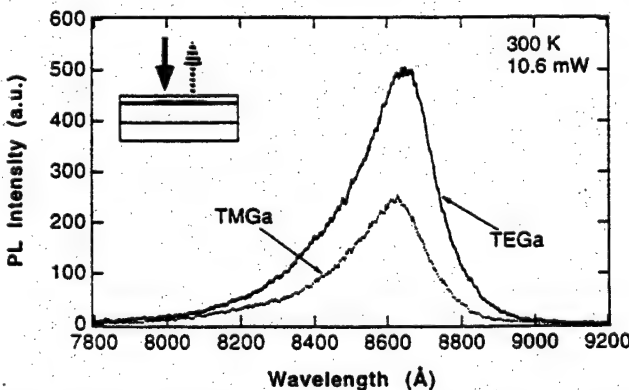


Fig. 6. Room temperature PL spectra from DHs with the central GaAs region grown by LALE using TEGa and TMGa in combination with AsH_3 .

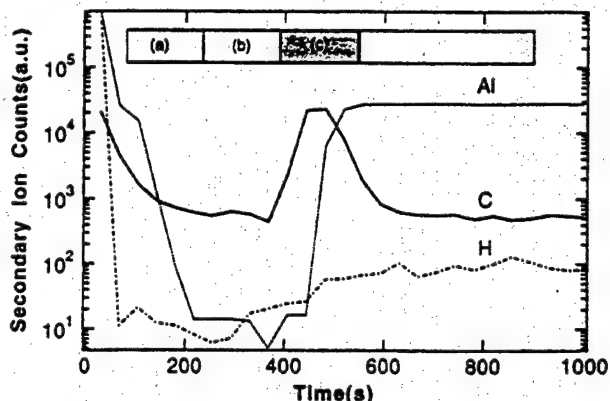


Fig. 7. The SIMS C and Al traces through the structure with the multilayered GaAs region grown by LALE using TEGa and AsH_3 , (layer a), TMGa and TBAs (layer b), and TMGa and AsH_3 , (layer c).

doping level is accompanied by the fact that Schottky contacts can be formed on top of the GaAs grown by LALE using TEGa with a reverse breakdown voltage as high as 20 V . Direct evidence of C reduction comes from our SIMS measurement as is shown in Fig. 7. The C level in the layer grown using TEGa and AsH_3 , (layer a) was not observed above the background level of the $\text{Al}_{0.3}\text{Ga}_{0.7}\text{As}$ layers used to isolate the LALE GaAs layers. On the contrary, an appreciable amount of C was detected in the layer grown using TMGa and AsH_3 . Growth chemistry is shown to have a substantial influence on the C incorporation in LALE as well as in MOCVD.

The influence of growth conditions on material quality is studied by observing the change in the PL efficiency of the same DH structures grown by LALE under different conditions. The results are summarized in Table 1. First, we see that the PL efficiency is improved by using higher laser intensity. It should be noted here that both intensities listed are within the intensity window for monolayer self-limiting growth. The use of multiple pulses is also seen to improve the PL efficiency. Although the second pulse is triggered 0.5 s after the cut-off of the first pulse and therefore is still overlapping with the 1.5 s TEGa injection pulse, it

TABLE I. The influence of growth parameters on the photoluminescence efficiency

Growth Parameters	Effect on PL Efficiency
Laser Intensity ($76 \Rightarrow 119\text{ W/cm}^2$)	Improved
Number of Pulses ($0.1 \Rightarrow 2 \times 0.1\text{ s}$)	Improved
TEGa Exposure ($0.45 \Rightarrow 1.3\text{ }\mu\text{mol}$)	Reduced

causes no additional thickness increase exceeding 1 ML cycle⁻¹. Furthermore, the PL efficiency is reduced with increasing TEGa exposure despite the fact that 1 ML cycle⁻¹ is obtained by virtue of the self-limiting behavior. This suggests that the ranges of TEGa exposure for material of good quality are narrower than those for obtaining monolayer self-limiting LALE growth.

The material characterization data presented above suggest the suitability of the quality of the GaAs material grown by LALE and the interfaces from hybridized growth for device application. We incorporated a single quantum well (QW) of size 100 Å grown by LALE using TEGa into the graded index separate confinement heterostructure (GRINSCH) laser structures. To exploit fully the strength of LALE for *in situ* fabrication, we have also employed Zn-doped p⁻-GaAs (200 Å thick) as the topmost layer to facilitate the alignment in locating the LALE QW region during device processing while providing good ohmic contact between the metal electrodes and the semiconductor. The whole device structure was formed in a single run with four temperature steps. The lower cladding layers (the n side) of the structure were grown first at 750 °C by conventional MOCVD. The substrate temperature was then reduced to 330 °C to carry out the LALE. The top cladding layers (the p side) were again grown at 750 °C. The LALE doping was carried out at 330 °C with the simultaneous injection of TEGa and diethylzinc. The devices were tested at room temperature with no deliberate heat sinking under pulsed conditions at a 10 kHz repetition rate. The device quality of the material and interfaces grown by LALE using TEGa is demonstrated for the first time with a threshold current density as low as 544 A cm⁻² for a cavity length of 570 μm.

4. Discussion

The laser intensity dependence of LALE growth rate shown in Fig. 2 for TEGa is similar to that for TMGa [9] except that the threshold intensity for obtaining 1 ML cycle⁻¹ is much (about an order of magnitude) lower. At such a low laser intensity as around 100 W cm⁻², laser induced heating is negligible. The contribution to LALE from localized heating can be ignored. Two other mechanisms are the surface photochemical reaction and the photocatalytic reaction. In a surface photochemical reaction, the molecular orbitals of the surface adsorbates are so modified that their absorption edge is shifted towards lower photon energy than that of the free molecules. For a purely single-photon event, the photons required to produce just 1 ML of surface Ga species should be a constant independent of the manner with which the photons are delivered.

This is not the case as has been shown in Fig. 3. More photons are used to produce 1 ML of surface Ga species when they are delivered at lower intensity for a longer time. In a photocatalytic reaction, the surface electronic states of the semiconductor are so modified that the surface provides one or more reaction pathway(s) for the reacting molecules to pass at a reduced energy barrier. By using an AlAs top layer to isolate the photocatalytic effect due to laser-induced charge transfer, Meguro and Aoyagi [10] showed that LALE can be initiated by the direct absorption of photons by the chemisorbed alkylgallium. In a more general case, both effects may be present as soon as the LALE GaAs becomes thick enough.

The reduction in C incorporation in the GaAs film grown by LALE using TEGa relative to that using TMGa is a result of different reaction mechanisms. The details of TEGa and TMGa decomposition on GaAs surfaces are still being developed. A comparison can be made only by inferring the mechanism from their gas phase decomposition behavior. One of the expected decomposition products from TEGa is C₂H₄ as opposed to a radical CH₃ in the case of TMGa. The stable C₂H₄ is much less reactive and less likely to be involved in processes resulting in C incorporation. The β-elimination model of TEGa decomposition leads to Ga species free of C. This is another advantage of using TEGa in LALE. However, because of the low stability of TEGa, the substrate temperature must be low in order to avoid homogeneous decomposition and to obtain selective area growth. This low substrate temperature may eventually become the limiting factor for achieving higher quality materials.

Both an increase in laser intensity and the use of additional laser pulses increase the number of photons irradiating the surface in each cycle. The excess photons, although not inducing further deposition in excess of 1 ML cycle⁻¹, are shown to be effective in improving the PL efficiency of the GaAs by LALE. The detailed mechanism for such improvement is not understood, possibly because of enhanced surface species mobility that promotes perfect lattice site registry. Excess TEGa exposure on the contrary causes not only more C to be trapped in the film but also more defects that act as the non-radiative recombination centers. More work is needed to unravel the nature of the defects.

5. Conclusions

LALE using TEGa and AsH₃ as precursors is studied. It is found that much lower intensity is required to achieve monolayer self-limiting LALE growth in this case than that using TMGa. Because of the reduced heating effect at low intensity, LALE using TEGa

Appendix 7

**N. C. Frateschi, M. Y. Jow, P. D. Dapkus, and A. F. J. Levi,
“InGaAs/GaAs quantum well lasers with dry etched mirror
passivated by vacuum atomic layer epitaxy,” Appl. Phys. Lett.
65, 1748 (1994)**

InGaAs/GaAs quantum well lasers with dry-etched mirror passivated by vacuum atomic layer epitaxy

N. C. Frateschi, M. Y. Jow, P. D. Dapkus, and A. F. J. Levi

Department of Electrical Engineering-Electrophysics, University of Southern California,
Los Angeles, California 90089-1112

(Received 17 May 1994; accepted for publication 29 July 1994)

We report measurements of strained InGaAs/GaAs quantum well laser diodes with electron cyclotron resonance (ECR) plasma etched mirrors that are passivated and smoothed with a novel technique involving the selective area growth of GaAs by vacuum atomic layer epitaxy. The threshold current of as-cleaved, etched, and passivated devices has been studied and a significant improvement in mirror feedback is shown with the passivation and smoothing of etched mirrors oriented along the [001] planes. © 1994 American Institute of Physics.

Etched mirrors for semiconductor laser diodes are needed for optoelectronic integration where monolithic placement of several lasers, waveguides, couplers, and transistors in a single opto-electronic integrated circuit (OEIC) is desired. Anisotropic dry-etching techniques such as reactive ion etching (RIE), ion milling (IM), and reactive ion beam etching (RIBE) have been investigated.¹ However, these processes owe a considerable part of their anisotropy to the physical etching caused by an intense ion bombardment that results either from the explicit nature of the process, as in the case of the last two techniques, or from the rf induced self-bias in the RIE case. In the presence of this physical etching, surface damage and roughness is expected and a degradation of mirror feedback can result. An alternative, potentially less damaging, dry-etching technique utilizes ECR plasma etching in which a GHz microwave source and high magnetic field confines electrons and efficiently ionizes the etchant gases with a much smaller plasma self-bias.² Results of preliminary work using this approach encourage us to employ ECR to etch high quality mirrors.³

In this letter we report passivation of ECR defined mirrors by growth of thin GaAs layers using vacuum atomic layer epitaxy (V-ALE).⁴ We show that V-ALE, which is a low-temperature, highly selective, and monolayer-controllable technique, is well matched to our purpose. The refractory metal tungsten is used both as a self-aligned contact and as a selective area growth mask. The tungsten process is compatible with existing very large scale integration (VLSI) metal insulator semiconductor field effect transistor (MISFET) technology and hence suitable for OEIC applications.

In this work we investigate several laser diodes fabricated from the same wafer. The laser diode structure consists of a strained InGaAs/GaAs single quantum well graded index separated confinement heterostructure (GRINSCH) grown epitaxially by metalorganic chemical vapor deposition (MOCVD) on a (100)-oriented substrate. The epitaxial layers are shown in Table I. The quantum well is designed and measured to provide gain in the wavelength range between $0.92 \mu\text{m} < \lambda < 1.01 \mu\text{m}$ and below $0.92 \mu\text{m}$ for $n=1$ and $n=2$ transitions, respectively.

Following epitaxial growth the sample was removed from the growth chamber and a 1000-Å-thick electron-beam evaporated tungsten layer was deposited over the wafer. 50-

μm-wide stripes separated by 250 μm were photolithographically defined and excess tungsten dry etched in a CF₄ plasma. The devices were then isolated using ECR etching in chlorine gas to remove the p^+ -doped GaAs cap layer between the tungsten metal stripes. Next, the sample was photolithographically patterned and a 5-μm-deep ECR etch resulted in vertical mirror faces. Figure 1 shows a scanning electron microscope (SEM) micrograph of the as-etched mirror. The cavity length of the laser is $L_C = 200 \mu\text{m}$.

Passivation and smoothing of the mirrors is achieved using selective area growth in a V-ALE chamber described elsewhere.⁴ In this experiment the tungsten stripes are used to mask epitaxial growth. The substrate was heated up to 620 °C for thermal cleaning and then cooled down to 530 °C for the growth sequence. The process cycle consists of trimethylgallium (TMGa) injection for 0.2 s followed by 4 s pumping, 2 s tertiarybutylarsine TBAs injection, and 2 s pumping. The exposure levels of TMGa and TBAs were 0.8×10^{-6} and 8.6×10^{-6} mole/s, respectively. This cycle was repeated 40 times to result in the growth of approximately 300 Å of GaAs on a (100) plane.

Finally, low-resistance ohmic contact metallization is achieved using electroplating. First the back side is plated with Au/Sn and alloyed in H₂ atmosphere for 15 s at 420 °C. Following this, the tungsten stripes and the back *n*-type con-

TABLE I. Layer structure for the lasers used in this study.

Material	Thickness (μm)	Impurity concentration (cm ⁻³)
GaAs	0.1	$p=5 \times 10^{18}$
Al _{0.5} Ga _{0.5} As	1.5	$p=5 \times 10^{17}$
Al _{0.5} Ga _{0.5} As Al _{0.3} Ga _{0.7} As grade	0.2	<i>i</i>
GaAs	0.0150	<i>i</i>
In _{0.2} Ga _{0.8} As	0.0095	<i>i</i>
GaAs	0.0150	<i>i</i>
Al _{0.3} Ga _{0.7} As Al _{0.5} Ga _{0.5} As grade	0.2	<i>i</i>
Al _{0.5} Ga _{0.5} As	1.5	$n=5 \times 10^{17}$
GaAs	0.2	$n=2 \times 10^{18}$
GaAs	Substrate	$n=2 \times 10^{18}$

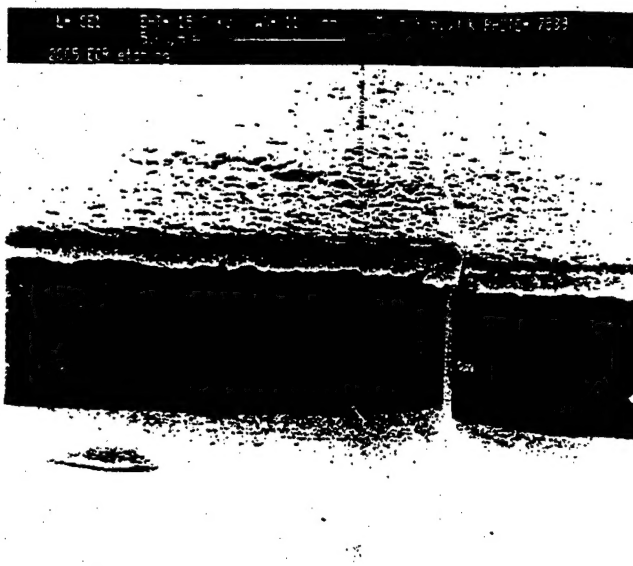


FIG. 1. SEM micrograph of the ECR etched laser mirror. The Au plated W contact layer is visible to the left of the image.

tact are plated with a thick Au layer. The series resistance of completed devices is less than 3Ω at $I = I_{sh}$.

As a reference, part of the same wafer was also processed with conventional cleaved mirrors along [011] planes. Threshold current versus cavity length along with the measured emission wavelength range for these cleaved devices is shown in Fig. 2(a). As commonly observed in this type of gain medium, the threshold current increases rapidly for $L_C < 400 \mu\text{m}$. In this range, as the cavity length reduces, the laser threshold becomes more dependent on the mirror losses. The needed increase in peak gain results in laser emission at shorter wavelengths. Using the logarithmic gain approach a transparency current of 152 A/cm^2 at $\lambda = 1 \mu\text{m}$ is estimated from this data. This good material quality indicates that laser performance is determined primarily by device processing issues.

We investigated the influence on mirror feedback with etched, passivated, and conventional cleaved mirrors for $L_C=200 \mu\text{m}$. This relatively short cavity length ensures that laser threshold current is sensitive to mirror quality [see Fig. 2(a)]. Table II summarizes our results. Lasers with conventional cleaved mirrors exhibit an $I_{th}=85 \text{ mA}$ ($J_{th}=0.85 \text{ kA cm}^{-2}$) current threshold with emission wavelength at $\lambda=0.94 \mu\text{m}$. The current threshold after ECR etching mirrors shows an average value of around $I_{th}=150 \text{ mA}$ ($J_{th}=1.5 \text{ kA cm}^{-2}$) indicating mirror degradation. Comparing this degra-

TABLE II. Average room-temperature threshold current and threshold current density for lasers at different stages of processing.

	Threshold current I_{th} (mA)	Threshold current density (kA/cm ²)
As cleaved	85	0.85
ECR etched	150	1.50
ECR etched plus passivation [011]	180	1.80
ECR etched plus passivation [001]	97	0.97

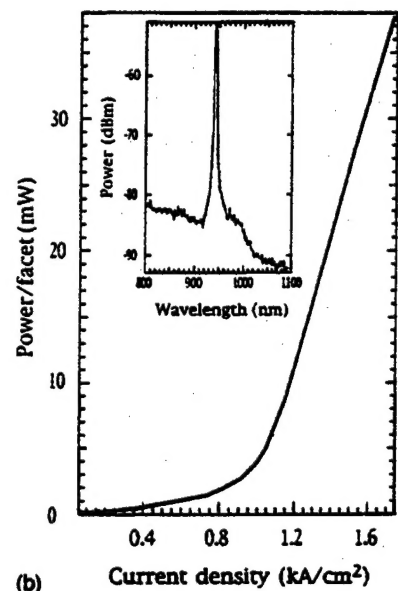
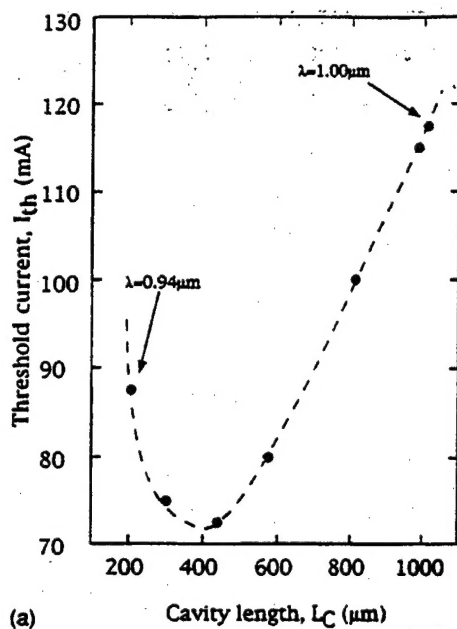


FIG. 2. (a) Room-temperature threshold current vs cavity length for lasers with cleaved mirrors. The lasing wavelength is shown for $L_C=200 \mu\text{m}$ and $L_C=1000 \mu\text{m}$. The laser stripe width is $50 \mu\text{m}$. (b) Room-temperature L - I characteristic for a laser with ECR etched mirrors and V-ALE passivation along the [001] crystal planes. $L_C=200 \mu\text{m}$ and stripe width is $50 \mu\text{m}$. The inset shows the laser spectrum measured for a drive current of $I=2I_{\text{th}}$. Optical emission peaks at wavelength $\lambda=0.94 \mu\text{m}$ and spectrometer resolution is 5 nm .

dation with that caused by other dry-etching techniques is inappropriate because previously published results use either longer cavity devices, cleaved-etched hybrid structures, post-etching passivation, and/or dielectric coatings.^{5,6} With the V-ALE passivation of ECR etched samples with mirrors aligned in the [011] plane we observe a further increase in threshold to around $I_{th}=180$ mA ($J_{th}=1.8$ kA cm⁻²) while after V-ALE regrowth on the [001] mirrors an improvement in current threshold is achieved. Threshold current as low as $I_{th}=97$ mA ($J_{th}=0.97$ kA cm⁻²) is obtained in the latter case

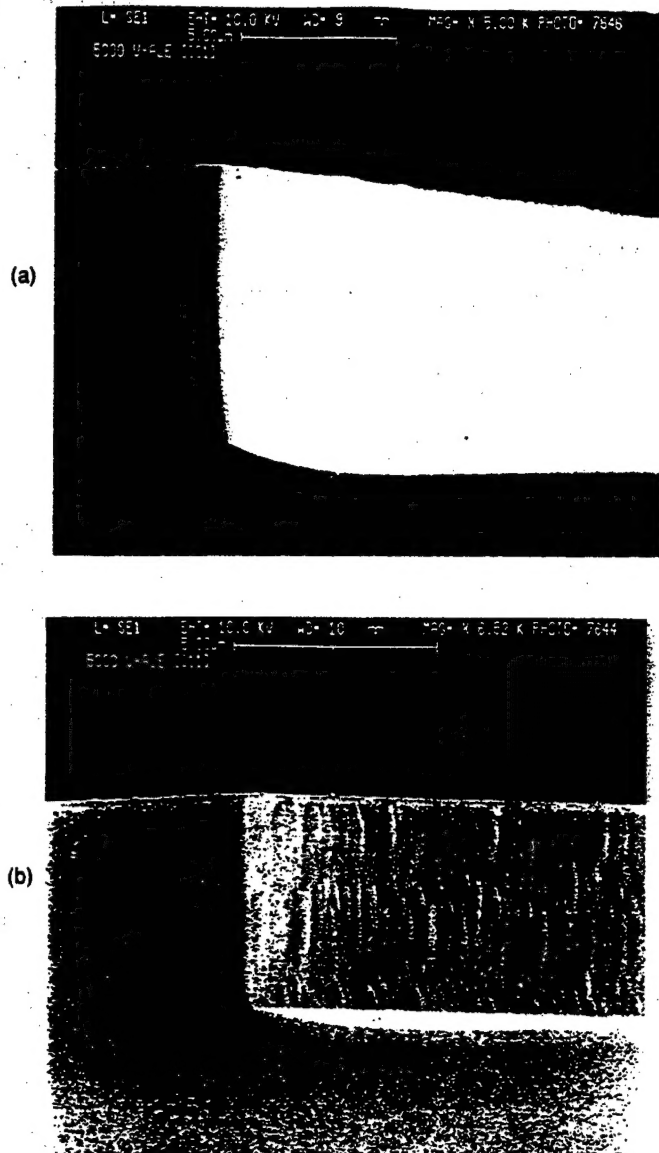


FIG. 3. SEM micrographs showing V-ALE growth morphology on vertically etched GaAs mirrors; (a) mirror in the [001] crystal plane, (b) mirror in the [011] plane.

indicating a reflectivity very close to the cleaved mirror value. Figure 2(b) depicts typical light-current ($L-I$) characteristics for the lasers with [001] passivated mirrors. The inset in Fig. 2(b) shows the lasing spectrum at current

$$I = 2I_{th} \text{ with peak emission at wavelength } \lambda = 0.94 \mu\text{m.}$$

The degradation observed for dry-etched mirrors aligned along conventional [011] cleave planes is probably a result of the strong crystal orientation dependence on surface reaction in ALE growth. It is this dependence which helps create a high spatial growth selectivity when using the tungsten stripe as a growth mask. On the other hand, the growth characteristics in crystallographic planes of different chemical nature is severely affected. While [001] planes are single atomic planes with more stable double bonds connecting the arriving As atoms to the Ga plane, [011] planes have 50% As and 50% Ga with the As atoms of a layer being weakly adsorbed by a single bond. High As desorption and consequently slow ALE growth rate results in the [011] planes as demonstrated by Isshiki *et al.*⁷ Therefore, given an etched [011] mirror, ALE growth will tend to occur more readily on the exposed [001] surfaces associated with roughness of a nonperfect etch. In this situation three dimensional defects are enhanced. For growth on the etched [001] plane the opposite is expected with the [011] surfaces associated with roughness being suppressed by V-ALE growth such that both good passivation and good smoothing is obtained. To verify the growth morphology in these two planes we grew a 5000 Å layer by V-ALE on samples etched along these two orientations. The SEM image in Fig. 3(a) shows the smooth growth that results in the [001] planes after the ALE growth. Figure 3(b) shows the growth for the [011] plane where the enhancement of the etching defects and consequent surface roughness is evident.

In conclusion, the performance of InGaAs/GaAs quantum well Fabry-Pérot lasers with ECR etched mirrors can be significantly improved by using selective V-ALE growth to passivate and smooth the mirrors. Improved mirror smoothing and passivation is found to occur on [001] crystal planes while surface roughness increases on [011] planes.

¹S. S. Ou, J. J. Yang, and M. Jansen, *Appl. Phys. Lett.* **60**, 689 (1992).

²J. Asmussen, *J. Vacuum Sci. Technol. A* **7**, 883 (1989).

³S. J. Pearson, F. Ren, T. R. Fullowan, J. R. Lothian, A. Karz, R. F. Kopf, and C. R. Aebernathy, *Plasma Source Technol.* **1**, 18 (1992).

⁴M. Y. Jow, B. Maa, T. Morishita, and P. D. Dapkus, *J. Electron. Mater.* (to be published).

⁵S. S. Ou, J. J. Yang, and M. Jansen, *Appl. Phys. Lett.* **57**, 1861 (1990).

⁶P. Tihanyi, D. K. Wagner, H. J. Vollmer, A. J. Roza, and C. M. Harding, *Electron Lett.* **23**, 772 (1987).

⁷H. Isshiki, Y. Aoyagi, and T. Sugano, *Appl. Phys. Lett.* **63**, 1528 (1993).